

The role of flooding in the activation of landslides in rail infrastructure

Iain Gareth Johnston

April 2022

The University of Leeds

School of Earth and Environment

Submitted in accordance with the requirements for the degree of Doctor of Philosophy

Declaration and author contributions

The candidate confirms that the work submitted is his own, except where work which has formed part of jointly authored publications has been included. The contribution of the candidate and the other authors to this work has been explicitly indicated below. The candidate confirms that the appropriate credit has been given within the thesis where reference has been made to the work of others.

The work presented in Chapter 2 was published as:

Johnston, I, Murphy, W and Holden, J (2021) A review of floodwater impacts on the stability of transportation embankments. *Earth-Science Reviews*, 215. 103553. ISSN 0012-8252 DOI: 10.1016/j.earscirev.2021.103553

I was responsible for the data search, data collection, data analysis, literature search, figure creation and writing the manuscript. William Murphy and Joseph Holden helped, in the form of supervisors, with advice on conception and direction of the study. They also assisted with comments, clarifications and proofreading the work.

Copyright declaration

This copy has been supplied on the understanding that it is copyright material and that no quotation from this thesis may be published without proper acknowledgement.

The right of Iain Johnston to be identified as Author of this work has been asserted by him in accordance with the Copyright, Designs and Patents Act 1988.

© 2022 Iain Johnston and the University of Leeds

Acknowledgements

Many thanks to my supervisors, Bill Murphy and Joe Holden, for their input and guidance throughout the duration of this project – and for their continued support, especially during periods when ever moving obstacles were being formed by events outside of our control.

The research undertaken in this thesis was possible due to funding from the Natural Environment Research Council, in conjunction with Network Rail, as part of a National Productivity Investment Fund award - number NE/R009813/1.

My thanks go to Clare Brint and other colleagues at Network Rail for providing access to internal failure reports and participating in discussions around their experiences with the dataset in question, and to Highways England for providing data about their assets.

My thanks to Kirk Handley and John Martin for their support with setting up and troubleshooting the design of laboratory experiments, Sam Allshorn for initially suggesting I use fluorescein and to James Woodman with his knowledge of the wide ranging uses of latex.

I thank those from RMEGGh and beyond who provided advice and direction on research topics I otherwise may not have considered, and those who attended Productivity Café for teaching me to use Python, and their general prompts to do some work. Romain, Dave and the rest of the Bike Hub crew – thank you for many educational and enjoyable lunch breaks, even if the nature of these has been curtailed by restrictions in more recent times.

To those who have held and shared ropes, travelled, camped, climbed, adventured and misadventured on trips big and small; thank you. Without these outlets this thesis may have been completed more quickly, but the process would have been far less fulfilling. To those who have spotted and caught falls - of all kinds - whether over a mat or pad, on a wall or slackline, in the lab or office, at home, and beyond – my appreciation is great, for without your help I would not be able to try the things I do. Finally, I would like to thank my parents, family, friends, and Sophie, for your continued support throughout.

Abstract

The effects of flood-induced embankment failures include infrastructure downtime, but, in more serious events, derailments and fatalities occur. From a review of global railway embankment failures, a new classification of four types of flood which cause slope failure was produced and key driving processes hypothesised. Internal erosion, driven by differential flood head, has the potential to cause material alteration following flooding by redistributing fine particles and altering material structure. Bender elements were used to measure material changes caused by internal erosion. Relationships between particle loss, shear wave velocity, permeability and sample strength were considered. Increases in the mass of material removed from samples caused reductions in sample strength. Following particle removal, multiple strain hardening-softening cycles developed during loading. High temporal resolution permeability and shear wave velocity measurement during seepage showed a relationship between the two properties; particle deposition is thought to have caused permeability reductions and shear wave velocity increases. Decimetre-scale physical slope models were used to identify where changes in material behaviour due to seepage-induced particle migration are likely to occur in slopes. Fines deposition caused mean grain size reductions of 4.5%, and 9% increases in coefficient of curvature, across the slope toe region. Increases in grain size, due to fine particle removal, occurred near water inflow. Coupled with evidence from triaxial testing, these data suggest that permeability barriers may form in embankments, increasing pore water pressures and decreasing slope stability. Numerical modelling predicted the effects of these material changes on displacement caused by live rail loading at an embankment scale. Areas of particle loss caused displacement increases. Zones of deposition showed less consistent increases in displacement. An improved understanding of flood types which cause destabilisation, failure recording practice alteration and non-intrusive monitoring of changes in slope properties following flooding will allow for enhanced predictions of failure behaviour and stability assessment.

Table of Contents

Chapter 1	15
1.1 Background	16
1.2 Aims and objectives	18
1.3 Thesis structure.....	18
1.4 Research methods summary	19
1.5 References	21
Chapter 2	23
2.1 Introduction	25
2.2 Landslide types and destabilisation processes affecting infrastructure.....	28
2.2.1 Landslide types recorded in embankments and cuttings	29
2.2.2 Landslides originating outside of geotechnical assets	31
2.3 Floods as a cause or trigger of slope failure and weakening	31
2.3.1 Types of flood.....	32
2.4 Flood induced landslide observations	34
2.5 Active processes in embankment slopes	40
2.5.1 Internal erosion.....	40
2.5.2 Effects of live loading during flooding	45
2.5.3 Scour	46
2.5.4 Sliding.....	49
2.5.5 Wetting front development.....	50
2.5.6 Discussion of process effects	51
2.6 Conclusions and further research	53
2.7 References	54
Chapter 3	61
3.1 Introduction	62
3.2 Methods.....	65
3.2.1 Sample material	65
3.2.2 Testing apparatus.....	66
3.2.3 Seepage and shearing	68
3.3 Results.....	70
3.3.1 Particle removal	70
.....	71
3.3.2 Shear wave velocity change.....	71
3.3.3 Drained shear strength and stiffness.....	74
3.3.4 Permeability change	74
3.3.5 Evidence of particle migration	75
3.4 Discussion.....	76
3.4.1 Implications for transportation embankments.....	79
3.5 Conclusions	80
3.6 References	81

Chapter 4	83
4.1 Introduction.....	84
4.2 Methods	85
4.2.1 Equipment design and slope structure	86
4.2.2 Slope material.....	88
4.2.3 Testing processes	88
4.3 Results	89
4.4 Discussion	94
4.5 Conclusion	97
4.6 References.....	97
Chapter 5	99
5.1 Introduction.....	100
5.2 Methods	103
5.2.1 Modelling structure.....	103
5.2.2 Model design.....	104
5.2.3 Transfer functions	106
5.3 Results	108
5.3.1 Displacement – frequency relationship	108
5.3.2 Base only altered model (BO-AM).....	109
5.3.3 Full slope altered model (FS-AM).....	111
5.3.4 Uniform model	114
5.3.5 Basal alteration – full slope alteration comparison	114
5.4 Discussion	115
5.5 Conclusion	117
5.6 References.....	117
Chapter 6	120
6.1 Overarching questions and objectives	121
6.2 Scaling.....	126
6.3 Monitoring and measurement	127
6.4 Applications.....	128
6.4.1 Application to industry	128
6.4.2 Application to wider fields	129
6.5 Limitations and further research.....	129
6.5.1 Limitations	129
6.5.2 Further research.....	130
6.6 Summary	132
6.7 References.....	133
Appendix 1	145

List of Figures

- Figure 1:** Potential progression of slope stability during a flood event. Some slopes will fail during (i), or shortly after (ii), flooding. Following flood recession the stability of slopes must be considered as stability may not rebound to its pre-flood condition (iii) - presenting questions about the effects of future live loading, flooding or other destabilisation events. 17
- Figure 2:** Schematic comparisons between cross sections of a typical UK embankment (left) and a modern road or rail embankment (right). After Briggs et al. (2017). 27
- Figure 3:** Embankments form linear barriers to flow: a) representation of flow interception - during river flooding, water level increases causing impoundment (i) where embankments cross floodplains; at the bottom of slopes, or where embankments are formed across slopes, runoff is trapped behind the embankment causing impoundment (ii); b) embankment intercepting river overbank floodwaters during flooding at Church Fenton, UK (copyright Network Rail, 2020). 28
- Figure 4:** Timescales over which flood related effects act on geotechnical assets..... 29
- Figure 5:** Process models of weakening and failure processes developing in slopes during flooding: a) offset head flood ; b) overtopping flood ; c) basal flood; d (over page): above slope flood. Solid arrow denotes surface water movement. Dashed arrow denotes ground water movement..... 33
- Figure 6:** Illustrations of rail slopes subjected to flooding: a) embankment failure following offset head flooding in Acquivavia, Italy (October 2005); b) Embankment failure in Conwy, UK, following overtopping flood (March 2019); c) failure of embankment following train loading during basal flooding in Ohio, USA (June 2018); d) floodwater development above slope, causing infiltration in UK (a) reproduced from Polemio and Lollino (2011); b) and d) courtesy of Network Rail; c) courtesy of Sioux County Sherriff. 37
- Figure 7:** Schematic representation of strain development during shearing post-seepage and associated fines loss. Increased particle loss causes material softening and samples to fail without displaying peak strength. Critical state strength reduces between samples containing increasing amounts of fines loss. 41
- Figure 8:** Soil structure development during seepage. A: Pre-flood soil skeleton. Fine particles are located in pore spaces and coat coarser grained particles. B: Water seepage drives particle motion through soil. C: Loss of fine particles forms an unstable soil skeleton. Higher strength and stiffness reductions and contraction behaviour development during shear are expected up-flow due to the loss of fine particles. D: Fines redeposition reduces pore space and creates a permeability barrier. Fine particles are concentrated at particle contacts. Strength increases may occur in zones where there is an accumulation of fine particles. WFD – water flow direction. 42
- Figure 9:** Rapid drawdown development (u = pore pressure)..... 44
- Figure 10:** Basal sliding develops when the shearing force applied by floodwaters overcomes the resistance caused by embankment mass. Displacement, d , can cause increases in substrata permeability and flow pathway development due to rupturing. If

<i>embankments are founded on weak substrata, the sliding plane may develop below the embankment-substrata interface.....</i>	50
Figure 11: <i>Grain size distribution for the soils tested.....</i>	66
Figure 12: <i>Experimental apparatus.....</i>	67
Figure 13: <i>Mass of material washed out from samples during seepage recorded against a) seepage volume and b) seepage duration.</i>	71
Figure 14: <i>Observed Vs and K over time during seepage for tests a) 30D, b) 30C, c) 15D, d) 30H, e) 30B and f) 15A. d-f are continued over page. Values are normalised by the initial value for the respective property. Trend lines on A-D are three point moving averages and are logarithmic on graphs E and F.</i>	72
Figure 15: <i>Friction angle change with percentage of material washed out from samples. ..</i>	74
Figure 16: <i>Shearing curves for tests on samples with (a) 15% and (b) 30% fines content. (c) Is the close up of low strain stress behaviour of samples with 30% fines content. Strains are axial, and were measured without on-sample measurement.</i>	75
Figure 17: <i>Seepage front development inside samples shown by fluorescence migration; samples were halved post-seepage and imaged using UV light. Fluorescence was initially located at the top of samples, before migrating downwards during seepage. a) Seepage development across the width of samples. b) Concentrated seepage development along a preferential seepage plane.....</i>	76
Figure 18: <i>Conceptual model of change in fine particle distribution and soil structure caused by seepage.....</i>	77
Figure 19: <i>Experiment design schematic.....</i>	86
Figure 20: <i>Grainsize distribution of material used during slope construction.</i>	89
Figure 21: <i>Geometric mean grain size values for slopes A - E. Colour bar 1 is used for slopes A - D, colour bar 2 refers to slope E. Lowest mean grain sizes are observed in the bottom rear portion of the slope. In slope C, transect (i) underwent the shortest duration of seepage. Transect D (i) was a control transect and underwent no seepage.</i>	92
Figure 22: <i>Mean Cc value for each sampling point in slopes A - E. In slopes C, transect (i) underwent the shortest duration of seepage. Transect D (i) was a control transect and underwent no seepage. Colour bar 1 refers to slope A, colour bar 2 to slopes B - D and colour bar 3 to slope E.</i>	93
Figure 23: <i>a) mean grain size and b) normalised mean Cc values at each sampling point for all transects of slopes A-D, excluding the control transect Di which did not undergo seepage. Average grain size values for each sampling cell show the mean of the geometric mean grainsize of each transect. Cc values were normalised by the average Cc value of all samples in slopes A-D combined.</i>	94
Figure 24: <i>Normalised mean grain size for each horizontal layer in slopes D and E. Transect 'D-i', measured without seepage, does not show geometric mean grain size variations between each vertical layer in comparison to transect D-ii, measured following seepage. Values normalised by the geometric mean grain size of each transect.....</i>	94

Figure 25: Fine particle accumulation at the toe of slope ‘A’. Fluorescein migration is also evident, with a fluorescent zone visible above the zone with fine particle deposition. . 95

Figure 26: Locations of material zones used in the altered models. a) Uniform model b) Basal alteration (BO-AM) c) Large scale embankment alteration (FS-AM). The same material regions and mesh were applied to all three models. The ground below the model continued uniformly to a depth of 40 m. Material properties are defined in Table 1. In B and C theoretical water table level is indicated by black dashed lines. Sampling point location descriptions and dynamic load inputs are labelled in A, and the same sampling points and load locations were used in all models. Sampling points were numbered 0-11 left and right, with 0 at the base of the embankment body on each side. Sampling points had a 0.5 m horizontal spacing. 102

Figure 27: Dynamic load Gaussian wave content. a) Time domain b) Frequency domain, calculated using a Fast Fourier transform. 105

Figure 28: Example transfer graph for an individual sampling point. The transfer value represents a change in signal amplitude between two datasets and is calculated for each frequency. 107

Figure 29: Fourier transform of displacement signal, displaying power – frequency relationship for all sampling points on the left hand slope face for the uniform model (the right hand slope face and altered model displayed displacements of a comparable amplitude). a) Vertical displacement b) Horizontal displacement. 108

Figure 30: Transfer functions for the BO-AM left embankment batter for a) Vertical displacement and b) horizontal displacement. The horizontal dashed black line across the plot denote points at which material boundaries were present on the slope face. c) The red line denotes the location of sampling points, with the black area the section of the slope where material alteration was modelled. 109

Figure 31: Transfer functions for the BO-AM right hand embankment batter, for a) Vertical displacement and b) horizontal displacement. The horizontal dashed black line across the plot denote points at which material boundaries were present on the slope face. c) The red line denotes the location of sampling points, with the black area the section of the slope where material alteration was modelled. 110

Figure 32: Transfer functions for the BO-AM showing differential change between the right and left sides of the embankment, for a) Horizontal displacement and b) Vertical displacement. The horizontal dashed black line across the plot denote points at which material boundaries were present on the slope face. 110

Figure 33: Transfer functions for the FS-AM left embankment batter for a) Vertical displacement and b) horizontal displacement. The horizontal dashed black lines across the plot denote points at which material boundaries were present on the slope face. c) The red line denotes the location of sampling points, with the black area the section of the slope where material alteration was modelled. 111

Figure 34: Transfer functions for the FS-AM right embankment batter for a) Vertical displacement and b) horizontal displacement. The horizontal dashed black lines across the plot denote points at which material boundaries were present on the slope face. c) The red line denotes the location of sampling points, with the black area the section of the slope where material alteration was modelled. 112

Figure 35: Transfer functions for the FS-AM showing differential change between the right and left sides of the embankment, for a) Vertical displacement and b) Horizontal displacement. The horizontal dashed black line across the plot denote points at which material boundaries were present on the slope face. 114

Figure 36: Transfer functions for the uniform model showing differential change between the right and left sides of the embankment, for a) vertical displacement and b) horizontal displacement. Black dashed lines represent the point mesh changes met the slope boundary. 115

List of Tables

Table 1: Summary of slope destabilisation caused by flooding by asset type and landslide type. Flood effects are based on all failures identified in this review. Landslide types are after Cruden and Varnes (1996). Y = slope is susceptible to this failure. N = slope is not commonly susceptible to this failure. R = slope is rarely susceptible to this landslide type.	30
Table 2: Examples of consequential flood-induced transport infrastructure failures identified during this review.....	35
Table 3: Descriptions and occurrence of the four classified types of flood. The number of failures is recorded as the number of discrete flooding events which have been identified where failure has occurred. Multiple landslides may develop during a single flooding failure event.	38
Table 4: Internal erosion processes.	40
Table 5: The effects of antecedent conditions on material preparation.	47
Table 6: Instability criteria to identify soils susceptible to internal instability.....	64
Table 7: Initial sample properties and test properties.	68
Table 8: Soil property changes comparing before and after seepage tests. For Vs and K change, negative values indicate a reduction after seepage. % changes are relative to initial values.	70
Table 9: Slope design properties. Slope density was not recorded for slope A due to procedural error.	87
Table 10: Slope material stability criteria. Materials with h/f values >1.3 are considered stable.....	88
Table 11: Material properties used in the models. Properties for the load slab, ballast and subgrade were taken from Connolly et al. (2013). Poisson’s Ratio, which varies from roughly 0.15-0.45 in soils (Olivier et al., 2016, Suwal and Kuwano, 2012) was set at a constant 0.3 for the embankment body.....	104
Table 12: Detail of the contents of transfer functions presented in results.	107
Table 13: Summary of destabilisation process development caused by each of the four identified flood types.....	122

Chapter 1

Introduction

Chapter summary

This chapter provides context for the research undertaken during this thesis and provides background information on the topics covered as a whole. The overall aims, objectives, and key research questions studied during this work are defined. The methodology used to address these questions and the structure of the thesis are then outlined.

1.1 Background

The flooding of linear infrastructure embankments is a persistent and somewhat frequent problem which can cause embankment degradation and failure (e.g. Polemio and Lollino, 2011, Tsubaki et al., 2017). Consequences of failure may include infrastructure damage and downtime, train derailment and, in some cases, fatalities (Mossa, 2007). With increases in the scale of modern infrastructure developments, ageing of existing assets, and increases in the severity of rainfall events due to climate change (Field et al., 2012), transport systems are increasingly subjected to more extreme and prolonged flood conditions (Lindgren et al., 2009). Furthermore, high speed rail development is increasing globally, as are associated ground vibrations (Bian et al., 2016).

Transport networks are vulnerable to flooding in many countries. On a global scale, approximately 7.5% of road and rail infrastructure assets are potentially vulnerable to 1 in 100 year flood events (Koks et al., 2019). The costs of flood damage related disruption to transportation infrastructure are high, with costs of £930 million to EU road and rail systems per year between 2000 and 2010 (Przyluski et al., 2011). In China flooding causes upwards of £40 million of damage to rail systems per year (Hong et al., 2015). In the UK, 17% of rail tracks are susceptible to river flooding, 9% to coastal flooding and 17% to groundwater and surface water flooding. A total of 2400 km of UK rail tracks, approximately 8% of the total, are considered to be at a high risk of flooding (Dawson et al., 2017). Network Rail (2016b) suggested that 35% of UK rail embankments are at risk of flooding. In addition to infrastructure disruption, a variety of consequential accidents have occurred following flood-induced embankment failure across the world. Five people were killed in Italy in 2005 following a road embankment collapse (Mossa, 2007). In the USA, 48 flood-related train accidents were recorded in the period 2001 – 2010, including 38 derailments, (Federal Railroad Administration, 2001-2010) and in Japan, an average of 202 rail incidents were recorded each year from 1991 to 2000 (Noguchi et al., 2000). In the UK, consequences of flooding have included trains travelling over failed embankments (RAIB, 2013c, RAIB, 2017b) and embankments failing during train passage (RAIB, 2013a). Given the likelihood of increased flooding (Field et al., 2012, Betts and Brown, 2021), flood-induced failures are likely to increase in the future.

Although landslide development in soil embankments is generally well understood, understanding of the effects of flooding on the stability of transportation slopes is less well developed (Polemio and Lollino, 2011). Extracting the effects of flooding, henceforth defined as the temporary presence of surface water on, or in close proximity to, an

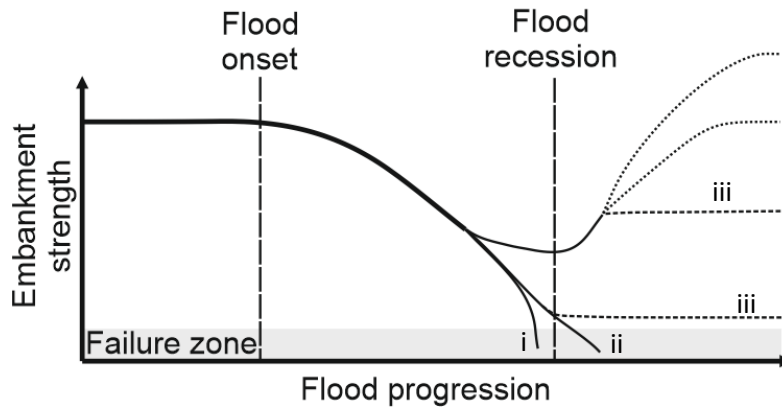


Figure 1: Potential progression of slope stability during a flood event. Some slopes will fail during (i), or shortly after (ii), flooding. Following flood recession the stability of slopes must be considered as stability may not rebound to its pre-flood condition (iii) - presenting questions about the effects of future live loading, flooding or other destabilisation events.

embankment, from the effects of persistent or intense rainfall presents a further challenge. The effects of flooding also have a temporal dimension: the stability of a slope can change during the rise and fall of an individual flood event. Overall stability may increase or decrease depending on the section of a slope considered and the extent of flood progression (e.g. Menan Hasnayn et al., 2017, Pinyol et al., 2008). In addition to causing failure, the processes induced in slopes by flooding can lead to lasting changes in material properties, including strength, stiffness and permeability, in sections of slopes which do not immediately fail (Figure 1) (Kelly et al., 2012, Chang and Zhang, 2011). The process of identifying stability changes in embankments in the field can be challenging as destabilisation processes can occur without leaving visible external destabilisation markers.

Lasting changes in slope stability following flood recession have received little research attention, although they are becoming more widely considered as a threat (Polemio and Lollino, 2011, Tsubaki et al., 2016). For material property alteration to be included in slope condition assessment, the types of weakening and potential signs of instability or processes which may cause instability must be identified – as must the conditions which promote stability change. Improved understanding of the likelihood of material alteration development, would allow for a better understanding of the condition of slopes affected by flooding. The severity of the hazards posed by flooding-induced slope alteration are currently poorly understood. In order for future embankment construction to be better designed and more resilient to future flood events, a better understanding of the processes involved is required. Furthermore, for existing embankments, an increased understanding

of how slopes are destabilised by flooding will permit infrastructure managers to better manage the condition of slopes and the risks posed following flooding events.

1.2 Aims and objectives

The overall aims of this thesis are to investigate the role of flooding in activation of landslides in rail embankments and to understand the potential for flooding to cause lasting weakening, following flood recession, in embankments which do not fail during flooding.

The thesis addresses the overarching research question of *“how do floods, and repeat flood events, cause slope failure and lasting slope condition alteration to develop in transportation infrastructure embankments”*, and there are four objectives:

- 1) To compile reports of global flood-induced embankment failures in order to identify (i) types of flood which affect embankments and (ii) flood-induced processes which promote slope destabilisation.
- 2) To understand the magnitude of material property alteration caused by specific flood-induced processes, with a focus on the effects of seepage and internal erosion on strength, stiffness and permeability.
- 3) To identify the sections of slopes where changes in material properties are most likely to occur due to flood-induced seepage, and to evaluate the best material parameters to identify these changes.
- 4) To identify the consequence of flood-induced property alterations in embankments, focusing on identifying the significance of changes in the magnitude of slope vibrations.

1.3 Thesis structure

In order to understand the effects of flooding on the stability of embankments, first it was necessary to identify the types of floods which cause slope failure. To this end, Chapter Two presents a paper published in *‘Earth-Science Reviews’* which collates and analyses failures caused by the flooding of rail and road embankments. From the identified failure events, the types of flood which cause embankment failure are defined. The specific processes which cause slope failure, and which cause destabilisation in slopes affected by flooding but which do not fail, are identified and their effects on material behaviour and slope stability are reviewed. Chapter Three considers the effects of internal erosion processes, driven by flood-induced seepage, and identified as key slope alteration processes in Chapter Two, on the physical properties of soils. Experiments were undertaken on samples in a laboratory

environment, using triaxial tests modified to allow seepage through samples and shear wave velocity monitoring prior to shearing. In Chapter Four the results of laboratory experiments identifying the locations of fine particle migration in slopes are presented. Tests utilised physical models representing an embankment. Chapter Five presents results from dynamic numerical models which explore the effects of material property changes identified in Chapters Three and Four on surface displacements in embankments caused by vibration loading. Chapter Six synthesises, discusses, and summarises the work presented in this thesis, identifies limitations and applications of this work and explores areas to be considered for further research.

1.4 Research methods summary

The overall approach utilised in this thesis was to identify the types of flood which cause embankment slopes to fail and to identify the distinct ways floods cause failure to occur. From the failures identified, the specific processes which cause slope destabilisation and their effects were ascertained. Laboratory testing was then undertaken to understand how specific processes caused changes in material properties and where in slopes these changes are likely to occur. Triaxial testing on constructed samples was undertaken to allow for more consistent initial sample conditions than would have been possible from using embankment derived soils. The controlled testing conditions of the laboratory setting also allowed for a better understanding of the material alteration than if testing had been undertaken on in-situ materials in a field environment. Upscaled laboratory models were used to identify locations of material movement to allow measurement of material changes in a controlled environment, with samples containing known starting materials and subjected to known seepage durations. Process acceleration was possible in comparison to sampling full-scale embankments. Results from laboratory testing were used to inform numerical modelling to understand the significance of slope alterations to live loading. A numerical modelling approach was utilised to provide an understanding of the effects of loading at a larger scale than was possible during laboratory testing. Models were run with material properties representing those which may develop following flood induced material alteration. Numerical modelling allowed for a number of testing scenarios to be considered, without the need for identification, and intrusive investigation of, embankments which had been altered to a known degree in field environments.

An outline of the methods used in each chapter is provided below. Method details are contained within subsequent chapters.

Chapter 1

Chapter 2 *A review of floodwater impacts on the stability of transportation embankments*

A review of flood-induced failures was undertaken using data from industry sources and a wider open literature search. The chapter provides more than a basic literature review as it analyses combined data from failure events in order to produce a new categorisation of embankment flood types, which may cause slope failure, and to understand their relative frequencies. The chapter therefore provides a combination of: i) a critical review of the international literature on the topic and ii) data compilation and interrogation. The failure events found in this data search were used to assess the types of flood which produce failure and identify the processes which were causing failure. Failure information was collated from a number of sources. Failure data relating to flooding were provided by Network Rail and Highways England. A broader open data search was also undertaken, including peer-reviewed literature, regulatory documents and news sources, focusing on failures in the UK and internationally.

Chapter 3 *Measuring the effects of internal erosion on granular soils used in transport embankments*

Laboratory testing was undertaken to understand the magnitude of changes to materials caused by seepage, in order to assess the potential for development of lasting changes in material properties after flood recession. Triaxial testing was utilised to allow for shear wave velocity measurement in samples during seepage, and to enable shear testing following the seepage process. Lateral bender elements were used to measure changes in shear wave velocity.

Chapter 4 *Redistribution of particles in model embankment slopes following seepage*

Laboratory testing was undertaken on physical slope models to establish the locations of soil alterations in slopes. Modelled slopes were utilised to upscale the changes and behaviours measured during smaller scale laboratory tests, and to allow for expatiated seepage and associated particle movement which would likely have taken longer to develop in field testing of full scale earthworks.

Chapter 5 *The effects of flood induced material alteration on embankment displacement due to dynamic loading*

Numerical modelling was undertaken in Rocscience's RS2 software to establish the effects of alterations to material properties measured during laboratory testing on embankment behaviour when subjected to live loading. The primary focus of the numerical modelling

was to assess how surface displacement changed between embankments affected and unaffected by flooding.

1.5 References

- BETTS, R. A. & BROWN, K. 2021. Introduction. In: The Third UK Climate Change Risk Assessment Technical Report [Betts, R.A., Haward, A.B. and Pearson, K.V.(eds.)]. Prepared for the Climate Change Committee, London.
- BIAN, X., JIANG, H. & CHEN, Y. 2016. Preliminary Testing on High-speed Railway Substructure Due to Water Level Changes. *Procedia Engineering*, 143, 769-781.
- CHANG, D. & ZHANG, L. 2011. A Stress-controlled Erosion Apparatus for Studying Internal Erosion in Soils. *Geotechnical Testing Journal*, 34, 579-589.
- DAWSON, R., GOSLING, S., CHAPMAN, L., DARCH, G., WATSON, G., POWRIE, W., BELL, S., PAULSON, K., HUGHES, P. & WOOD, R. 2017. UK Climate Change Risk Assessment 2017 Evidence Report: Chapter 4, Infrastructure.
- FEDERAL RAILROAD ADMINISTRATION 2001-2010. Railroad Safety Statistics Annual Report. Federal Railroad Administration Office of Safety Analysis.
- FIELD, C. B., BARROS, V., STOCKER, T. F. & DAHE, Q. 2012. *Managing the risks of extreme events and disasters to advance climate change adaptation: special report of the intergovernmental panel on climate change*, Cambridge University Press.
- HONG, L., OUYANG, M., PEETA, S., HE, X. & YAN, Y. 2015. Vulnerability assessment and mitigation for the Chinese railway system under floods. *Reliability Engineering & System Safety*, 137, 58-68.
- KELLY, D., MCDOUGALL, J. & BARRETO, D. Effect of particle loss on soil behaviour. Proc., 6th Int. Conf. on Scour and Erosion, Publications SHF, Paris, 2012. 639-646.
- KOKS, E. E., ROZENBERG, J., ZORN, C., TARIVERDI, M., VOUSDOUKAS, M., FRASER, S. A., HALL, J. W. & HALLEGATTE, S. 2019. A global multi-hazard risk analysis of road and railway infrastructure assets. *Nature Communications*, 10, 2677.
- LINDGREN, J., JONSSON, D. K. & CARLSSON-KANYAMA, A. 2009. Climate Adaptation of Railways: Lessons from Sweden. *European Journal of Transport and Infrastructure Research*, 9, 164-181.
- MENAN HASNAYN, M., JOHN MCCARTER, W., WOODWARD, P. K., CONNOLLY, D. P. & STARRS, G. 2017. Railway subgrade performance during flooding and the post-flooding (recovery) period. *Transportation Geotechnics*, 11, 57-68.
- MOSSA, M. 2007. The floods in Bari: What history should have taught. *Journal of Hydraulic Research*, 45, 579-594.
- NETWORK RAIL 2016b. Task 106: JBA Trust, 4 March 2016, Overtopping (Earthworks at Flood Risk).
- NOGUCHI, T., FUJII, T. J. J. R. & REVIEW, T. 2000. Minimizing the effect of natural disasters. *Japan Railway & Transport Review*, 23, 52-59.
- PINYOL, N. M., ALONSO, E. E. & OLIVELLA, S. 2008. Rapid drawdown in slopes and embankments. *Water Resources Research*, 44, W00D03.
- POLEMIO, M. & LOLLINO, P. 2011. Failure of infrastructure embankments induced by flooding and seepage: a neglected source of hazard. *Natural Hazards and Earth System Sciences*, 11, 3383.
- PRZYLUCKI, V., HALLEGATTE, S. & TOMOZEIU, R. 2011. V. Przyluski, S. Hallegatte (SMASH-CIRED), R. Tomozeiu, C.Cacciamani (ARPA-ER) V. Pavan (ARPAER), C. Doll (Fraunhofer-ISI) (2011): —Weather trends and economy-wide impacts|| Deliverable 1 within the research project WEATHER (Weather Extremes: Impacts on Transport Systems and Hazards for European Regions) European Commission, 7th framework

Chapter 1

programme. Project co-ordinator: FraunhoferISI. Karlsruhe, Paris, Bologna, October 2011.

RAIB 2013a. Derailment of a freight train at Barrow upon Soar, Leicestershire. *Rail Accident Report*. Rail Accident Investigation Branch, Department for Transport.

RAIB 2013c. Train ran onto a washed-out embankment near Knockmore, Northern Ireland 28 June 2012. Rail Accident Investigation Branch, Department for Transport.

RAIB 2017b. Report 03/2017: Trains passed over washed out track at Baildon.

TSUBAKI, R., BRICKER, J. D., ICHII, K. & KAWAHARA, Y. 2016. Development of fragility curves for railway embankment and ballast scour due to overtopping flood flow. *Natural Hazards and Earth Systems Sciences*, 16, 2455-2472.

TSUBAKI, R., KAWAHARA, Y. & UEDA, Y. 2017. Railway embankment failure due to ballast layer breach caused by inundation flows. *Natural Hazards*, 87, 717-738.

Chapter 2

A review of floodwater impacts on the stability of transportation embankments

Chapter summary

This chapter presents a paper, published in *Earth-Science Reviews*, of flood-induced failures of transport infrastructure and identifies the types of floods which cause failure of embankments, the types of failure they induce, and their relative levels of occurrence. This is followed by detailing the specific processes which cause destabilisation for each of the flood types identified. The way each of these processes alters slope stability is assessed, with examination of factors including antecedent conditions, the driving mechanism for the process and the effects of the process on slope behaviour. This chapter concludes by considering the effects of repeated flooding events on slopes and identifying significant research gaps in the field.

Johnston, I, Murphy, W and Holden, J (2021) A review of floodwater impacts on the stability of transportation embankments. *Earth-Science Reviews*, 215. 103553. ISSN 0012-8252 DOI: 10.1016/j.earscirev.2021.103553

A review of floodwater impacts on the stability of transportation embankments

I. Johnston^{a,b*}, W. Murphy^a and J. Holden^b

^aSchool of Earth and Environment, University of Leeds, Leeds, LS2 9JT, UK

^bwater@leeds, School of Geography, University of Leeds, Leeds, LS2 9JT, UK

*ee16igj@leeds.ac.uk

Abstract

Infrastructure embankment failures due to flooding have been recorded in many countries. The consequences of flood-induced embankment failures have mainly been limited to infrastructure downtime; however, failures have caused fatalities and include multiple near-miss events. Here we review the types of flood which cause transportation embankment failure and the associated types of failure, processes which cause failure, and the potential for lasting slope weakening after flooding. Four types of flood which cause transport embankment failure are identified; offset head, overtopping, basal floods at slope toes and floods above slopes. Failure is caused by flood-specific processes including rapid drawdown, sliding, scour and internal erosion in addition to the development of destabilisation from effective normal stress decrease and saturation loading. Existing destabilisation modelling tends to focus on single flood events which cause failure, with limited consideration of repeat flooding and the long-term degradation of embankment strength which may occur following rainfall and flooding. Although there is a well-developed understanding of generic landslide development, we suggest that there has been limited consideration of the destabilising effects caused by dynamic conditions which develop during repeat flooding. Furthermore, while the effects of live traffic loading from high speed trains during flooding have previously been considered and shown to cause destabilisation, such previous work is found to be limited to specific embankment structures which are not representative of the wider rail network and considerable uncertainty exists for older earthworks. We conclude this review by identifying future research priorities to help improve prediction and mitigation of flood-induced embankment instability.

2.1 Introduction

Flooding has caused structural transport infrastructure failures in countries including the UK, Italy and Japan (e.g. Tsubaki et al., 2017, Polemio and Lollino, 2011, Network Rail, 2016a) and is considered one of the most prominent weather-related concerns for railways in the USA (Rossetti, 2007). While consequences of flood-driven embankment failures have largely been limited to infrastructure disruption, five people were killed in Italy in 2005 following a road embankment collapse (Mossa, 2007). Additionally, incidents have included trains travelling over failed embankments (RAIB, 2013c, RAIB, 2017b, Bisantino et al., 2016) and embankment failures during train passage (RAIB, 2013a).

In the context of this review, 'failure' is considered as a shear displacement of an asset which compromises the performance of the embankment itself or causes a measurable displacement of the road or track bed. This displacement is sometimes identified as a 'rough ride' by train drivers at early stages of movement. Other processes that might contribute to displacement, such as dynamic compaction, are not considered in this review. 'Triggers' of failure are considered as the direct events which caused failure to occur; 'causes' of failure move a slope towards instability but may not be directly attributed to failure in themselves. For the purposes of this review, flooding is defined as the temporary presence of surface water on, or in close proximity to, an embankment.

In this review we draw on global literature and datasets where possible. Nevertheless, a significant portion of our findings utilise data and experience from UK rail networks, with which the authors are most familiar. UK rail embankment systems often have an aged legacy and may therefore be susceptible to a wide range of failure types and a long period of exposure to environmental conditions. However, the identified processes and recommendations are applicable to, and draw upon, the broader context of global scenarios and infrastructure asset types.

In China, approximately £40 million were spent per year between 2000 and 2010 on flood-related railway disruption (Hong et al., 2015) and in Austria flooding caused over £100 million of damage to railways between 2006 and 2013 (Kellermann et al., 2016). In the USA, there were 48 flood-related train accidents between 2001 and 2010, causing 38 derailments (Federal Railroad Administration, 2001-2010). In Japan, an average of 202 interruptions to rail operation occurred per year due to flooding between 1991 and 2000 (Noguchi et al., 2000). Globally, approximately 7.5% of road and rail infrastructure assets are potentially vulnerable to 1 in 100 year flood events (Koks et al., 2019). However, while

Chapter 2

there are frequent media reports of incidents from around the world, there is no global database of flood-driven transportation infrastructure failures, so their true frequency is not known.

Transportation infrastructure landslides are relatively common in the UK, with over 160 failures recorded across UK road and rail networks in the winter of 2000-2001 alone (Ridley et al., 2004, Rail Engineer, 2012) and 381 rail earthwork failures between 2014 and 2019 (Network Rail, 2018). In addition to the obvious cost implications of network downtime and the challenges created for users, multiple near-miss incidents have been recorded in recent years. These include derailments and the trapping of 57 people on a road section between two failures during the Glen Ogle landslides in 2004 following heavy rainfall (Gibson et al., 2013, Winter et al., 2005, Winter et al., 2016). While only a subset of landslides on infrastructure assets are directly related to flooding, disentangling the mechanisms resulting from the presence of standing water, as opposed to effects of intense rainfall, remains challenging. The 2017 UK Climate Change Risk Assessment stated that 17% of UK railway tracks are susceptible to river flooding, 9% to coastal flooding and 17% to groundwater and surface water flooding (Dawson et al., 2017). The report further highlighted that circa 2400 km of UK tracks are considered at a high risk of flooding. Network Rail (2016a), who maintain and operate the rail infrastructure in the UK, suggested that 35% of UK rail embankments are at risk of flooding. Recent evidence suggests changing rainfall patterns will result in an increased incidence of flooding (Field et al., 2012). In addition, the growth of road and rail traffic leads to larger live load application, and an ageing asset inventory means there is a growing vulnerability to damage. This is particularly true for rail embankments where larger and faster trains are being used on the rail network.

UK rail embankments were primarily built during the late 19th century meaning there is often little known about the geotechnical history of individual sites. The construction techniques and materials used are rarely well recorded and there are limited data on maintenance and historical instability (Nelder et al., 2006, Network Rail, 2018). The majority of rail embankments were constructed using locally sourced materials. Additional fill, often granular material, has been added to many assets to allow for rail expansion or to accommodate for settlement, failure or subsidence of original fill materials (Figure 2). Assets were often constructed via end-tipping with little or no compaction and little regard for long term stability. Although more modern highway embankments utilise low

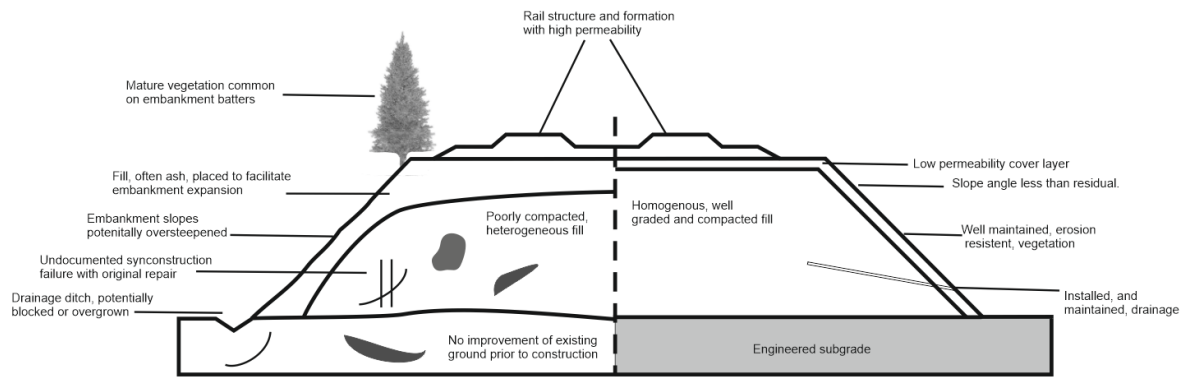


Figure 2: Schematic comparisons between cross sections of a typical UK embankment (left) and a modern road or rail embankment (right). After Briggs et al. (2017).

permeability materials, maintained drainage and compaction (Loveridge et al., 2010), this is less true of rail embankments due to highly permeable ballast toppings.

Unlike in constructed levees, water impoundment is not a primary design focus during transport embankment construction. Construction of levees includes seepage control through substrata, using impermeable blankets or cut-offs, and through embankment bodies, using drainage and low permeability barriers. Granular fills are not generally used in levees protecting human life due to high permeability, low resistance to overtopping erosion and susceptibility to liquefaction (USACE, 2000). Liquefaction susceptibility is higher in poorly consolidated, loose, granular materials (Marto and Soon, 2011). Furthermore, transportation infrastructure has the potential to form linear barriers to flow over large areas of land where it intersects natural flow paths (Figure 3). This can cause flood head development against transport embankments following rainfall (e.g. in *Whalley v. Lancashire and Yorkshire Railway Company* (Bennett, 1884)), following dam breach (e.g. Brown et al., 2008), or following river level rise (e.g. the Conwy valley (Wales) failures in 2015 (Rail Engineer, 2016) and flooding of the Asa River (Japan) in 2010 (Tsubaki et al., 2016)).

Through assessment of slope failure databases, individual flood-induced earthwork failure reports, geotechnical testing studies of soils subjected to seepage and other flood processes and studies monitoring and modelling slopes subjected to flooding, the aims of this review are to identify:

- 1) The types of flood and related processes which cause failure, long-term degradation and weakening of slopes;
- 2) Good practice in the recording of asset deformations associated with flood events;
- 3) The effects of traffic loading during flooding;

- 4) Current understanding of how flooding acts as a trigger of landslides and how this can be applied to geotechnical assets.

2.2 Landslide types and destabilisation processes affecting infrastructure

Landslide threats posed to geotechnical assets can be classed as internal (those that happen on the asset itself, such as material softening due to slope wetting and drying cycles) and external (those that have an origin outside the asset, such as floodwater induced head loading). External processes predominantly have an immediately deleterious

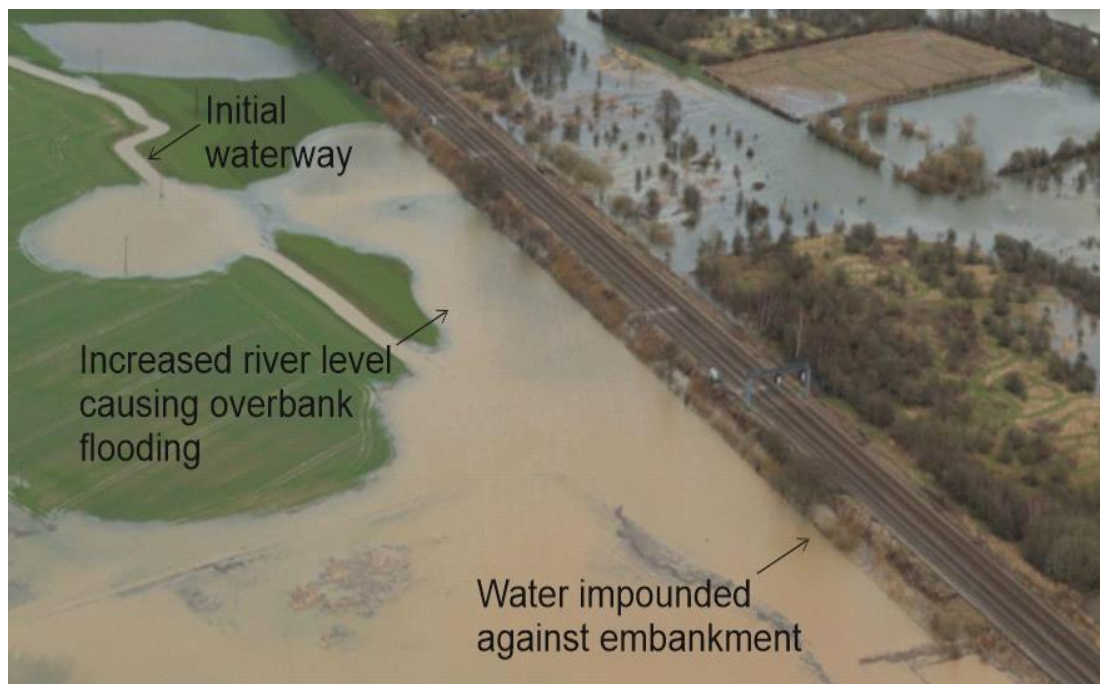
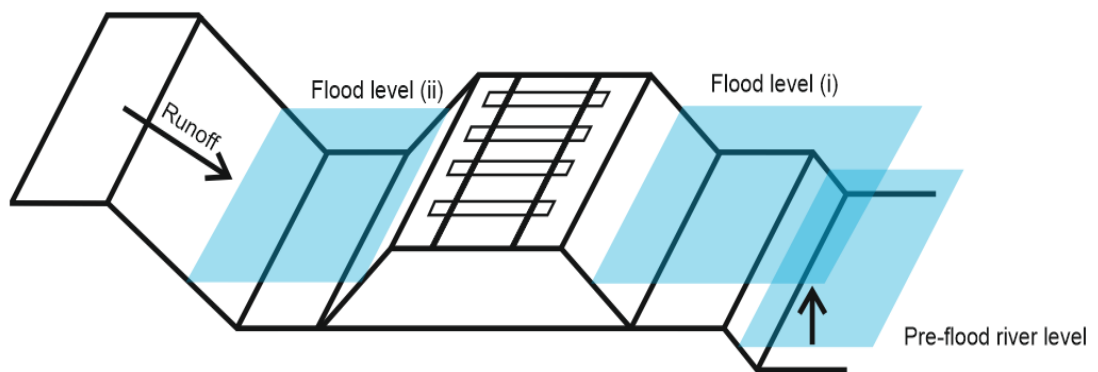


Figure 3: Embankments form linear barriers to flow: a) representation of flow interception - during river flooding, water level increases causing impoundment (i) where embankments cross floodplains; at the bottom of slopes, or where embankments are formed across slopes, runoff is trapped behind the embankment causing impoundment (ii); b) embankment intercepting river overbank floodwaters during flooding at Church Fenton, UK (copyright Network Rail, 2020).

effect on the stability of the slope; internal processes mainly cause long-term changes in material properties. Longer-term alterations may be thought of as preparatory processes which allow later triggers to be effective. Figure 4 illustrates the key processes driving asset failure and the timescales over which they occur.

One of the most significant challenges in examining the impact of flooding on geotechnical assets is that no one single dataset in the public domain is sufficiently detailed to allow for primary research, nationally or internationally. Therefore, observations examined herein are a combination of a review of the published literature informed by additional UK-based field data provided by Network Rail and Highways England.

2.2.1 Landslide types recorded in embankments and cuttings

It is important to consider asset type when assessing failure types; cuttings, embankments and natural slopes have different predominant failure modes due to their composite materials and construction (Table 1). Flooding effects on landslides are dependent on both asset and flood type.

Generally, earth and debris falls and topples as defined by Hungr et al. (2014) do not occur in embankments as the slopes are insufficiently steep; rock falls and topples are common in cuttings (Lato et al., 2012). Embankment oversteepening may occur due to rapid erosion during flooding, leading to debris and earth falls and topples. Debris flows which affect infrastructure commonly develop at structure intersections, such as tunnel portals and the end of embankments, due to focusing of runoff. Translational failures often occur in cover layers overlying embankment cores (Perry, 1989). Rotational failures can develop following live loading of embankments over clays (Lehtonen et al., 2015).

Loveridge et al. (2010) indicated that while shallow failures occur both in rail and road asset groups, deep seated failures ($\approx 2\text{m}$ depth (Briggs et al., 2016)) are currently rare in highway slope assets but occur more commonly in rail cuttings and embankments. Differences in the

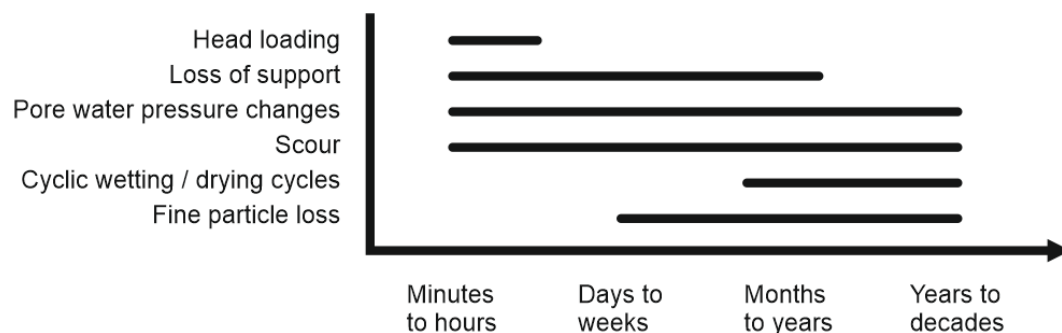


Figure 4: Timescales over which flood related effects act on geotechnical assets.

Table 1: Summary of slope destabilisation caused by flooding by asset type and landslide type. Flood effects are based on all failures identified in this review. Landslide types are after Cruden and Varnes (1996). Y = slope is susceptible to this failure. N = slope is not commonly susceptible to this failure. R = slope is rarely susceptible to this landslide type.

Landslide type	Cuttings		Flood effects	Embankments		Flood effects
	Rock	Debris/earth		Cohe-sive	Gran-ular	
Falling	Y	N	Erosion along discontinuities; development of water pressures in tension cracks	R	N	Rapid erosion relating to flooding can result in localised oversteepening.
Toppling	Y	N		R	N	
Sliding	R	Y	Erosion along discontinuities; development of water pressures in tension cracks; changes in effective stress state	Y	Y	Changes in effective stress state; scour of embankment toe; weakening of materials through internal erosion processes.
Slumping	R	Y	Rare in rock cuttings due to limited height and insufficient driving forces; in soil cuttings slumping can occur due to changes in water pressures (see text)	Y	Y	
Flowing	N	Y	Debris flows caused by water flow localisation are common phenomena in soil and weak rock assets. These can result in washouts. Large debris flows are more likely to be external risks.	R	Y	Erosion of top of embankment develops into breach; flow down embankment batters causes debris flows and washouts.
Complex	Y	Y		Y	Y	Changes in stress state cause rotational failures; these can develop into flows or flow-slides due to high liquid contents.

occurrence of deep seated failures between assets groups were assigned to younger ages of highway assets (Loveridge et al., 2010) and the increased height of rail earthworks to maintain shallower route gradients. Shallow translational failures occur due to increasing pore pressures near the slope surface, following rainfall (Briggs et al., 2016). In embankments, deep-seated, rotational failures occur in most commonly in slopes formed

of cohesive materials (Perry et al., 2003) and are often triggered by prolonged periods of rainfall, flooding or slope load variations (Network Rail, 2018).

Infrastructure earthwork failures are commonly recorded as ‘washouts’, a broad term encompassing post-failure slope morphologies where material is removed from a supporting structure or a slope face by water flow. Failures recorded as ‘washouts’ range from full slope loss to the localised removal of material from soil pipe outflow. Classification of failures recorded as washouts (following Cruden and Varnes (1996)) includes flow-slides (e.g. Railrodder, 2011), localised and full slope debris flows (RAIB, 2013c), translational failures and scour-erosion from runoff (RAIB, 2017b). Washout geomorphologies may be formed by ‘complex’ landslide events, described according to their final morphology but with differing initial and secondary failure types; these data are not routinely recorded for failures in infrastructure.

Due to the broad usage and ill-defined nature of the term ‘washout’, we suggest that the term washout or phrase ‘a slope washout occurred’ should not be used to describe failure in slopes. Instead, the term ‘washout’ should only be used to describe post failure slope geomorphology with, where applicable, an additional description of the mechanism of slope failure - i.e. ‘a debris flow failure resulting in a washout’.

2.2.2 Landslides originating outside of geotechnical assets

External landslide risks to infrastructure are primarily related to failures which develop on slopes outside of asset boundaries before travelling across open land. These failures are primarily debris flows such as at Rest and Be Thankful, Scotland (BGS, 2012). Individual rock blocks can travel significant distances through bounding/rolling on steep, rough terrain. Jaboyedoff and Labiouse (2011) outlined a methodology where such hazards can be assessed. External risks are often difficult to predict, or account for, due to the increased number of factors which must be considered during analysis – many of which may be unknown. While important to consider, risks from external landslides that originate elsewhere in the landscape and might then impact rail infrastructure are not discussed further in this review as they develop on natural slopes due to a wide array of additional processes not further discussed.

2.3 Floods as a cause or trigger of slope failure and weakening

One of the challenges associated with understanding the role that flooding has on geotechnical assets is disentangling the effects of the flood and the effects of intense

rainfall. Such rainfall has the capacity to create slope instability regardless of whether ponding of water occurs. Therefore, to identify a landslide as being caused or triggered by flooding it must meet the following criteria:

- 1) The landslide is spatially related to, and interacts with, floodwater prior to or during failure;
- 2) The landslide occurs after water has started to accumulate. That water can be ponded or flowing;
- 3) The floodwater causes a stress state response in the slope;
- 4) The proximity of floodwater is appropriate to the mechanism of movement (e.g. if the landslide is triggered by erosional processes downslope, the floodwater should not be on the other side of the embankment). On the basis of these criteria, we identified forms of instability related to flooding, outlined in section 2.4.

2.3.1 Types of flood

We collated the available information on failure events which developed from flooding for UK road and rail infrastructure, as well as notable events recorded in news reports and academic literature globally. Events with a direct impact on live loads are recorded in Table 2; a list of all identified failures is presented in Appendix 1. From the identified failures, we suggest four key types of floods which cause failures, as illustrated in Figures 5 and 6. These are:

Offset Head Floods (Figure 5a): Offset head development occurs when embankments act as a temporary dam; flood head primarily develops behind one side of a slope. Partial drainage (e.g. through culverts) and/or water input on the leeside of the slope can cause differential increases in head on both sides of a slope. Internal erosion can develop through embankments, and / or substrata, causing slope weakening without external expression.

Overtopping Floods (Figure 5b): Overtopping floods occur when floodwaters go over the top of an embankment. Overtopping floods often initiate as offset head flood events prior to further floodwater rise. Overtopping floods can cause complete submergence of a slope. It is more common for overtopping floods to flow down the leeside of an embankment, prior to potential breach and lee-slope erosion. Although processes common with offset head floods may develop prior to slope overtopping, these are superseded by overtopping processes, removing altered material.

Basal Flood Development (Figure 5c): Basal floods develop with or without ground saturation. Shallow water presence at the toe of a slope, either an embankment or cutting, increases water levels in slopes, increasing pore pressures and reducing slope strength. Although slope weakening develops, basal floods are primarily causes of failure. In all identified events, live loading was reported as being needed to act as a failure trigger.

Above Slope Floods (Figure 5d): Above slope floods develop above cuttings. During above slope floods, flow occurs down slopes from open land or at the end of constrictions (for example where a cutting stops and an embankment starts), or through slope faces. If above slope floods form in depressions behind slope crests, overtopping may not occur and seepage into and through slopes may be the primary destabilisation method. Mass failures can develop due to wetting front development and saturation. Piping development (Bernatek-Jakiel and Poesen, 2018) and seepage outflow on slope faces can cause localised failures in addition to large scale slope weakening.

Mechanisms associated with each of these four flood types are broadly outlined in Table 3.

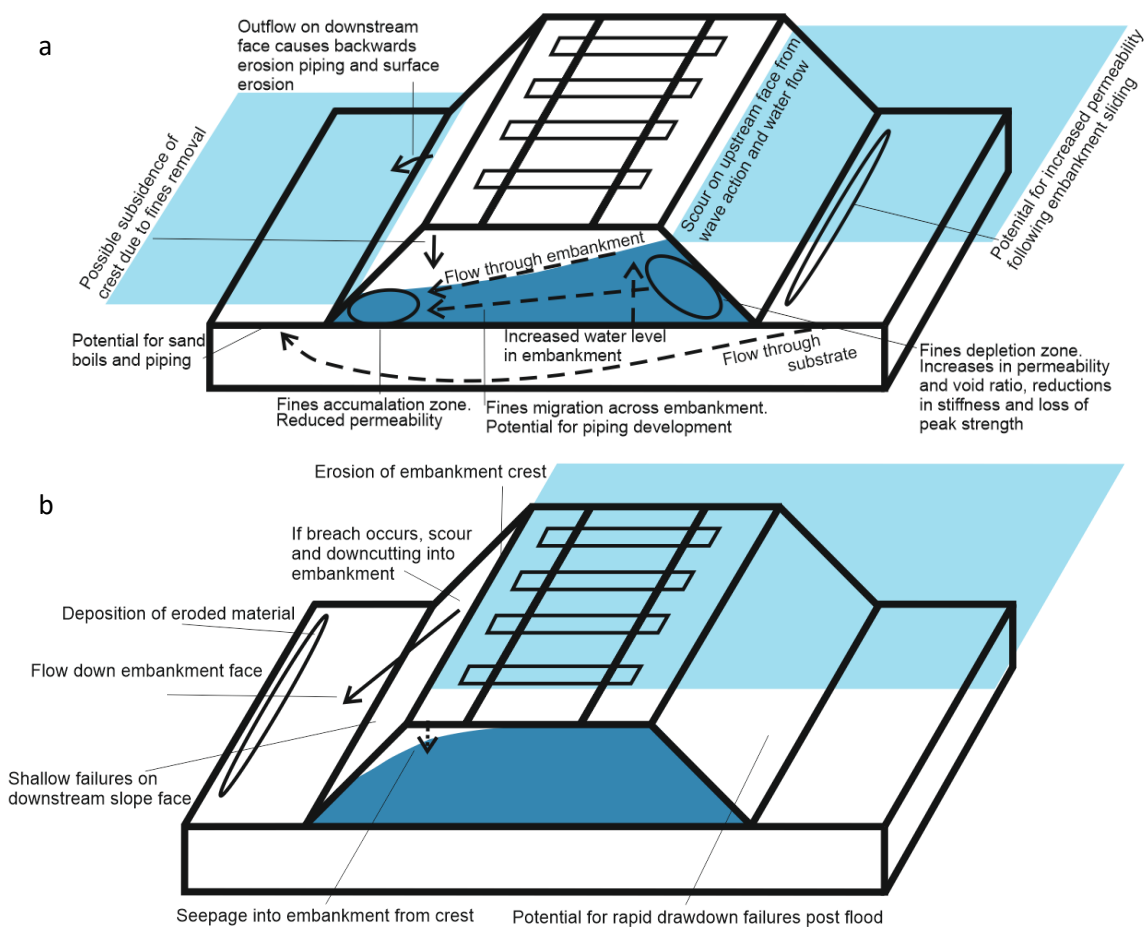


Figure 5: Process models of weakening and failure processes developing in slopes during flooding: a) offset head flood ; b) overtopping flood ; c) basal flood; d (over page): above slope flood. Solid arrow denotes surface water movement. Dashed arrow denotes ground water movement.

2.4 Flood induced landslide observations

Prior detailed analysis of the number of earthwork landslides following flooding was not identified; this is thought to be related to limited public recording of failures and prioritisation of re-establishing network operation. Available public datasets are predominantly comprised of summary information, without detailed information on material properties or factors such as failure type, flooding history and flood duration. Our analysis of failures comprises data collected from Network Rail and Highways England in the UK, in addition to failures reported in public literature and media globally. Failures identified in media reports were classified using observations of photographic evidence. Agency data was acquired from database extracts and individual failure reports. Offset head floods are identified as the most likely cause of slope failure, accounting for 36% of recorded flood induced failure events. A total of 23 offset head floods, 12 above slope floods, 13 basal floods and 16 cases of overtopping were identified as causing failure (Table 3). The three most commonly recorded causes of slope failure due to flooding in the USA

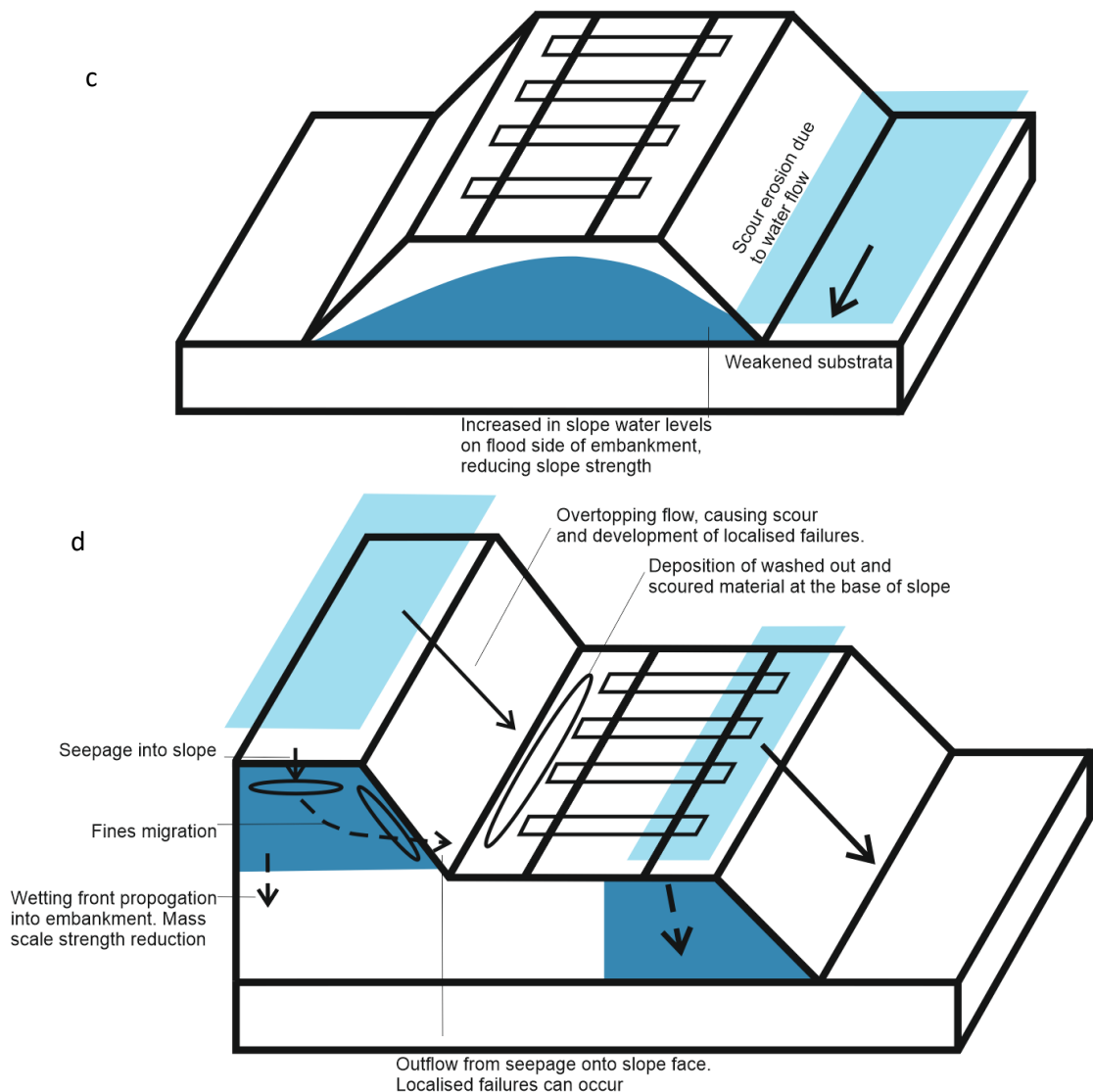


Table 2: Examples of consequential flood-induced transport infrastructure failures identified during this review.

Failures	Country and Year	Failure type and number.	Failure result and damage	Flood type	Detail	Reference
Acquaviva,	Italy, 2005	Single major + multiple minor	Washout, injuries to 27 people	Offset head	6.3m of water impoundment against rail embankment in six hours. Embankment was constructed of rockfill core with soil cladding. Failure occurred as a high speed train drove over the failure site. Additional translational failures of cladding material.	Bisantino et al. (2016), Polemio and Lollino (2011).
Knockmore	N. Ireland, 2012	Single major	Washout	Offset head	0.7m head developed across the rail embankment, with water increases on both sides following heavy rain. Construction was a clay base overlain by ash and ballast. Failure occurred when impounded water overtopped clays, causing granular ash to washout.	RAIB (2013b).
Barrow upon soar	United Kingdom, 2012	Single Rotational	Train derailment	Basal flood	The rail embankment was constructed of a clay core with an outer ash layer. Failure occurred as a freight train passed over the site.	RAIB (2013a)
Baildon	United Kingdom, 2016		Washout	Above slope flood	Water running along rail tracks exited at the end of an embankment, causing erosion and washout.	(RAIB, 2017)
Sayo River	Japan, 2009		Multiple failures over 13km	Overtopping + base of slope	12 embankment failures, 9 severe embankment breaches and 56 ballast washouts occurred. Flooding was caused by record breaking rainfall, up to 327mm causing the Sayo River to overflow.	Tsubaki et al. (2017)
Bietto	Italy, 2005		Five fatalities	Impoundment		Mossa (2007)
Stackpool	Canada, 2011	Initial rotational	Washout	Impoundment	Floodwaters are reported to have occurred due to the break of a beaver dam upstream of the site, causing the rail embankment to fail.	Railrodder (2011)

Desert Road	USA, 2008		Washout	Offset head + overtopping	Floodwaters formed against one side of the road, however the culvert was not big enough to prevent water level rise and overtopping.	Fowler (2008)
Paris	France, 2018		Washout. Derailment	Impoundment	During heavy rains, floodwaters in drainage ditch impounded against rail embankment. Train drove over failed section, causing derailment.	RATP (2018)
Doon	USA, 2018		Derailment. Oil spill	Base of slope	Floodwaters at the base of both sides of rail embankment. Train drove onto embankment, causing failure and derailment.	(Independent, 2018)
Black hills Julia Creek	USA, Australia, 2015		Washout Train derailment	Impoundment Base of slope	Water impounded against rail embankment, causing failure. Floodwaters formed against a rail embankment, causing failure during freight train passage and train derailment.	USGS (2009) (Australian Transport Safety Bureau, 2016)
Navarro County	USA		Derailment	Overtopping	Floodwaters overtopping rail embankment. Train drove onto failed section, derailing.	(CNN, 2015)
Stonehaven	Scotland, 2020	Debris flow	Derailment and three fatalities	Above slope flood	Floodwaters overtopped a drainage culvert, causing localised debris flow onto tracks. A train hit the landslide debris, causing derailment.	(Haines, 2020)

are recorded as overtopping (50%), soil softening due to saturation (31%) and internal erosion (19%) (Transportation Research Board et al., 2016).

Shear failures through embankment bodies, as opposed to underlying strata, have been recorded following basal floods and offset head floods. Above slope floods can cause debris flows, when flow channelisation occurs, and shallow translational failures when water runs down the sides of slopes. Debris flows also occur following offset head and overtopping floods, however these may form as latter stages of complex failures and do not necessarily represent initial failure type. All identified flood related failures in the UK occurred in rail assets. Due to the scarcity of recording internationally, quantification of landslide types most commonly caused by flooding, and asset types most vulnerable to flood related failure, was not possible.

Differences between types of flood-triggered failures categorised above and those identified in previous studies (e.g. Network Rail, 2016a, Transportation Research Board et al., 2016) are attributed to the size and consequence of failures associated with each flood type, and the likelihood of their recording in open literature. Small breaches caused by overtopping are less likely to be widely, accurately, and precisely recorded and reported



Figure 6: Illustrations of rail slopes subjected to flooding: a) embankment failure following offset head flooding in Acquivavia, Italy (October 2005); b) Embankment failure in Conwy, UK, following overtopping flood (March 2019); c) failure of embankment following train loading during basal flooding in Ohio, USA (June 2018); d) floodwater development above slope, causing infiltration in UK (a) reproduced from Polemio and Lollino (2011); b) and d) courtesy of Network Rail; c) courtesy of Sioux County Sherriff.

than large-scale individual, discrete failures which are directly consequential. The disparity between the prevalence of overtopping failures (25% of recorded events) found by our investigations, which combine data from public literature and news reports with agency information from Network Rail, and the study by Transportation Research Board et al. (2016) (where overtopping failures comprise 50% of recorded events) is likely due to the Transportation Research Board et al. (2016) study including a greater number of small-scale localised floods.

Table 3: Descriptions and occurrence of the four classified types of flood. The number of failures is recorded as the number of discrete flooding events which have been identified where failure has occurred. Multiple landslides may develop during a single flooding failure event.

Type of Flood	Mechanisms (<i>less common italicised</i>)	Materials	Case examples (Table 2)	Number of identified failure event	References
Offset head	Internal erosion Sliding Force Subsidence Rapid drawdown	Poorly sorted, Gap-graded	Acquaviva Knockmore	23 (36%)	Polemio and Lollino (2011), Transportation Research Board et al. (2016)
Overtopping	Surface erosion on lee-side of slope Ground saturation causing material weakening Rapid drawdown	Granular	Sayo River, Japan Conwy Valley	16 (25%)	Tsubaki et al. (2017) (Rail Engineer, 2016)
Basal flood development	Water egress prevented, increasing water level in slope. Scour during flows, causing toe erosion and over steepening.	Scour most prominent in granular materials	Barrow-upon-soar Doon, Iowa	13 (20%)	RAIB (2013a) (Independent, 2018)
Above slope	Surface erosion from water flowing down embankment batters. Saturation from ponded water, causing pore pressure increase. Internal erosion and piping development through slopes.	Erosion most prominent in granular	Baildon	12 (19%)	(RAIB, 2017b) Zhang et al. (2011).

Failures recorded in the literature show that following flooding there are often groups of smaller failures, rather than large discrete events. Examples include the Conwy Valley (Wales) failures in 2015 (Rail Engineer, 2016) and the failures in Sayo, Japan, in August 2009 (Tsubaki et al., 2017, Tsubaki et al., 2012) where fluvial floods caused embankment failures at multiple locations during individual flooding events. Full details of such failures are generally not recorded. There is limited recording of specific details of multiple failures which occur following widespread flooding in open literature. Therefore, failure reviews conducted by agencies (e.g. Transportation Research Board et al., 2016) are likely to include more inconsequential and small scale failures. Differences in recording practice between agencies and asset owners increase uncertainties in identifying how many failures have occurred in different locations. Two conclusions can be drawn from the lack of failures in road assets: i) when flooding does occur, the more modern road earthwork network is more resilient against flooding; ii) road embankments are constructed in less flood prone areas, or with better drainage, and road earthworks may be equally susceptible to failure as rail embankments if flooding does occur. As limited recorded information is available for flood events affecting transport infrastructure but not causing failure, it is not possible to differentiate between these two potential scenarios.

The lack of information about inconsequential floods inhibits development of accurate empirical models of slope degradation due to flooding and the effects of repeat flooding on slope properties. The lack of detailed failure descriptions in the UK creates difficulty in improving reactive maintenance practices, due to a poor understanding of the frequency of individual failure types and slope alterations caused by different flood types. Re-establishing embankment operability, rather than understanding failure process development, is the main focus of asset owners post-failure. We suggest that for slopes impacted by flooding, the following should be, where available, routinely recorded to allow for a developed understanding of how flooding alters slope behaviour: flood water depth, the relative height of flooding in comparison to slope height, duration of flood presence, flood flow direction. Additionally, in the event that a failure occurs, the initial failure mechanism and post failure geomorphology should be recorded.

2.5 Active processes in embankment slopes

Although properties of materials are often assumed to be static over the design life of any given structure, it has to be recognised that there are numerous processes ongoing in slopes that will impact on the in-service performance of any geotechnical asset. Such process involving weathering, strain softening (or hardening) or anything that alters the state of effective stress in the ground will result in changes in the slope forming materials. In many cases, these changes may be negligible. However, there are suites of processes that act in embankments which are deleterious to the performance of the asset over design timescales.

2.5.1 Internal erosion

Internal erosion develops in embankments during flooding when a hydraulic gradient is induced through a slope, causing seepage. Hydraulic gradients primarily develop due to offset head development across slopes. Internal erosion develops through embankment

Table 4: *Internal erosion processes.*

Process	Process description	Susceptible materials	References
Suffusion and suffosion	The movement of fines through the soil skeleton due to seepage forces without volume change (suffusion) due to skeleton contact or with change in volume suffosion) due to pore collapse.	Internally unstable soils - Gap graded and/or poorly sorted materials. Soils with angular grains are thought to be less susceptible to suffosion	Slangen and Fannin (2017), Wan and Fell (2008), Chang and Zhang (2013b)
Concentrated leakage erosion / Contact erosion	Entrainment of particles in existing soil pathways, e.g. voids, and contacts of coarse and fine grained materials, causes macropore development.	Existing pathways in soils	Polemio and Lollino (2011)
Piping / backwards erosion	Erosion initiates at the seepage discharge point on the downstream face of an embankment when seepage forces are strong enough to cause fluidization of material on the free surface. Erosion develops towards the upstream embankment face, forming macropores/pipes.	Most common in uniform sands. Less common in slopes with cohesive, low permeability, outer layers. Pipes may also develop where fine particle loss allows for concentrated flow and movement of larger particles.	Bonelli et al. (2007b), Beek et al. (2013)

substrata if the ground is sufficiently permeable in comparison to embankment permeability (Chang and Zhang, 2013b). Particle loss from internal erosion has the potential to cause changes in soil density, structure, strength, stiffness, differential settlement and the formation of in-slope permeability barriers. In extreme cases, internal erosion can sufficiently weaken slopes to cause failure. There are three main types of internal erosion (Table 4); suffusion/suffosion, concentrated leakage erosion and backwards erosion/piping development (Polemio and Lollino, 2011, USBR, 2015, Bonelli et al., 2007b).

Although an individual flood event may not cause slope failure or visible changes in slope morphology, it is essential to consider the lasting slope degradation which may be caused by a flood. Internal erosion has been shown to cause changes in soil strength behaviour (Figure 7), permeability, stiffness (Yang et al., 2018) and void ratio amongst other factors (e.g. Ke and Takahashi (2012), Chang and Zhang (2011), Ouyang and Takahashi (2015), Sato and Kuwano (2016)). Additionally, internal migration development from the collapse of pipes causes embankment subsidence (Polemio and Lollino, 2011, Bonelli et al., 2007b). Localised subsidence may also develop following weathering or dissolution of embankment materials (Ingles and Aitchison, 1969). If subsidence does not occur, material property change development may not be noted by infrastructure owners. Particle migration development is dependent on hydraulic gradient. Internal erosion testing is most commonly undertaken in flexible skinned triaxial apparatus (e.g. Chang and Zhang, 2011) and rigid wall permeameters (e.g. Ke and Takahashi, 2012). Bian et al. (2016) showed internal erosion can cause loss of track support in rail embankments, however slope-scale internal erosion studies are lacking in the wider literature.

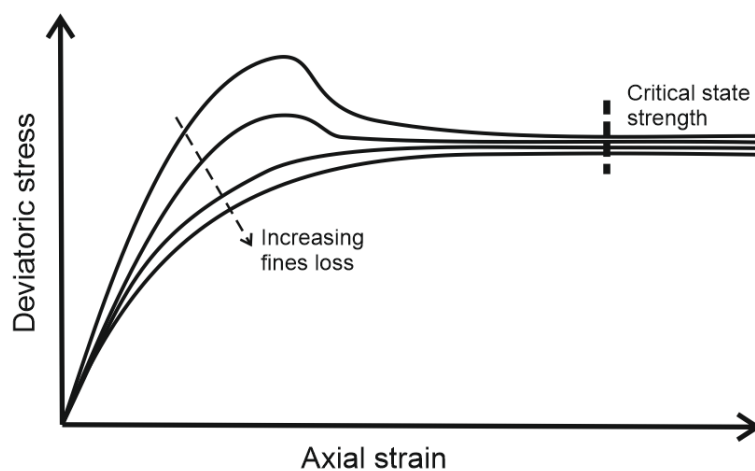


Figure 7: Schematic representation of strain development during shearing post-seepage and associated fines loss. Increased particle loss causes material softening and samples to fail without displaying peak strength. Critical state strength reduces between samples containing increasing amounts of fines loss.

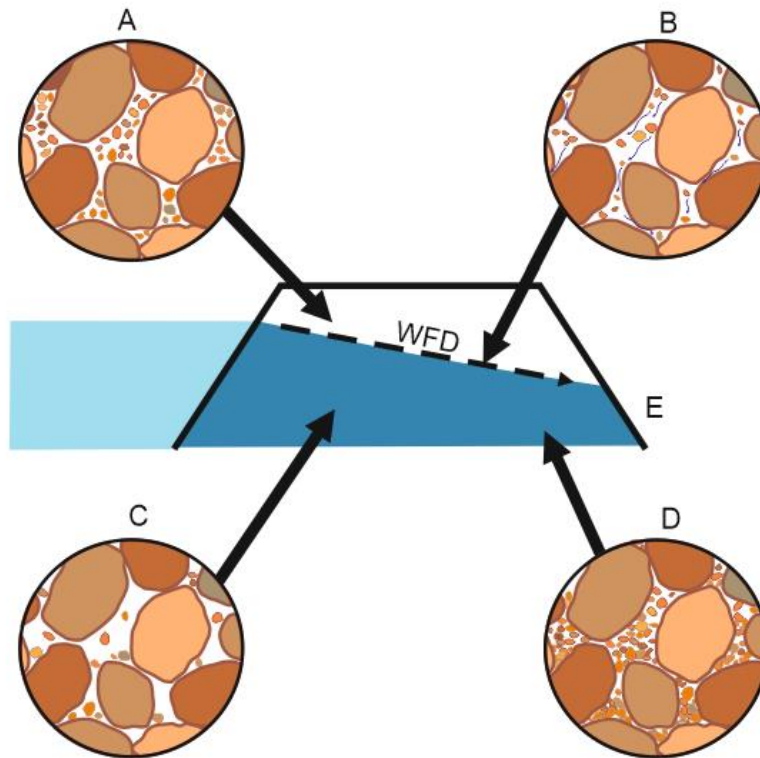


Figure 8: Soil structure development during seepage. A: Pre-flood soil skeleton. Fine particles are located in pore spaces and coat coarser grained particles. B: Water seepage drives particle motion through soil. C: Loss of fine particles forms an unstable soil skeleton. Higher strength and stiffness reductions and contraction behaviour development during shear are expected up-flow due to the loss of fine particles. D: Fines redeposition reduces pore space and creates a permeability barrier. Fine particles are concentrated at particle contacts. Strength increases may occur in zones where there is an accumulation of fine particles. WFD – water flow direction.

Materials are considered internally unstable if they are susceptible to internal erosion development. The primary factor that controls the vulnerability of a soil to internal erosion development is grain size distribution. Gap-graded and well-graded materials, with fines contents of 10-35% and 5-25% respectively, are considered as potentially internally unstable. Above these maximum values, fine particles become loaded, preventing migration (Chang and Zhang, 2013b). Internal stability of soils with fines contents between 10-35% for gap-graded soils and 5-25% for well-graded soils can be assessed using stability criteria, based on the relative distribution of coarse and fine particles (e.g. Wan and Fell, 2008, Chang and Zhang, 2013b, Kenney and Lau, 1985, Indraratna et al., 2011, Fannin and Moffat, 2006). Increased angularity and reduced roundness of soil particles reduces the susceptibility of a soil to internal erosion development, due to increased interparticle contact and resistance to particle rotation (Slangen and Fannin, 2017, Shire and O’Sullivan,

2013). Additionally, initial soil density (Ke and Takahashi, 2012) can alter the susceptibility of soil to internal erosion.

Experimental results from Chang and Zhang (2011), and Ouyang and Takahashi (2015) show that the removal of fines from upstream sections of soils produces a small reduction in the angle of shearing resistance of soil material. There is a potential increase strength on the downstream side of samples or embankments. However, the implication of this loss is that the soil may become highly contractive in shear, resulting in the collapse of the soil skeleton (Chang and Zhang, 2011). There may be reductions in the critical strength of material at constant volume shearing. The associated processes are outlined in Figure 8. Reductions in soil strength, and increases in contraction, are greater with larger amounts of fine particle removal. Redeposition of fine particles can cause localised increases in soil strength. Strength increases have been attributed to the re-distribution of fine particles into the contacts between coarse-grained particles. Prior to seepage, fine particles are located in void spaces and coat coarse-grained particles (Alramahi et al., 2010). In strength testing undertaken using triaxial apparatus, failure develops through the weakest part of samples. Particle loss is non-linear and causes vertical sample stratification due to particle movement with seepage (e.g. Chang and Zhang, 2011). The evidence suggests that contractile behaviour development due to internal erosion comes in tandem with reductions in material strength. Though this means slopes are more likely to fail, in the setting of rail embankments contractile behaviour may lead to the development of rough rides prior to full slope failures. This has the benefit of providing an early warning of slope instability, allowing for intervention before full slope failure. In contrast, failures which occur in dilative materials are likely to have less prior warning as movements will be sudden – however likely occur in materials with higher peak strength.

Fine particle removal from soils causes increases in soil permeability. However, localised changes in permeability develop when material is moved through soils. Laboratory testing undertaken by Xiao and Shwiyhat (2012) and Chang and Zhang (2011) has shown differential permeability change in samples following seepage. Pore spaces open in upstream zones due to particle removal, increasing sample permeability. Permeability reduces in areas of particle deposition downstream, clogging pore spaces and blocking flow pathways. In embankments, differential particle movement across slopes following flooding has the potential to form permeability gradients across slopes and permeability barriers in depositional zones. Pore-water pressure increases and slope strength reductions are expected in slopes with permeability barriers. Rapid drawdown is the recognised

phenomenon that occurs when a water body recedes more rapidly than pore pressures are able to dissipate (Morgenstern, 1963). This pore pressure change can combine with the rapid reduction of the toe weight applied by water. Destabilisation is generated by the onset of strong out-of-slope seepage forces and excess pore water pressure build up in the slope (Figure 9) (Rickard, 2009, Pinyol et al., 2008). Although rapid drawdown failures in granular embankments are rare, reductions in slope permeability following particle clogging will increase the likelihood of rapid drawdown development following flood recession.

In laboratory tests, shear wave velocity (V_s) reductions of up to 40% (Kelly et al., 2012) and 26% (Truong et al., 2010) have been observed following removal of fine particles via dissolution. Reductions in surface wave velocity of up to 30% at the point of failure caused by piping development have been reported in large scale (28 m long x 4 m high) physical

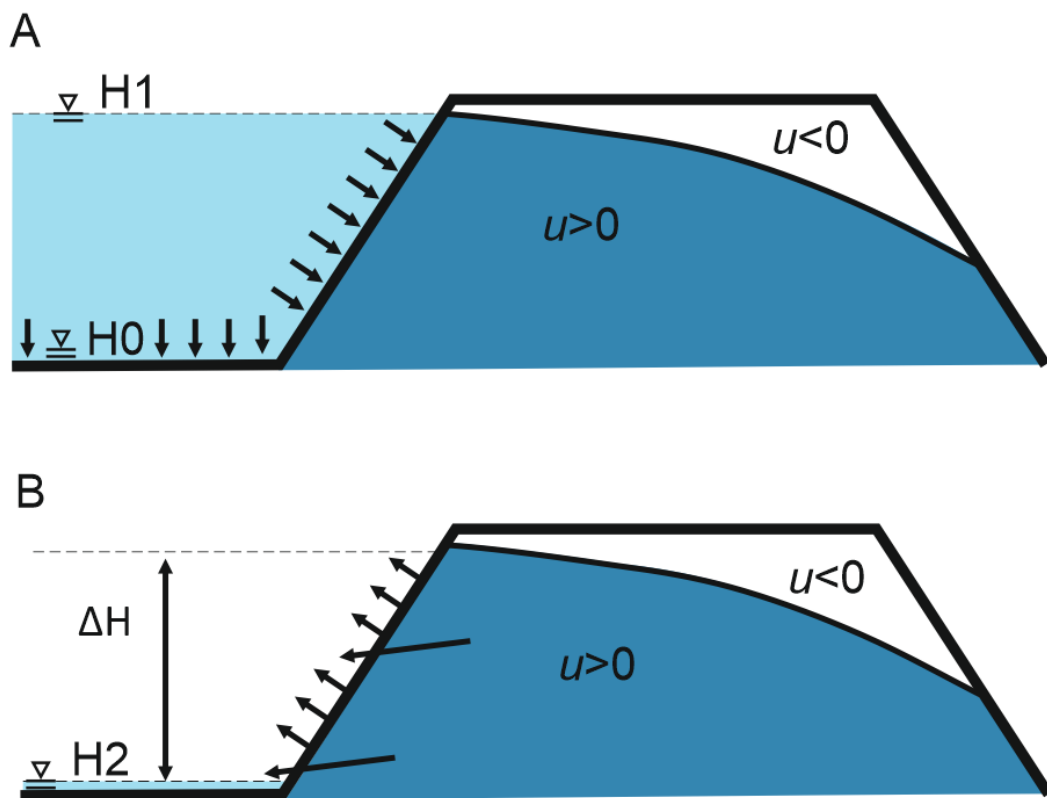


Figure 9: Rapid drawdown development (u = pore pressure).

9a) Stage 1: Flood head increase. Initial water level (H_0) raises due to flooding to H_1 , increasing slope saturation and pore pressures, decreasing slope stability. Floodwaters apply confining pressures and aid slope stability.

9b) Stage 2: Drawdown phase. Floodwaters recede to a new level (H_2) and the stabilising effect of floodwater weight is lost. In-slope pore water pressures remain high and strong out of slope seepage forces form. Slope stability decreases when pore water pressures dissipate more gradually than surface waters recede, potentially resulting in slope failure. Soils with higher permeability undergo more rapid u reductions, reducing drawdown effects.

model tests (Planès et al., 2016). Parekh (2016) also recorded reductions in V_s following internal erosion throughout a soil mass in a limited number of internal erosion tests. Reductions in acoustic velocity were attributed to reductions in sample stiffness and density, caused by the removal of fine particles and the loss of particle contact (Truong et al., 2010). Fine particle removal allows for a lack of constriction of load-bearing, coarser-grained particles forming the soil skeleton, allowing for increased material movement. Although laboratory testing has shown overall decreases in sample stiffness following internal erosion development, localised increases in stiffness may occur due to the redeposition of fine particles and increases in density. Additionally, the transport of fine particles during seepage causes re-distribution of fine particles to inter-particle contacts during seepage flow (Alramahi et al., 2010). This can cause localised increases in soil stiffness. Stiffness reductions have the potential to cause exacerbations of ground vibrations caused by train passage due to reductions in embankment critical velocity (Madshus and Kaynia, 2000). While internal erosion testing has not been undertaken on materials specific to infrastructure embankments, these processes are applicable to such materials.

2.5.2 Effects of live loading during flooding

Changes in shear modulus have multiple impacts on embankment function. During flooding, increased saturation and pore water pressures reduce soil shear modulus, increasing deformation and reducing V_s in embankments (Jiang et al., 2016). This is important because of the potential for excessive vibrations in embankments where V_s is low. This concept is known as critical velocity and describes the state where train speed exceeds the velocity of the Rayleigh wave (a type of surface wave) generated by the train. When this condition is reached it can result in excessive ground vibration and material weakening. This problem is generally associated with high speed rail and soft ground (e.g. low density materials such as peat), where Rayleigh wave velocities are as low as 40 m s^{-1} (Madshus and Kaynia, 2000).

Critical velocity exceedance has been recorded in railways over soft ground in Sweden, causing excessive vibrations and restrictions on rail speed (Madshus and Kaynia, 2000, Bian et al., 2016). Jiang et al. (2016), Bian et al. (2016), and Jiang et al. (2015) analysed the effects of high speed rail loading on slopes with varying water tables and flood conditions using a full-scale ballastless embankment model. Water tables at the top of the subgrade caused saturation, which reduced subgrade resonant frequency. In turn, this saturation reduced the critical velocity required to cause embankment degradation and failure,

resulting in failure during loading, mimicking high speed rail traffic, up to velocities of 360 km h⁻¹. Failure was attributed to internal erosion processes, including piping, developing in the outer embankment. Increased vibrations have been shown to increase the amount of fine particles removed from an embankment during a flood event (Jiang et al., 2015). Removal of fine particles may reduce material strength (Chang and Zhang, 2011); in turn the loss of support at the outer embankment section could cause increased loading by the central portion of the rail slab - potentially overcoming the reduced subgrade strength. These behaviours are different from the behaviour of ballasted tracks (Jian et al., 2014). Additionally, although loading from low-speed rail, which has velocities lower than 200 km hr⁻¹ (UIC, 2018), is less likely to exceed critical velocities, in areas of soft ground there is the potential for low speed rail to exceed critical velocity thresholds – more so following ground weakening by flooding.

During flood events, trains may continue to travel at speeds >40 m s⁻¹, suggesting that train speeds are not inherently reduced during flooding. For example, significant train damage was only prevented during flooding and embankment failure in Acquaviva, Italy (October 2005), during train transit due to the high train speed which allowed the train to move past the developing landslide (Ficarella, 2005). Additionally, during a derailment at Stonehaven, Scotland, in August 2020 the train was travelling close to the permitted line speed while flooding was present in the area (Haines, 2020). Consideration is generally not given to the performance of embankments when applying speed restrictions due to flooding; rail speed reductions during flooding are generally applied by operators to prevent train damage (RSSB, 2015). However, in environments where earthworks are vulnerable to flood inundation, we argue that slope instability should be considered as an important factor influencing the implementation of speed restrictions.

2.5.3 Scour

There is a significant body of research considering effects and consequences of scour on bridge foundations and other transportation structures (e.g. Lamb et al., 2019, Van Leeuwen and Lamb, 2014, Landers and Mueller, 1996), but earth embankment scour and breaching processes are poorly understood (Schmocker and Hager, 2012) and research is lacking in specific areas. Two distinct types of flood scour develop on embankments: i) overtopping, transverse flow causing cutdown into embankment crests (Tsubaki et al., 2017); ii) parallel flow, causing scour of individual embankment batters. Overtopping is a more commonly a cause of embankment slope failure (ASCE, 2011).

Table 5: *The effects of antecedent conditions on material preparation.*

Condition	Effect	References
Ground desiccation	Detachment of desiccated blocks increases scour Moisture content decrease increases soil strength Desiccation crack formation increases infiltration into slope	Thorne (1982), Lawler et al. (1997), Lawler (1991), Couper and Maddock (2001)
Freeze thaw weathering	Increased erosion due to loosening of upper soil layers which causes weakening and increases in permeability.	Papanicolaou et al. (2006), Lawler et al. (1997), Lawler (1991), Wolman (1959)
Rainfall intensity	Low intensity rainfall allows desiccation cracks to swell and close. High rainfall intensity exploits desiccation features.	Bell (2000), Lawler et al. (1997)
Prolonged flooding and rainfall	Weakening of bank materials due to increased water content.	Simon et al. (2000)
Vegetation	Increased cohesion and reductions in soil moisture content from roots increase stability. Dense, low level, vegetation is shown to decrease erosion rates. Increased scour can occur around trees and exposed root networks during flood flows.	Lawler et al. (1997), Papanicolaou et al. (2006), Abernethy and Rutherford (2000), Keller and Swanson (1979)

Parallel flow-induced scour is most commonly found in fluvial environments. Basal floods are rarely voluminous enough to cause damage beyond surface erosion and translational failures of near-surface materials. Scour-induced failures initiate as concentrated flow erosion, causing slope instability, followed by mass wasting of destabilised slopes (Qin et al., 2018). Localised features, such as fence posts, overhead rail power line stanchions, and trees, have been shown to cause increased scour and localised failure (Gilvear et al., 1994). River morphology and bank roughness also alter scour occurrence (Blanckaert, 2011, Blanckaert et al., 2012); scour induced failure has increased prevalence on the outside of meanders. Although particle entrainment occurs at a large scale when threshold flow velocities are exceeded, turbulence can cause entrainment when mean velocities are below threshold entrainment values (Niño et al., 2003, Thorne, 1982). Threshold entrainment velocities are variable for given grain sizes or lithologies due to variations in angularity, inter-particle forces, compaction and sorting (Buffington and Montgomery, 1997). Additionally, there is a poor understanding of cohesive sediment erosion during different flow conditions and of relationships between physical soil properties and erodibility (Thorne, 1982, Julian and Torres, 2006, Utley and Wynn, 2008).

Chapter 2

Susceptibility to entrainment is also dependent on antecedent conditions and the wetting-drying history of a slope (Table 5). These factors make it difficult to assess whether specific floods will develop near-bank shear stresses capable of causing localised or mass slope failures. However, flooding scour of slopes is important to consider due to toe scour and undercutting as potential causes of landslides (Freeborough et al., 2016, Perry, 1989). Parallel flow is more likely to cause scour and failure of slopes with granular faces, due to reduced erodibility of cohesive materials (Julian and Torres, 2006, Thorne, 1982, Hooke, 1980).

Overtopping-driven scour cuts down into embankments. In rail embankments, ballast removal forms an initial breach, leading to water downcutting into embankment bodies (Tsubaki et al., 2017). Breach development in granular embankment bodies has been shown to develop in two stages. Initially, a breach channel forms due to erosion, followed by mass wasting events to cause breach widening (Mohamed et al., 2002, Pickert et al., 2011). In embankments formed of cohesive and less erodible soils, breach formation develops through back cutting – i.e. a series of retrogressive ‘steps’ form on the downstream embankment face (Morris et al., 2009, Zhu et al., 2011). It is important to consider these differences in relation to duration and size of downcutting until crest height begins to reduce, and the stability of slopes remaining after flooding ceases. Embankment breaches caused by overtopping flow form a washout morphology, either in topping ballast or through full embankment height. Initial soil saturation (Al-Riffai and Nistor, 2013), compaction (Asghari Tabrizi et al., 2017) and grain size (Schmocker et al., 2014, Pickert et al., 2011) have influence on the erosion potential and speed of breach development for embankments constructed from non-cohesive materials. Breach development can lead to localised increases in embankment stability due to breached faces acting as a drainage pathway, increasing slope drainage and reducing pore water pressure in the slope forming materials (Pickert et al., 2011). No evidence has been identified of lasting slope weakening of un-scoured slope regions. Numerical modelling to identify the probability of slopes failing due to overtopping flow has been undertaken. Tsubaki et al. (2016) identified broad regions of rail embankments susceptible to failure, with the accuracy of their models limited by the precision and accuracy of localised topography mapping and knowledge of embankment properties and construction methods. Morris et al. (2009) and ASCE (2011) provided comprehensive reviews of earth embankment breaching processes. Ultimately, the role of scour in generating slope instability comes in terms of changing the state of effective stress. Most commonly, this results from a change to σ_3 , however overtopping scour potentially

changes σ_2 (σ_2 and σ_3 are the intermediate and minor principal stresses, respectively).

Given that the majority of 2D plane strain slope stability models do not consider σ_2 , this is potentially a change which is not factored into embankment analysis.

Antecedent conditions have a greater effect on the erodibility of cohesive soils as they are more prone to cracking following desiccation than granular soils (Bell, 2000). However, the impact of desiccation is dependent on the intensity and development of rainfall and flooding (Lawler et al., 1997, Bell, 2000). Longer periods between flood events allow accumulation of weathered material, which can increase permeability and create a system that is more susceptible to rapid erosion during flooding (Network Rail, 2018, Lawler, 1995); high river flows erode weakened material which has accumulated over the preceding period of low flow (Prosser et al., 2000). The duration since previous scour events can be used as a proxy for the amount of weakened weathered material and should be considered when assessing embankment stability and scour susceptibility. In the majority of infrastructure assets, slow weathering rates and active infrastructure management will prevent significant accumulation of weakened material between flooding events.

The influence of antecedent conditions is dependent on the type of failure and scale of slope being considered. Scour and shallow failures, such as debris flows and shallow translational slides of surface material layers, are less dependent on long term antecedent conditions than deep seated failures as smaller amounts of water are needed, and at shallower depths, in order to promote failure (Van Asch et al., 1999, Bunce, 2008). The lower permeability of fine grained and un-fissured soils makes them more responsive to longer durations of water input – from flooding and rainfall – as water is not able to drain as freely. Antecedent soil moisture content has also been considered as a correlating factor for landslide development (e.g. Posner and Georgakakos, 2015, Ponziani et al., 2012). Additionally, multi-peak and prolonged flood events have the potential to cause material weakening by increasing in-slope water levels and reducing effective stress; large flood events following preceding dry periods are less likely to cause erosion (Simon et al., 2000).

2.5.4 Sliding

The pushing effect caused by a flood behind embankments can have a destabilising effect, with the potential to cause basal sliding (Figure 10) (Morris et al., 2007). Although translational mass failures may occur, sliding movements are often minor, causing substrata damage. Affected ground may have increased permeability, increasing the chances of under-embankment seepage. The small scale of many geotechnical assets, such

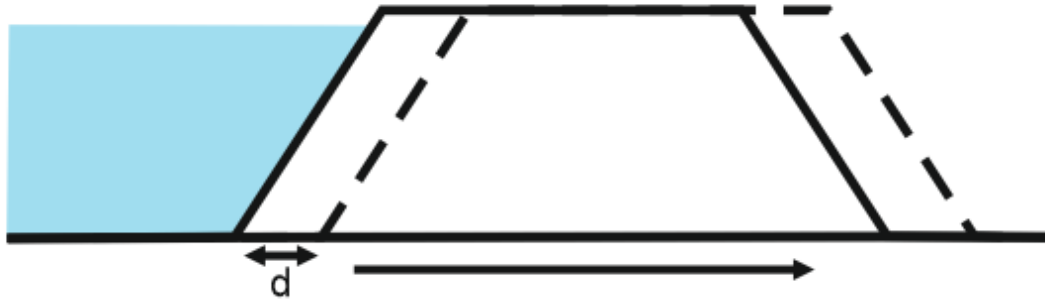


Figure 10: Basal sliding develops when the shearing force applied by floodwaters overcomes the resistance caused by embankment mass. Displacement, d , can cause increases in substrata permeability and flow pathway development due to rupturing. If embankments are founded on weak substrata, the sliding plane may develop below the embankment-substrata interface.

as rail and road embankments, does not allow sufficient head for basal sliding to develop solely from changes in pressures (Tsubaki et al., 2017).

2.5.5 Wetting front development

During prolonged floods there is adequate water supply to allow for infiltration rate to exceed infiltration capacity, allowing a saturated wetting front to develop to an extended depth - increasing pore water pressures and reducing or eradicating matric suctions. These strength reductions have been shown to cause translational landslides at depths of 1-2 m due to reductions in mobilised shear strength (Fourie, 1996, Simon et al., 2000, Zhang et al., 2011). Shallow failures often occur in cover material or weakened surface layers which overlie more competent slope core materials (Perry, 1989). Large-scale, deep-seated, instabilities are produced by longer periods of inundation and pore pressure development as more water is needed to cause slope destabilisation (Van Asch et al., 1999). Infiltration periods must be longer than the time taken for wetting fronts to reach a given depth (Pradel and Raad, 1993, Fourie, 1996, Zhang et al., 2011). In addition to failures caused by wider wetting front development, macropore presence can allow for rapid water infiltration to depth in soils, creating localised zones of high pore-water pressure and failure (Zhang et al., 2011). Permeability barrier development in slopes, caused by internal migration, can lead to pore water pressure development during flooding and increased chances of slope failure. A detailed review of rainfall and infiltration-based slope destabilisation is provided by Zhang et al. (2011).

Failures associated with rapid drawdown are most commonly observed in reservoirs where water levels are rapidly reduced following semi-permanent high water levels (Alonso and Pinyol, 2016, Pinyol et al., 2008, Johansson and Edeskär, 2014). Flooding has been shown to

cause rapid drawdown after sustained or prolonged flood events (Rickard, 2009, USBR, 2015) or following periods of prolonged rainfall (USBR, 2015). Rapid drawdown failures have been recorded in transport embankments (Transportation Safety Board, 1997). In addition, river embankment landslides often occur during the falling limb of flood hydrographs (Thorne, 1982, Lawler et al., 1997, Simon et al., 2000) suggesting the influence of rapid drawdown effects, despite minor changes in flood head. Localised partial failures, for example caused by macropore fluid input or low levels of rapid drawdown, have the potential to develop into larger scale ‘retrogressive failures’ due to localised stress redistributions (Jia et al., 2009).

While susceptibility to rapid drawdown is identified as a ‘common fault’ and regular cause of failure in flood embankments (Bettess and Reeve, 1995), there is limited rapid drawdown research on small-scale scenarios (Alonso and Pinyol, 2016, Pinyol et al., 2008). The scarcity of detailed embankment failure analyses is partly due to a lack of case examples (Dyer, 2004). There has been some consideration of smaller slopes using physical models (e.g. Jia et al., 2009); river embankment and flood defence monitoring scenarios, which show rapid drawdown as a cause of slope failure with as little as 1m of head loss (Rinaldi et al., 2004, Liang et al., 2015, Dyer, 2004); and numerical models (e.g. Morgenstern, 1963). However, this physical model work has only considered situations where initial water levels are at slope crests - not the rate of water level rise, height of water level rise or duration of standing water presence. Sensitivity analysis undertaken by Franczyk et al. (2016) indicated that flood stage, duration of high water and the rate of fall of water are important to consider during rapid drawdown analysis. Furthermore, in many scenarios, floodwaters will not reach the full height of embankments – and when they do, overtopping processes often dominate failures. Seepage from rapid drawdown can cause development of internal erosion due to strong out of slope seepage forces (Li et al., 2019), causing lasting slope weakening. Flooding is most likely to cause rapid drawdown related instability following prolonged flood events, and instability is more likely following repeated hydraulic loading cycles (Jadid et al., 2020). Given the potential for flood events to cause rapid drawdown failure, if there is the possibility of floodwater forming next to a slope for a prolonged period, the effects of rapid drawdown should be considered during stability analysis.

2.5.6 Discussion of process effects

Menan Hasnayn et al. (2017) showed that flooding significantly reduced the long-term quality of rail subgrade materials, with settlement increasing significantly following flooding

due to soil suction reduction. However, only one flood cycle was used during their testing programme. Without maintenance it is possible that additional destabilisation events could further reduce material quality. This is important for embankments which are repeatedly loaded over a wet season or multiple seasons without visible degradation. The importance of the dynamic nature of railway assets has also been highlighted by results from physical models. Take and Bolton (2004), for example, identified the role of cyclic loading in the development of pore pressures. Physical and numerical models have also been used to investigate the role of vegetation on embankment stability. Reductions in pore water pressures and associated stability increases have been found to be caused by the presence of mature trees; tree removal causes wetting of embankments and decreases in slope stability (Briggs et al., 2014). Generally, physical and process models have been used to understand the fundamental processes occurring in slopes subject to flood processes. These models have not been used as a design tool, and there is little evidence of their use in a forensic capacity.

Lasting strength reductions, such as the loss of peak material strengths, mean that future flooding and live loading events may act on pre-weakened structures and unexpectedly cause failure. This is of additional concern when there is not visible evidence of material property alteration, for example following suffusion. It is likely that any material property changes and internal erosion derived subsidence will be spatially variable across an embankment site due to directional seepage gradients. Furthermore, subsidence caused by internal erosion during flooding can lead to embankment overtopping, creating larger-scale failures (Wan and Fell, 2008). Grain structure collapse, due to vibrations from vehicle passage with time, may cause subsidence in flooding-altered materials. We are not aware of any completed monitoring programmes which assess the condition change of transport embankments which have been subjected to flooding.

Failures which develop in rail embankments often begin with ballast breaching, developing into lee-slope erosion. Tsubaki et al. (2017) suggested overtopping failures should be considered the primary failure cause in low embankments, as sufficient head to drive other processes is not able to develop. This is consistent with failure causes recorded by the Transportation Research Board et al. (2016), but not with all failures we identified in this study (Table 3). The trigger of flood induced landslide failures is likely to be pore pressure increase from wetting front development. Without other destabilising factors, including internal erosion and scour, failure likelihood is reduced.

2.6 Conclusions and further research

We classified four major types of flooding impacting rail embankments: offset head, overtopping, basal and above slope floods. These can cause slope failure during individual flood events and progressive weakening during repeat flooding. Rapid flood recession can also lead to failure via rapid drawdown. Slope destabilisation and failure are triggered by scour, live loading and pore water pressure increases. Internal erosion was identified as a major cause of lasting slope and substrata weakening. Overtopping floods most frequently cause failure. However, failures from all flood types have been identified. Factor of safety changes in slopes that have been affected by flooding and not failed should be considered, as should the effects of live loading events. A fully developed understanding of flood effects on slopes and the development of empirical flood-failure relationships is limited by the poor recording of embankment flooding data. Further work is needed to understand how alteration following repeat flooding events develops. Challenges related to producing such understanding are partially caused by the dearth of records of floods which occur on embankments but do not cause failure, and also by the inconsistent phraseology adopted in record keeping. Specifically, the term 'washout' should be reserved for describing post-failure slope morphology and not used to describe failure processes. There is a well-developed understanding of the ground response to rainfall and the landslide activation processes that develop on infrastructure embankments. However, there are important elements for which there is considerably less information. The most significant of these knowledge gaps relate to:

- 1) Dynamic interactions which develop between slopes, flooding and traffic loading;
- 2) The effects of repeat flood events and how materials' properties change over the design life of an asset;
- 3) The intensity of flooding, based on flood height and duration, required to cause slope failure.

Developing a wider understanding of infrastructure failures, including failure types, would allow for identification of how different processes, including flooding, cause failures and also may inform prevention methods which could be utilised. For this to be achieved, geotechnical assessment of landslides in infrastructure should be undertaken prior to clearance and reconstruction. Additional research is needed to assess the lasting impacts of flooding on embankment slopes and this may also help us understand appropriate mitigation measures. The redistribution of fines and how it affects strength, permeability

and shear modulus are all potentially significant knowledge gaps for the rail industry especially with the growth of high speed rail globally. Although strength and property degradation have been analysed to some extent in material samples, and potential mechanisms for lasting reductions in the strength of slope forming materials have been identified, it remains unclear what the quantifiable impacts on material degradation of such effects may be during repeat flooding events acting on a slope. Developing an understanding of degradation processes will help to inform the identification of floods which cause failure of embankments, and how these differ with varying initial conditions, lithologies, construction methods, loading histories and loading scenarios. Better understanding of the processes causing failure would allow for identification of the size and type of floods which are likely to cause failure for a given site. Although flood events have been shown to cause failure without traffic loading, the effect of dynamic traffic loads on embankments during floods is an area with little research. Further numerical and physical modelling work is needed to assess traffic speeds which may cause failure during flood conditions for ballasted and ballastless tracks with differing substrate lithologies and structures. Research into flood-destabilisation analysis should also develop process models which predict whether forecasted flood events will cause failure and the potential operational restrictions which may be needed to prevent failure. For this to be undertaken accurately, a detailed understanding of flood destabilisation processes will be needed.

2.7 References

- ABERNETHY, B. & RUTHERFURD, I. D. 2000. The effect of riparian tree roots on the mass-stability of riverbanks. *Earth Surface Processes and Landforms*, 25, 921-937.
- AL-RIFFAI, M. & NISTOR, I. Influence of seepage on the erodibility of overtopped noncohesive embankments. Proceedings of the 21st Canadian Hyrotechnical Conference, 2013.
- ALONSO, E. E. & PINYOL, N. M. 2016. Numerical analysis of rapid drawdown: Applications in real cases. *Water Science and Engineering*, 9, 175-182.
- ALRAMAHI, B., ALSHIBLI, K. A. & FRATTA, D. 2010. Effect of Fine Particle Migration on the Small-Strain Stiffness of Unsaturated Soils. *Journal of Geotechnical and Geoenvironmental Engineering*, 136, 620-628.
- ASCE 2011. Earthen Embankment Breaching. *Journal of Hydraulic Engineering*, 137, 1549-1564.
- ASGHARI TABRIZI, A., ELALFY, E., ELKHOLY, M., CHAUDHRY, M. H. & IMRAN, J. 2017. Effects of compaction on embankment breach due to overtopping. *Journal of Hydraulic Research*, 55, 236-247.
- BEEK, V. V. A. N., BEZUIJEN, A. & SELLMEIJER, H. 2013. Backward Erosion Piping. *Erosion in Geomechanics Applied to Dams and Levees*. John Wiley And Sons, Inc.
- BELL, F. G. 2000. *Engineering properties of soils and rocks*, Oxford, Elsevier.
- BENNETT, E. H. 1884. Court of Appeal. Whalley v. Lancashire and Yorkshire Railway Co. *The American Law Register (1852-1891)*, 32, 633-640.

- BERNATEK-JAKIEL, A. & POESEN, J. 2018. Subsurface erosion by soil piping: significance and research needs. *Earth-Science Reviews*, 185, 1107-1128.
- BETTESS, R. & REEVE, C. E. 1995. Performance of River Flood Embankments. Ministry of Agriculture, Fisheries and Food.
- BGS. 2012. *Rest and Be thankful (A83) landslide, 2012* [Online]. Available: <http://www.bgs.ac.uk/landslides/RABTAug2012.html> [Accessed 2018 May 2018].
- BIAN, X., JIANG, H. & CHEN, Y. 2016. Preliminary Testing on High-speed Railway Substructure Due to Water Level Changes. *Procedia Engineering*, 143, 769-781.
- BISANTINO, T., PIZZO, V., POLEMIO, M. & GENTILE, F. 2016. Analysis of the flooding event of October 22-23, 2005 in a small basin in the province of Bari (Southern Italy). *Journal of Agricultural Engineering*, 47, 8.
- BLANCKAERT, K. 2011. Hydrodynamic processes in sharp meander bends and their morphological implications. *Journal of Geophysical Research: Earth Surface*, 116, F01003.
- BLANCKAERT, K., DUARTE, A., CHEN, Q. & SCHLEISS, A. J. 2012. Flow processes near smooth and rough (concave) outer banks in curved open channels. *Journal of Geophysical Research: Earth Surface*, 117, F04020.
- BONELLI, S., MAROT, D., TERNAT, F. & BENAHMED, N. 2007b. Assessment of the risk of internal erosion of water retaining structures: dams, dykes and levees. Intermediate Report of the European Working Group of ICOLD Deutsches TalksperrenKomitee.
- BRIGGS, K., SMETHURST, J. & POWRIE, W. 2014. Modelling the Influence of Tree Removal on Embankment Slope Hydrology. 2014 2014 Cham. Springer International Publishing, 241-246.
- BRIGGS, K. M., LOVERIDGE, F. A. & GLENDINNING, S. 2016. Failures in transport infrastructure embankments. *Engineering Geology*, 219, 107-117.
- BROWN, A., CHAPMAN, A., JACOBS, U., GOSDEN, J. & SMITH, F. The influence of infrastructure embankments on the consequences of dam failure. 15th British Dams Society Conference, Warwick, 2008.
- BUFFINGTON, J. M. & MONTGOMERY, D. R. 1997. A systematic analysis of eight decades of incipient motion studies, with special reference to gravel-bedded rivers. *Water Resources Research*, 33, 1993-2029.
- BUNCE, C. M. 2008. *Risk estimation for railways exposed to landslides*. PhD thesis, University of Alberta.
- CHANG, D. & ZHANG, L. 2011. A Stress-controlled Erosion Apparatus for Studying Internal Erosion in Soils. *Geotechnical Testing Journal*, 34, 579-589.
- CHANG, D. S. & ZHANG, L. M. 2013b. Extended internal stability criteria for soils under seepage. *Soils and Foundations*, 53, 569-583.
- COUPER, P. R. & MADDOCK, I. P. 2001. Subaerial river bank erosion processes and their interaction with other bank erosion mechanisms on the River Arrow, Warwickshire, UK. *Earth Surface Processes and Landforms*, 26, 631-646.
- CRUDEN, D. M. & VARNES, D. J. 1996. Landslide Types and Processes. *Special Report* Transportation Research Board, National Academy of Sciences.
- DAWSON, R., GOSLING, S., CHAPMAN, L., DARCH, G., WATSON, G., POWRIE, W., BELL, S., PAULSON, K., HUGHES, P. & WOOD, R. 2017. UK Climate Change Risk Assessment 2017 Evidence Report: Chapter 4, Infrastructure.
- DYER, M. 2004. Performance of flood embankments in England and Wales. *Proceedings of the Institution of Civil Engineers - Water Management*, 157, 177-186.
- FANNIN, R. J. & MOFFAT, R. 2006. Observations on internal stability of cohesionless soils. *Géotechnique*, 56, 497-500.
- FEDERAL RAILROAD ADMINISTRATION 2001-2010. Railroad Safety Statistics Annual Report. Federal Railroad Administration Office of Safety Analysis.

- FICARELLA, I. 2005. *Il day after di una catastrofe 'Bari risparmiata grazie alla cava'* [Online]. Available: <https://ricerca.repubblica.it/repubblica/archivio/repubblica/2005/10/25/il-day-after-di-una-catastrofe-bari.html> [Accessed 2020].
- FIELD, C. B., BARROS, V., STOCKER, T. F. & DAHE, Q. 2012. *Managing the risks of extreme events and disasters to advance climate change adaptation: special report of the intergovernmental panel on climate change*, Cambridge University Press.
- FOURIE, A. B. 1996. PREDICTING RAINFALL-INDUCED SLOPE INSTABILITY. *Proceedings of the Institution of Civil Engineers - Geotechnical Engineering*, 119, 211-218.
- FRANCZYK, A., DWORNIK, M. & LEŚNIAK, A. 2016. Numerical modelling of the impact of flood wave cyclicity on the stability of levees. *E3S Web Conf.*, 7, 03022.
- FREEBOROUGH, K. A., DIAZ DOCE, D., LETHBRIDGE, R., JESSAMY, G., DASHWOOD, C., PENNINGTON, C. & REEVES, H. J. 2016. Landslide hazard assessment for National Rail Network. *Procedia Engineering*, 143, 689-696.
- GIBSON, A. D., CULSHAW, M. G., DASHWOOD, C. & PENNINGTON, C. V. L. 2013. Landslide management in the UK—the problem of managing hazards in a ‘low-risk’ environment. *Landslides*, 10, 599-610.
- GILVEAR, D., DAVIES, J. & WINTERBOTTOM, S. 1994. Mechanisms of floodbank failure during large flood events on the rivers Tay and Earn, Scotland. *Quarterly Journal of Engineering Geology and Hydrogeology*, 27, 319-332.
- HAINES, A. 2020. Interim report to the Secretary of State for Transport following the derailment at Carmont, near Stonehaven. Network Rail.
- HONG, L., OUYANG, M., PEETA, S., HE, X. & YAN, Y. 2015. Vulnerability assessment and mitigation for the Chinese railway system under floods. *Reliability Engineering & System Safety*, 137, 58-68.
- HOOKE, J. M. 1980. Magnitude and distribution of rates of river bank erosion. *Earth Surface Processes*, 5, 143-157.
- HUNGR, O., LEROUEIL, S. & PICARELLI, L. 2014. The Varnes classification of landslide types, an update. *Landslides*, 11, 167-194.
- INDEPENDENT. 2018. *Crude oil pours into river after train derails in US* [Online]. Available: <https://www.independent.co.uk/news/world/americas/oil-spill-train-derailment-water-contamination-iowa-rock-river-doon-a8413626.html> [Accessed 2019].
- INDRARATNA, B., NGUYEN, V. T. & RUJIKIATKAMJORN, C. 2011. Assessing the potential of internal erosion and suffusion of granular soils. *Journal of Geotechnical and Geoenvironmental Engineering*, 137, 550-554.
- INGLES, O. & AITCHISON, G. 1969. *Soil-water disequilibrium as a cause of subsidence in natural soils and earth embankments*, Division of Soil Mechanics, CSIRO.
- JABOYEDOFF, M. & LABIOUSE, V. 2011. Preliminary estimation of rockfall runout zones. *Natural Hazards Earth System Sciences*, 11, 819–828.
- JADID, R., MONTOYA, B. M., BENNETT, V. & GABR, M. A. 2020. Effect of repeated rise and fall of water level on seepage-induced deformation and related stability analysis of Princeville levee. *Engineering Geology*, 266, 105458.
- JIA, G. W., ZHAN, T. L. T., CHEN, Y. M. & FREDLUND, D. G. 2009. Performance of a large-scale slope model subjected to rising and lowering water levels. *Engineering Geology*, 106, 92-103.
- JIAN, W., XU, Q., YANG, H. & WANG, F. 2014. Mechanism and failure process of Qianjiangping landslide in the Three Gorges Reservoir, China. *Environmental Earth Sciences*, 72, 2999-3013.
- JIANG, H., BIAN, X., CHEN, Y. & HAN, J. 2015. Impact of Water Level Rise on the Behaviors of Railway Track Structure and Substructure. *Transportation Research Record: Journal of the Transportation Research Board*, 2476, 15-22.

- JIANG, H., BIAN, X., JIANG, J. & CHEN, Y. 2016. Dynamic performance of high-speed railway formation with the rise of water table. *Engineering Geology*, 206, 18-32.
- JOHANSSON, J. & EDESKÄR, T. 2014. Effects of external water-level fluctuations on slope stability. *The Electronic journal of geotechnical engineering*, 19, 2437-2463.
- JULIAN, J. P. & TORRES, R. 2006. Hydraulic erosion of cohesive riverbanks. *Geomorphology*, 76, 193-206.
- KE, L. & TAKAHASHI, A. 2012. Strength reduction of cohesionless soil due to internal erosion induced by one-dimensional upward seepage flow. *Soils and Foundations*, 52, 698-711.
- KELLER, E. A. & SWANSON, F. J. 1979. Effects of large organic material on channel form and fluvial processes. *Earth Surface Processes*, 4, 361-380.
- KELLERMANN, P., SCHÖNBERGER, C. & THIEKEN, A. H. 2016. Large-scale application of the flood damage model RAILway Infrastructure Loss (RAIL). *Nat. Hazards Earth Syst. Sci.*, 16, 2357-2371.
- KELLY, D., MCDUGALL, J. & BARRETO, D. Effect of particle loss on soil behaviour. Proc., 6th Int. Conf. on Scour and Erosion, Publications SHF, Paris, 2012. 639-646.
- KENNEY, T. & LAU, D. 1985. Internal stability of granular filters. *Canadian Geotechnical Journal*, 22, 215-225.
- KOKS, E. E., ROZENBERG, J., ZORN, C., TARIVERDI, M., VOUSDOKAS, M., FRASER, S. A., HALL, J. W. & HALLEGATTE, S. 2019. A global multi-hazard risk analysis of road and railway infrastructure assets. *Nature Communications*, 10, 2677.
- LAMB, R., GARSIDE, P., PANT, R. & HALL, J. W. 2019. A Probabilistic Model of the Economic Risk to Britain's Railway Network from Bridge Scour During Floods. *Risk Analysis*, 39, 2457-2478.
- LANDERS, M. N. & MUELLER, D. S. 1996. Channel scour at bridges in the United States.
- LATO, M. J., DIEDERICHS, M. S., HUTCHINSON, D. J. & HARRAP, R. 2012. Evaluating roadside rockmasses for rockfall hazards using LiDAR data: optimizing data collection and processing protocols. *Natural Hazards*, 60, 831-864.
- LAWLER, D. 1995. The Impact of Scale on the Processes of Channel-Side Sediment Supply: A Conceptual Model. *IAHS Publications-Series of Proceedings and Reports*.
- LAWLER, D., COUPERTHWAITTE, J., BULL, L. & HARRIS, N. 1997. Bank erosion events and processes in the Upper Severn basin. *Hydrology and Earth System Sciences Discussions*, 1, 523-534.
- LAWLER, D. M. 1991. A New Technique for the Automatic Monitoring of Erosion and Deposition Rates. *Water Resources Research*, 27, 2125-2128.
- LEHTONEN, V. J., MEEHAN, C. L., LÄNSIVAARA, T. T. & MANSIKKAMÄKI, J. N. 2015. Full-scale embankment failure test under simulated train loading. *Géotechnique*, 65, 961-974.
- LI, Z., YE, W., MARENCE, M. & BRICKER, J. D. 2019. Unsteady seepage behavior of an earthfill dam during drought-flood cycles. *Geosciences*, 9, 17.
- LIANG, C., JAKSA, M. B., OSTENDORF, B. & KUO, Y. L. 2015. Influence of river level fluctuations and climate on riverbank stability. *Computers and Geotechnics*, 63, 83-98.
- LOVERIDGE, F. A., SPINK, T. W., O'BRIEN, A. S., BRIGGS, K. M. & BUTCHER, D. 2010. The impact of climate and climate change on infrastructure slopes, with particular reference to southern England. *Quarterly Journal of Engineering Geology and Hydrogeology*, 43, 461-472.
- MADSHUS, C. & KAYNIA, A. M. 2000. High-speed railway lines on soft ground: Dynamic behaviour at critical train speed. *Journal of Sound and Vibration*, 231, 689-701.
- MARTO, A. & SOON, T. 2011. Short Review on Liquefaction Susceptibility. *International Journal of Engineering Research and Applications*, 2, 2115-2119.

- MENAN HASNAYN, M., JOHN MCCARTER, W., WOODWARD, P. K., CONNOLLY, D. P. & STARRS, G. 2017. Railway subgrade performance during flooding and the post-flooding (recovery) period. *Transportation Geotechnics*, 11, 57-68.
- MOHAMED, M. A., SAMUELS, P., MORRIS, M. & GHATAORA, G. Improving the accuracy of prediction of breach formation through embankment dams and flood embankments. *River Flow*, 2002.
- MORGENSTERN, N. 1963. Stability Charts for Earth Slopes During Rapid Drawdown. *Géotechnique*, 13, 121-131.
- MORRIS, M., DYER, M. & SMITH, P. 2007. Management of Flood Embankments. A good practice review. Department for Environment, Food and Rural Affairs.
- MORRIS, M., HASSAN, M., KORTENHAUS, A. & VISSER, P. 2009. Breaching Processes: A state of the art review. *FLOOD site Project Report, T06-06-03*.
- MOSSA, M. 2007. The floods in Bari: What history should have taught. *Journal of Hydraulic Research*, 45, 579-594.
- NELDER, L. M., GUNN, D. & REEVES, H. 2006. Investigation of the geotechnical properties of a Victorian Railway Embankment. *Proc. 1st Int. Conf. Railway Foundations, 2006* 2006. 34-47.
- NETWORK RAIL 2016a. Task 106: JBA Overtopping (Earthworks at Flood Risk).
- NETWORK RAIL 2018. Earthworks Asset Policy January 2018. Network Rail Infrastructure Ltd.
- NIÑO, Y., LOPEZ, F. & GARCIA, M. 2003. Threshold for particle entrainment into suspension. *Sedimentology*, 50, 247-263.
- NOGUCHI, T., FUJII, T. J. J. R. & REVIEW, T. 2000. Minimizing the effect of natural disasters. *Japan Railway & Transport Review*, 23, 52-59.
- OUYANG, M. & TAKAHASHI, A. 2015. Influence of initial fines content on fabric of soils subjected to internal erosion. *Canadian Geotechnical Journal*, 53, 299-313.
- PAPANICOLAOU, A., DEY, S., RINALDI, M. & MAZUMDAR, A. 2006. Research issues for riverine bank stability analysis in the 21st century. *Iowa City*.
- PAREKH, M. L. 2016. *Advancing internal erosion monitoring using seismic methods in field and laboratory studies*. Colorado School of Mines. Arthur Lakes Library.
- PERRY, J. 1989. A survey of slope condition on motorway earthworks in England and Wales. Wokingham, Berkshire United Kingdom Transport and Road Research Laboratory (TRRL).
- PERRY, J., PEDLEY, M., BRADY, K. & REID, M. 2003. Briefing: Embankment cuttings: condition appraisal and remedial treatment. *Proceedings of the Institution of Civil Engineers - Geotechnical Engineering*, 156, 171-175.
- PICKERT, G., WEITBRECHT, V. & BIEBERSTEIN, A. 2011. Breaching of overtopped river embankments controlled by apparent cohesion. *Journal of Hydraulic Research*, 49, 143-156.
- PINYOL, N. M., ALONSO, E. E. & OLIVELLA, S. 2008. Rapid drawdown in slopes and embankments. *Water Resources Research*, 44, W00D03.
- PLANÈS, T., MOONEY, M. A., RITTGERS, J. B. R., PAREKH, M. L., BEHM, M. & SNIEDER, R. 2016. Time-lapse monitoring of internal erosion in earthen dams and levees using ambient seismic noise. *Géotechnique*, 66, 301-312.
- POLEMIO, M. & LOLLINO, P. 2011. Failure of infrastructure embankments induced by flooding and seepage: a neglected source of hazard. *Natural Hazards and Earth System Sciences*, 11, 3383.
- PONZIANI, F., PANDOLFO, C., STELLUTI, M., BERNI, N., BROCCA, L. & MORAMARCO, T. 2012. Assessment of rainfall thresholds and soil moisture modeling for operational hydrogeological risk prevention in the Umbria region (central Italy). *Landslides*, 9, 229-237.

- POSNER, A. J. & GEORGAKAKOS, K. P. 2015. Soil moisture and precipitation thresholds for real-time landslide prediction in El Salvador. *Landslides*, 12, 1179-1196.
- PRADEL, D. & RAAD, G. 1993. Effect of Permeability on Surficial Stability of Homogeneous Slopes. *Journal of Geotechnical Engineering*, 119, 315-332.
- PROSSER, I. P., HUGHES, A. O. & RUTHERFURD, I. D. 2000. Bank erosion of an incised upland channel by subaerial processes: Tasmania, Australia. 25, 1085-1101.
- QIN, C., ZHENG, F., WELLS, R. R., XU, X., WANG, B. & ZHONG, K. 2018. A laboratory study of channel sidewall expansion in upland concentrated flows. *Soil and Tillage Research*, 178, 22-31.
- RAIB 2013a. Derailment of a freight train at Barrow upon Soar, Leicestershire. *Rail Accident Report*. Rail Accident Investigation Branch, Department for Transport.
- RAIB 2013c. Train ran onto a washed-out embankment near Knockmore, Northern Ireland 28 June 2012. Rail Accident Investigation Branch, Department for Transport.
- RAIB 2017b. Report 03/2017: Trains passed over washed out track at Baildon.
- RAIL ENGINEER. 2012. *Managing Earthworks* [Online]. Rail Engineer. Available: <https://www.railengineer.uk/2012/03/16/managing-earthworks/4/> [Accessed 2018].
- RAIL ENGINEER. 2016. *The Conwy Crisis* [Online]. Available: <https://www.railengineer.uk/2016/03/18/conwy-crisis/> [Accessed 2018].
- RAILRODDER. 2011. *CN Ruel Subdivision Roadbed Failure* [Online]. Available: <https://www.youtube.com/watch?v=Pb3pZIK6UFQ> [Accessed].
- RICKARD, C. E. 2009. Floodwalls and flood embankments. *The Fluvial Design Guide*. Environment Agency.
- RIDLEY, A., MCGINNITY, B. & VAUGHAN, P. 2004. Role of pore water pressures in embankment stability. *Proceedings of the Institution of Civil Engineers - Geotechnical Engineering*, 157, 193-198.
- RINALDI, M., CASAGLI, N., DAPPORTO, S. & GARGINI, A. 2004. Monitoring and modelling of pore water pressure changes and riverbank stability during flow events. *Earth Surface Processes and Landforms*, 29, 237-254.
- ROSSETTI, M. A. 2007. Analysis of weather events on US Railroads.
- SATO, M. & KUWANO, R. 2016. Effects of internal erosion on mechanical properties evaluated by triaxial compression tests. *Japanese Geotechnical Society Special Publication*, 2, 1056-1059.
- SCHMOCKER, L., FRANK, P.-J. & HAGER, W. H. 2014. Overtopping dike-breach: effect of grain size distribution. *Journal of Hydraulic Research*, 52, 559-564.
- SCHMOCKER, L. & HAGER, W. H. 2012. Plane dike-breach due to overtopping: effects of sediment, dike height and discharge. *Journal of Hydraulic Research*, 50, 576-586.
- SHIRE, T. & O'SULLIVAN, C. 2013. Micromechanical assessment of an internal stability criterion. *Acta Geotechnica*, 8, 81-90.
- SIMON, A., CURINI, A., DARBY, S. E. & LANGENDOEN, E. J. 2000. Bank and near-bank processes in an incised channel. *Geomorphology*, 35, 193-217.
- SLANGEN, P. & FANNIN, R. J. 2017. The role of particle type on suffusion and suffosion. *Géotechnique Letters*, 7, 6-10.
- TAKE, W. A. & BOLTON, M. D. 2004. Identification of seasonal slope behaviour mechanisms from centrifuge case studies. *Advances in geotechnical engineering: The Skempton conference*.
- THORNE, C. 1982. Processes and mechanisms of river bank erosion. In: R. D. HEY, J. C. B. C. R. T. (ed.) *Gravel-bed rivers*. Wiley.
- TRANSPORTATION RESEARCH BOARD, NATIONAL ACADEMIES OF SCIENCES, E. & MEDICINE 2016. *Minimizing Roadway Embankment Damage from Flooding*, Washington, DC, The National Academies Press.

- TRANSPORTATION SAFETY BOARD 1997. Interim railway safety recommendations concerning the identification and detection of railway roadbed instability. TSB Recommendation# 05/97. *Transportation Safety Board, Quebec, Canada.*
- TRUONG, Q. H., EOM, Y. H. & LEE, J. S. 2010. Stiffness characteristics of soluble mixtures. *Géotechnique*, 60, 293-297.
- TSUBAKI, R., BRICKER, J. D., ICHII, K. & KAWAHARA, Y. 2016. Development of fragility curves for railway embankment and ballast scour due to overtopping flood flow. *Natural Hazards and Earth Systems Sciences*, 16, 2455-2472.
- TSUBAKI, R., KAWAHARA, Y., SAYAMA, T. & FUJITA, I. 2012. Analysis of Hydraulic and Geomorphic Conditions Causing Railway Embankment Breach due to Inundation Flow. *Journal of hydroscience and hydraulic engineering*, 30, 87-99.
- TSUBAKI, R., KAWAHARA, Y. & UEDA, Y. 2017. Railway embankment failure due to ballast layer breach caused by inundation flows. *Natural Hazards*, 87, 717-738.
- UIC. 2018. *The definition of High Speed Rail* [Online]. Available: https://www.uic.org/com/uic-e-news/596-high-speed/article/the-definition-of-high-speed-rail?page=thickbox_enews [Accessed June 2018 2018].
- USACE 2000. Design and construction of levees. *Engineering and Design*. U.S. Army Corps of Engineers.
- USBR 2015. Best Practices in Dam And Levee Safety Risk Analysis. 4 ed.
- UTLEY, B. C. & WYNN, T. M. 2008. Cohesive Soil Erosion: Theory and Practice. *World Environmental and Water Resources Congress 2008*.
- VAN ASCH, T. W. J., BUMA, J. & VAN BEEK, L. P. H. 1999. A view on some hydrological triggering systems in landslides. *Geomorphology*, 30, 25-32.
- VAN LEEUWEN, Z. & LAMB, R. 2014. Flood and scour related failure incidents at railway assets between 1846 and 2013. *Railway Safety & Standards Board*.
- WAN, C. F. & FELL, R. 2008. Assessing the Potential of Internal Instability and Suffusion in Embankment Dams and Their Foundations. *Journal of Geotechnical and Geoenvironmental Engineering*, 134, 401-407.
- WINTER, M., MACGREGOR, F. & SHACKMAN, L. 2005. *Scottish road network landslides study*.
- WINTER, M. G., SHEARER, B., PALMER, D., PEELING, D., HARMER, C. & SHARPE, J. 2016. The Economic Impact of Landslides and Floods on the Road Network. *Procedia Engineering*, 143, 1425-1434.
- WOLMAN, M. G. 1959. Factors influencing erosion of a cohesive river bank. *American Journal of Science*, 257, 204-216.
- XIAO, M. & SHWIYHAT, N. 2012. Experimental Investigation of the Effects of Suffusion on Physical and Geomechanic Characteristics of Sandy Soils. *Geotechnical Testing Journal*, 35, 890-900.
- YANG, Y., KUWANO, R. & XU, C. 2018. A preliminary study on the piping erosion of soils using glucose dissolution method. *Environmental Earth Sciences*, 77, 31.
- ZHANG, L. L., ZHANG, J., ZHANG, L. M. & TANG, W. H. 2011. Stability analysis of rainfall-induced slope failure: a review. *Proceedings of the Institution of Civil Engineers - Geotechnical Engineering*, 164, 299-316.
- ZHU, Y., VISSER, P. J., VRIJLING, J. K. & WANG, G. 2011. Experimental investigation on breaching of embankments. *Science China Technological Sciences*, 54, 148-155.

Chapter 3

Measuring the effects of internal erosion on granular soils used in transport embankments

Chapter summary

The flooding of embankments used for rail and other infrastructure has the potential to cause lasting weakening of slopes via the movement of fine particles induced by seepage. In laboratory experiments, internal erosion was induced in granular soil samples, with properties consistent with those used to construct transportation embankments, to assess how particle migration through, and out of, samples caused shear wave velocity, strength, stiffness and permeability changes. Shear wave velocity changes, measured using horizontal bender elements, of up to 19% were observed following fine particle removal of up to 1% of initial sample mass. Shear wave velocity change was found to be a proxy for the development of permeability change during seepage-induced particle migration. Median measured permeability changes were +5% and -34% for samples containing 15% and 30% fines, respectively. The largest directly observed permeability and stiffness changes occurred during the initial stages of seepage. Negative correlation was observed between mass of material removed from samples and peak friction angle. Following seepage, soils displayed a dual stiffness behaviour. Stiffness and strength changes were attributed to redistribution of fine particles and opening of pore spaces. My results have implications for the monitoring of earthworks affected by flooding and seepage as the associated redistribution of fine particles may lead to large changes in slope properties.

3.1 Introduction

Failures from flooding in transport embankments are relatively common (e.g. Tsubaki et al., 2017, Polemio and Lollino, 2011) and have been associated with several fatalities (Mossa, 2007). Although transport embankments are often not designed for flood retention, flooding behind linear infrastructure embankments is relatively common as they can act as barriers to runoff along the base of slopes and across alluvial floodplains (e.g. Mossa, 2007, Bennett, 1884). With increases in extreme rainfall events and flooding expected under climate change (Field et al., 2012, Tabari, 2020), understanding the impact of flooding on slope-forming material properties and increasing the resilience of embankments to flooding will become ever more important, especially in areas with ageing infrastructure. Seepage can affect the strength of the material and therefore has an impact on mid to long term embankment stability (Sato and Kuwano, 2016). In addition to changes in strength and soil behaviour, characteristic changes in shear modulus throughout an embankment may create localised instability during dynamic loading applied by high-speed trains on rail infrastructure. Given the global expansion of high-speed rail it is important to understand processes which can impact on embankment stability over the whole asset lifespan.

Flooding can cause enhanced head development along an embankment which may, in turn, enhance seepage flow through the embankment. Seepage-driven destabilisation can cause failure through sliding or internal erosion-driven weakening (Polemio and Lollino, 2011), which highlights the importance of this process for infrastructure engineering. There is a dearth of studies which consider geotechnical hazards associated with seepage processes during and after flood events around embankments. Embankment failure may not occur in the immediate aftermath of the flood, as seepage-driven processes may cause weakening which allows for a later trigger (Johnston et al., 2021). Therefore, it is important to be able to measure changes in slope strength, stiffness and behaviour following flooding, particularly where internal erosion processes have occurred due to seepage processes. There are three main types of internal erosion; i) suffosion and suffusion, ii) soil piping and backwards erosion and iii) contact erosion (Bonelli et al., 2007a, USBR, 2015, ICOLD, 2017). Here I focus primarily on suffosion and suffusion, which are the erosion of fine soil particles due to seepage flow with and without volume change respectively (Fannin and Slangen, 2014), due to their ability to alter embankment properties without visible deterioration. Materials susceptible to suffosion and suffusion are said to be internally unstable. Following the removal (washing out) of fine particles, changes have been shown to occur in soil

properties including strength, void ratio, small strain stiffness and permeability (Kelly et al., 2012, Chang and Zhang, 2011, Parekh, 2016).

Internal stability criteria can be used to assess the internal stability of soils based on grain size distribution (Kenney and Lau, 1985, Kenney and Lau, 1986). Commonly used stability criteria are shown in Table 6. For soils or earthworks to be susceptible to suffosion or suffusion, fine-grained particles must fit through pore spaces in the matrix between coarse-grained particles. The proportion of fine-grained particles must also be low enough so that fines do not fill voids between coarse-grained particles, causing fines loading and preventing particle migration (Wan and Fell, 2008). Chang and Zhang (2013b) showed that approximately 20% and 35% fines content is needed for fines loading to develop in well graded and gap graded soils, respectively.

Internal erosion can develop when a hydraulic gradient is induced across a sample, or slope, with strong enough seepage forces to cause fine particle movement (Wan and Fell, 2008). Triaxial tests (e.g. Chang and Zhang, 2011, Sato and Kuwano, 2016, Luo et al., 2013) show peak sample strength reduction and development of contractional soil behaviour during shearing following particle loss from internal erosion. In addition, initial increases in sample permeability have been shown to occur as washout is initiated, with subsequent reductions in permeability when clogging of basal soil pores develops (Chang and Zhang, 2011, Ke and Takahashi, 2014, Fannin and Moffat, 2006). Greater losses of fine particles occur in the upstream areas of samples. Migrations of material have been measured in simplified embankment models, with sizes in the range of decimetres (Horikoshi and Takahashi, 2015), and are further discussed in Chapter 4.

Surface wave monitoring of model embankments in laboratory settings has indicated deterioration of embankment properties subject to seepage, with surface wave velocity reductions of up to 30% attributed to pore pressure increases and effective stress reductions (Planès et al., 2016). In field environments, seasonal variations in surface wave velocity have been measured and attributed to variations in embankment saturation and pore water pressure (Gunn et al., 2018, Bergamo et al., 2016). In addition to short-term moisture controlled variations in soil properties, it is important to understand permanent changes in material properties - for example caused by seepage-induced particle movement, which likely causes deterioration of earthworks (Sato and Kuwano, 2016). Studies assessing changes in soil stiffness and shear wave velocity (V_s) following particle loss are limited. In laboratory-scale testing, fine particle presence in pore fluids has been shown

to increase sample stiffness due to deposition of fine particles onto the contacts of larger grains in soils composed of glass beads (Alramahi et al., 2010). Bender elements have been used to identify changes in V_s following changes in localised effective stress (Parekh, 2016) and following dissolution of salt fines, used as a proxy for internal erosion, with V_s reductions of up to 26% (Truong et al., 2010) and 40% (Kelly et al., 2012) recorded. However, I could not identify studies assessing changes in V_s in samples undergoing internal erosion.

I sought to test how strength, shear wave velocity and permeability change in granular embankment materials subject to seepage forces, for two fines contents typical of those used in embankment construction. In particular, I sought to determine the degree to which internal fine particle movement led to changes in sample shear wave velocity, stiffness, permeability and strength, due to the removal of fines from pore spaces, fines redeposition and downstream accumulation, and the removal of fines from samples. I aimed to assess whether these processes were enhanced for larger hydraulic heads and for longer time periods under flood simulation. To support my assessment I measured changes in sample V_s , using micro seismic techniques during seepage flow, and mass of outflow sediment.

Table 6: *Instability criteria to identify soils susceptible to internal instability.*

D_x – size of sieve which passes $x\%$ of a soil sample by weight. D_x^f refers to the fine soil fraction, D_x^c refers to the coarse soil fraction. f is the weight fraction finer than grain size d . h is the weight fraction between grain size d and $4d$, where d is specified by the user.

Author	Criteria
Kezdi (1979)	$D_{15}^c/D_{85}^f < 4$, material is considered internally stable.
Kenney and Lau (1985)	$h/f > 1.3$ = stable $h/f < 1.3$, transition $h/f < 1$, unstable
Wan and Fell (2008)	Transition zone: $15/\log(D_{20}/D_5) < 22$ and $30/\log(D_{90}/D_{60}) > 80$ Unstable zone: $15/\log(D_{20}/D_5) < 15$ and $30/\log(D_{90}/D_{60}) > 110$ Unsuitable for fines <15%
Indraratna et al. (2011)	Stable zone: $D_{35}^c/d_{85}^f < 0.73$ Transition zone: $0.73 \leq D_{35}^c/d_{85}^f \leq 0.82$ Unstable zone: $D_{35}^c/d_{85}^f > 0.82$

3.2 Methods

Internal erosion testing was undertaken on soils with fines contents of 15% and 30% in a flexible skinned triaxial cell. Strength, permeability, shear wave velocity and particle loss were monitored during testing. V_s measurement was undertaken using horizontal bender elements; horizontal bender elements were used because vertical elements would only show V_s change following complete particle removal. Horizontal elements measure change perpendicular to the flow direction, which allowed for monitoring of material movement during seepage. Shear waves were used in this context as they allowed for near continuous monitoring of change. Additionally, the same parameters control surface waves and shear waves. Therefore, there is a direct link to two of the geophysical methods used for embankment monitoring (Gunn, 2011). Eight seepage tests with shearing were undertaken for each fines content. A control test which was saturated, consolidated and sheared but without seepage was undertaken to assess whether any material washout occurred due to the testing procedure was undertaken on a sample containing 30% fines. A control test was not possible on a sample containing 15% fines due to facility closure at the onset of COVID-19 restrictions. Test duration (d) and hydraulic gradient (i) were varied between tests. Though high resolution shear wave velocity measurements allowed for a large number of results to be produced per test, individual test replicates were not undertaken due to testing limitations and material loss caused by the implementation of COVID-19 shutdowns and restrictions.

3.2.1 Sample material

Sample soils were comprised of sub-rounded to angular sands and silt. Sieving was used to split bulk samples, comprising sharp sands and river sands, into 12 bands between 43 μm and 2 mm; material from individual grain size bands were then combined to create a soil with the desired grain size distribution (Figure 11). Soil mixes were formed to meet UIC 719R – the specification for high-speed rail embankment material given by the International Union of Railways – which stipulates $Cu > 6$ (Eq. 3.1) and $1 < Cc < 3$ (Eq. 3.2):

$$Cu = D_{60}/D_{10} \quad [3.1]$$

$$Cc = D_{30}^2 / (D_{10}D_{60}) \quad [3.2]$$

where Cu is the coefficient of uniformity, Cc is the coefficient of curvature, and D_x is the grainsize at a given grainsize distribution percentile. Soil ‘fines’ were categorised as those $< 125 \mu\text{m}$. Fines contents of 15% and 30% were used for the two sets of test undertaken (Figure 11). Though the soils used in these samples meet the UIC 719R

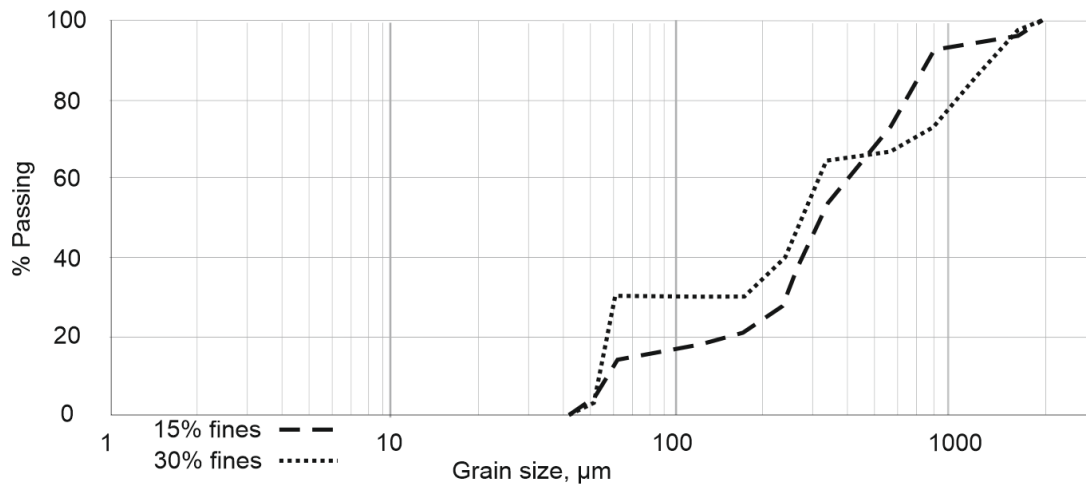


Figure 11: Grain size distribution for the soils tested.

specification for high-speed rail embankment materials for modern rail embankments, they are likely more representative of older embankments and those designed without the specific purposes of water retention. More modern slopes, and those designed to withstand water impoundment, are likely to be constructed of materials with smaller gap rations.

Samples were prepared via moist compaction, using de-aired water, to prevent fines separation during preparation (Kwan and Mohtar, 2018b). Samples were prepared inside a metal split mould and tested inside a flexible latex membrane. Seven lifts with decreasing thicknesses were used during the construction of individual samples to prevent overcompaction. During each lift, a funnel was used to minimise the drop height of soil to prevent soil segregation. Samples were 100 mm high x 50 mm diameter. Sample material was well graded and categorised as unstable by the stability indices listed in Table 6. Initial sample properties and test conditions are shown in Table 7.

3.2.2 Testing apparatus

Testing was undertaken in a Wykehan Farrance triaxial system modified to include horizontally-orientated bender elements (e.g. Pennington et al., 1997), vertical fluid flow through samples and washout collection (Figure 12). De-aired water flow through samples was controlled by a pump with volume accuracy of $\pm 1 \text{ mm}^3$, pressure accuracy $\pm 1 \text{ kPa}$ and a volume of 200 cm^3 . The basal platen consisted of a 1 mm thick steel mesh with 1 mm circular holes and 2 mm pitch to allow for fines migration from the base of samples while supporting the coarse fraction of the sample. Tubing around the outside of the mesh prevented the blocking of mesh pores and base densification. A porous plate was used at

the top of the sample to ensure water distribution from the flow input across the sample area.

Bender elements were inserted horizontally across the middle of the samples after the samples were removed from the mould. Liquid latex sealant was used to ensure sample isolation from confining pressure water. Bender elements had an 11 mm wide, 4 mm deep and 2 mm high intrusion into samples. Wave travel times were measured using the peak to peak time domain method to remove error associated with picking first arrivals caused by the near-field effect and P wave reflections (Yamashita et al., 2007). The distance between elements was taken as the tip to tip distance, after Yamashita et al. (2009). Wave frequencies of 30 or 50 kHz were used during tests on samples with 15% fines content and

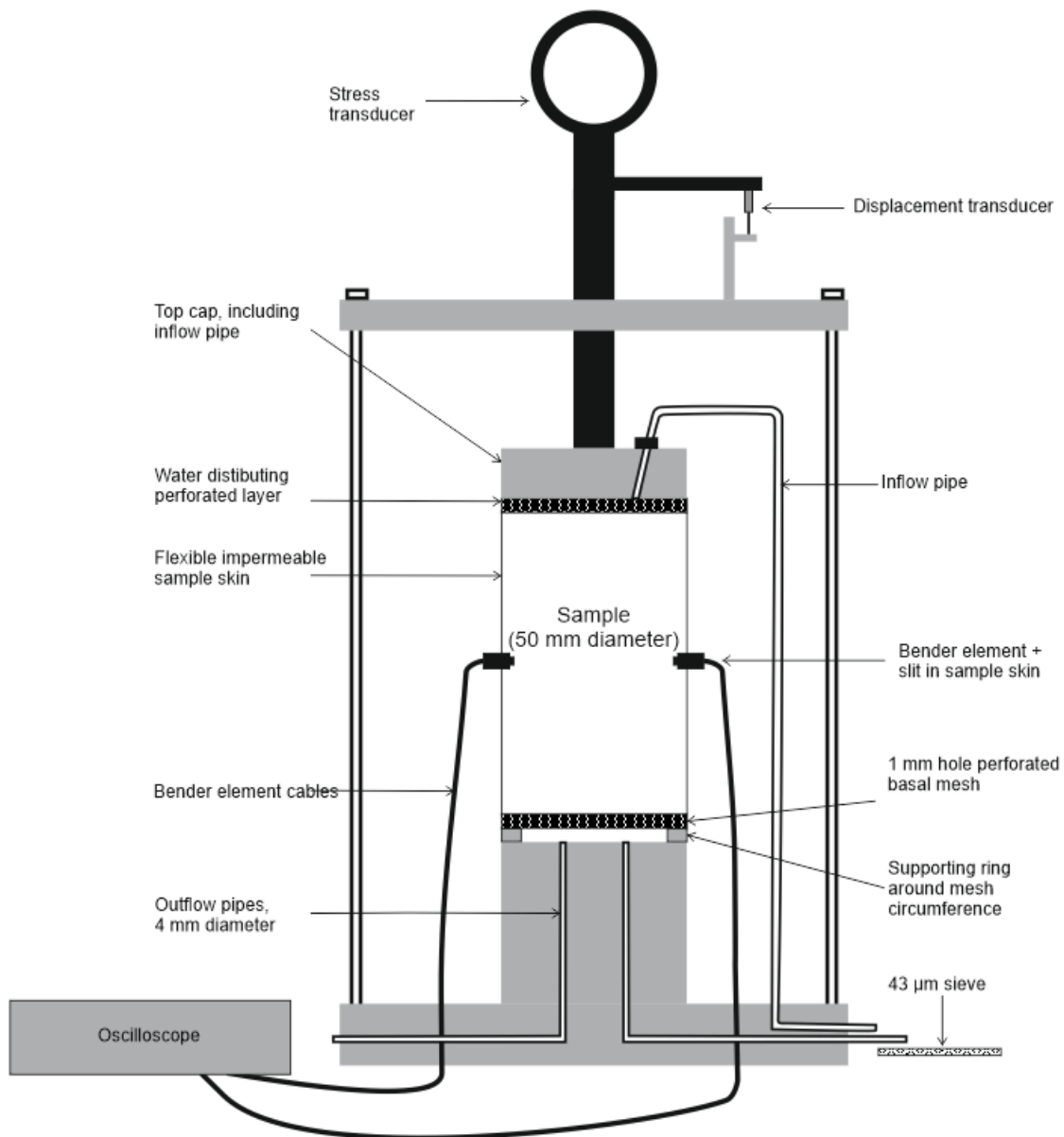


Figure 12: Experimental apparatus for bender element and seepage modified triaxial tests.

10 or 15 kHz during tests with 30% fines content; lower frequency waves were utilised in samples where the initial higher frequency wave did not produce an observable output signal. Input signals were sent as individual sinewave pulses, with readings taken every 2-3 minutes during seepage. Signal stacking was utilised for all readings to reduce signal noise. Shear wave velocities measured using the bender elements had an error of +/- 1.0 m s⁻¹.

3.2.3 Seepage and shearing

Samples underwent isotropic consolidation and saturation prior to the initiation of seepage. Back pressure was gradually increased to minimise particle disturbance prior to seepage. Minimum B-values of 0.86 were achieved during saturation; though below the recommended B-value of 0.95 in BS EN 17892:2018, further increases in confining pressure did not produce increases in B value so saturation was considered complete (British Standards Institution, 2018). Back pressure was not maintained during seepage, as the base of samples was open to atmospheric pressure; back pressure was re-imposed prior to shearing. Due to the necessity of altering pore water pressures and confining pressures during testing, effective stress changes developed within samples during the testing process. Increases in effective stress after seepage through samples was complete had the potential to alter, through compression, the soil structure created by particle movement. While increases in pore water pressures are likely to occur on embankment slopes in field environments, significant changes in confining pressure are unlikely to occur. Therefore,

Table 7: Initial sample properties and test properties.

Test	Density, g cm ⁻³	Initial K , m s ⁻¹ x10 ⁻⁷	Hydraulic gradient	Seepage duration, mins	Water seepage volume, cm ³	Confining pressure during shear, kPa	Back pressure during shear, kPa
15A	1.74	37.9	3	299	1110	60	30
15B	1.62	34.9	3	100	1200	66	27
15C	1.73	11.3	3	348	120	60	25
15D	1.68	35.8	3	132	157	66	30
15E	1.68	44.4	3	88	90	66	39
15F	1.89	45.1	5	91	1200	62	22
15G	1.76	4.6	5	267	860	60	27
15H	1.72	21.6	3	184	2240	52	30
30A	1.80	339	3	100	1260	56	40
30B	1.81	21.0	5	106	1390	56	40
30C	1.84	39.5	5	206	1800	70	48
30D	1.81	37.1	3	200	1400	70	30
30E	1.82	12.6	3	51	30	67	30
30F	1.83	230	5	50	650	70	50
30G	1.53	-	-	0	0.00	70	30

material compression is less likely to occur in full scale embankments. Sample saturation was maintained by ensuring the outflow pipe was above the height of the sample base. Pressurised seepage flow was downwards using de-aired tap water. Seepage was non-continuous and 200 cm³ of water flowed through samples before a period of zero flow while the pump was refilled. The refilling period lasted approximately eight minutes. Recorded seepage times do not include the refilling period. During refilling, cell drainage taps were closed to maintain sample condition.

As washout mass could only be recorded at the end of tests, seepage durations were chosen to provide a range of endpoints, to identify potential relationships between seepage and washout mass. Permeability (in this case saturated hydraulic conductivity, K) and V_s measurements were taken throughout the duration of seepage. Permeability was calculated by measuring the volume of water entering samples over time for a fixed hydraulic gradient. Hydraulic gradients (i) of 3 or 5 were used for each test during seepage; values were chosen in order to accelerate particle movement, reducing seepage duration. Wave frequency was kept constant throughout individual tests to prevent alteration of V_s readings. Seepage outflow was passed through a 43 μm sieve to collect particles washed out of samples and the testing cell. Material washed out of samples which remained in the testing cell was collected at the end of shearing, preventing the continuous monitoring of washed out material mass. Following seepage, consolidated drained shearing was undertaken.

p' values were chosen to represent conditions found in embankments, with values primarily representative of materials in the upper 3-6m of embankment bodies. As pressures were maintained by individual pumps and on-cell pressure transducers, rather than a centralised computer system, coupled with the relatively low pressures used in the tests, maintaining exact pressures between tests was not possible. During the drained shear stage, loading was rate controlled. The loading rate specified on the load frame ensured pore water pressure increases did not occur within samples and did not exceed 10% per hour, as specified by BS EN ISO 17892-9:2018 (British Standards Institution, 2018). Additional seepage tests without shearing were undertaken in samples containing fluorescein powder on the top surface to track seepage front development. Fluorescein testing was undertaken on samples with both 15% and 30% fine material content. In samples containing fluorescein, seepage was halted when fluorescent water first exited samples, to prevent dilution of fluorescein to unobservable levels, and these samples were not sheared to avoid disrupting seepage pathways.

3.3 Results

Table 8: Soil property changes comparing before and after seepage tests. For V_s and K change, negative values indicate a reduction after seepage. % changes are relative to initial values.

Test	V_s change, m s^{-1}	V_s change, %	K change, $\text{m s}^{-1} \times 10^{-7}$	K change, %	Loss, $\text{g m}^{-2}\text{L}^{-1}$	Total loss, g	Total loss, %
15A	-4.6	-1.5	-26.4	-70	0.610	1.33	0.41
15B	0.10	0.0	2.5	7	0.292	0.69	0.21
15C	0	0.0	-10.2	-90	0.696	0.16	0.05
15D	-0.7	-0.2	3.5	10	0.303	0.94	0.28
15E	21	6.7	-1.7	-4	0.328	0.64	0.19
15F	2.7	0.6	1.1	3	0.480	1.13	0.33
15G	-16	-3.7	0.4	9	0.384	0.65	0.19
15H	-4.6	-1.2	3.0	14	0.424	1.86	0.53
30A	18	7.5	87.1	26	0.980	2.43	0.68
30B	-3.2	-1.6	25.1	120	0.519	1.38	0.40
30C	44	19.0	-17.7	-45	0.293	1.02	0.29
30D	-1.5	-0.7	-24.1	-65	0.431	1.15	0.32
30E	-2.0	-0.9	-11.2	-88	12.684	0.81	0.24
30F	-1.1	-0.5	-12.1	-5	0.545	0.72	0.21
30G	-	-	-	-	-	0.03	0.01
30H	6.7	4.7	-151	-34	0.312	1.72	0.52

3.3.1 Particle removal

Particle loss and volume of seepage water were very strongly positively correlated in samples containing 15% fines content, ($r = 0.878$, $p < 0.001$) and moderately positively correlated in samples containing 30% fines content ($r = 0.626$, $p < 0.1$) (Figure 13a).

Discoloured water, which became paler with additional seepage, was observed exiting the sample cell throughout the duration of the tests, providing qualitative evidence that material migration was prevalent throughout the majority of test durations. In all tests, the majority (>60%) of particles that were washed out from samples were <125 μm with 67% or more of particles <210 μm . The removal of mass per cross sectional sample area per litre of seepage water ($\text{g m}^{-2}\text{L}^{-1}$) reduced with increasing seepage volume (Table 8). A total of 0.03 g (<0.01%) of material was removed from sample 30G, which underwent the saturation and shearing processes but not seepage, representing the washout mass loss caused by non-seepage processes during testing (Table 8). Seepage duration and washed out material mass were not correlated (Figure 13b). Sample volume change was not observed during seepage, as additional confining pressure water was not added to the cell and confining pressure drops were not observed during seepage.

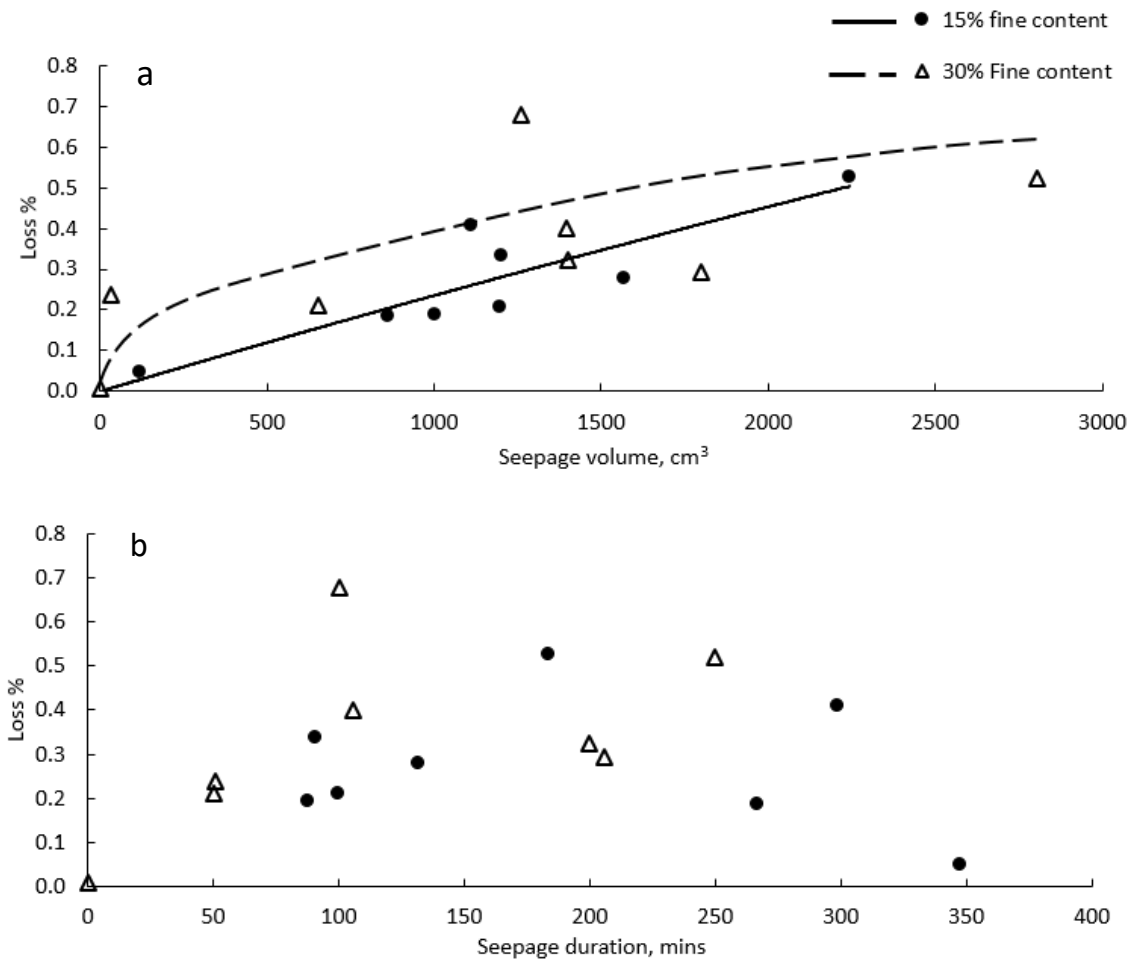


Figure 13: Mass of material washed out from samples during seepage recorded against a) seepage volume and b) seepage duration.

3.3.2 Shear wave velocity change

Total V_s change in samples over the full duration of tests was not related to particle mass loss or seepage volume. During seepage, V_s change predominantly occurred over short time periods during the initial phases of seepage (Figure 14). More gradual V_s changes were observed during prolonged seepage. V_s variations frequently occurred in tandem with changes in sample permeability (Figure 14). For the full test durations, V_s increases and decreases greater than measurement error were recorded in five and eight tests, for 15% and 30 % fines respectively (Table 8; Figure 14). Maximum recorded V_s change was 19% of initial V_s . More commonly, full test duration V_s changes ranged from 0-7% of initial V_s (Table 8) with similar magnitudes found for tests with 15% and 30% fines content.

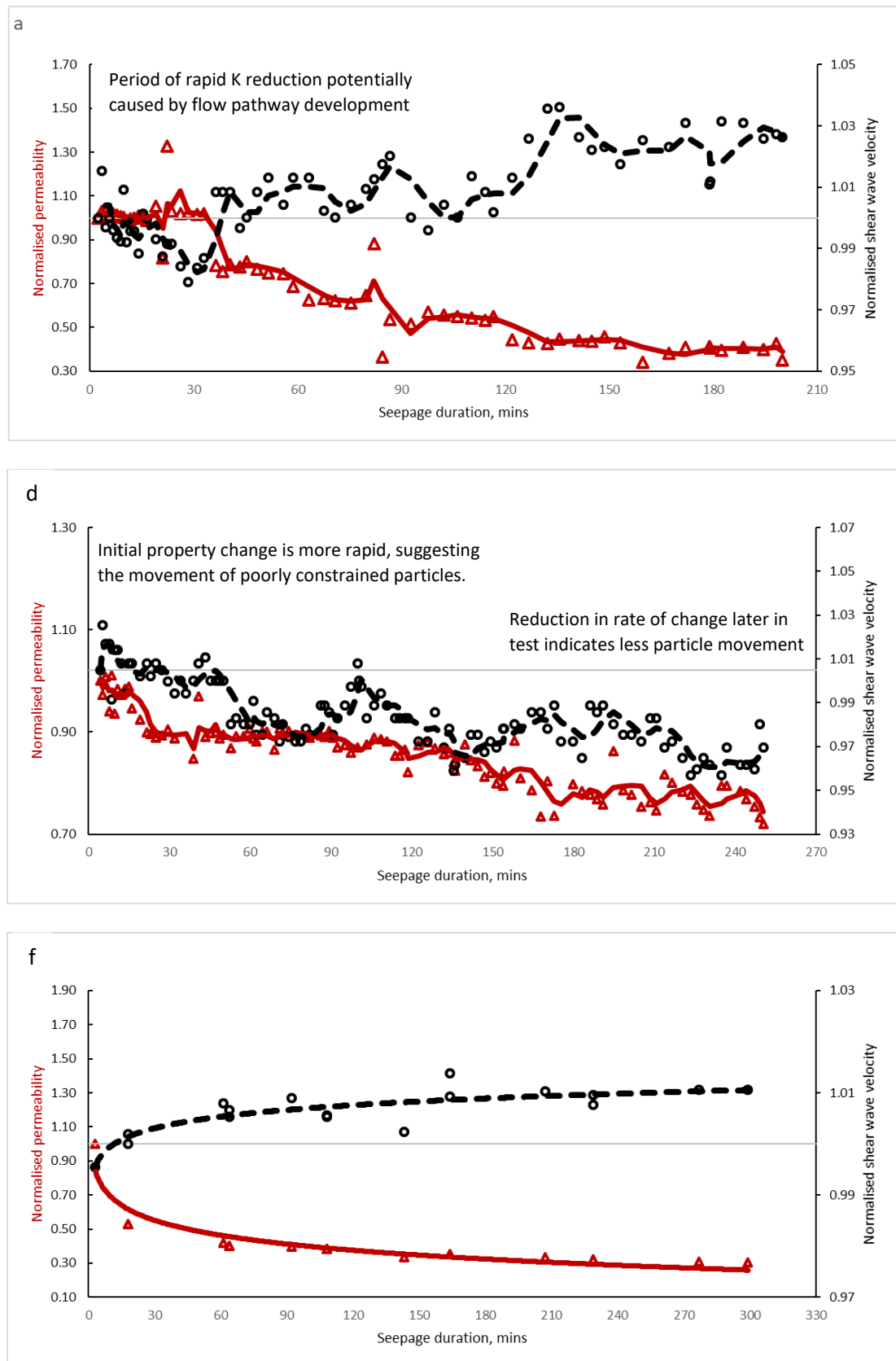
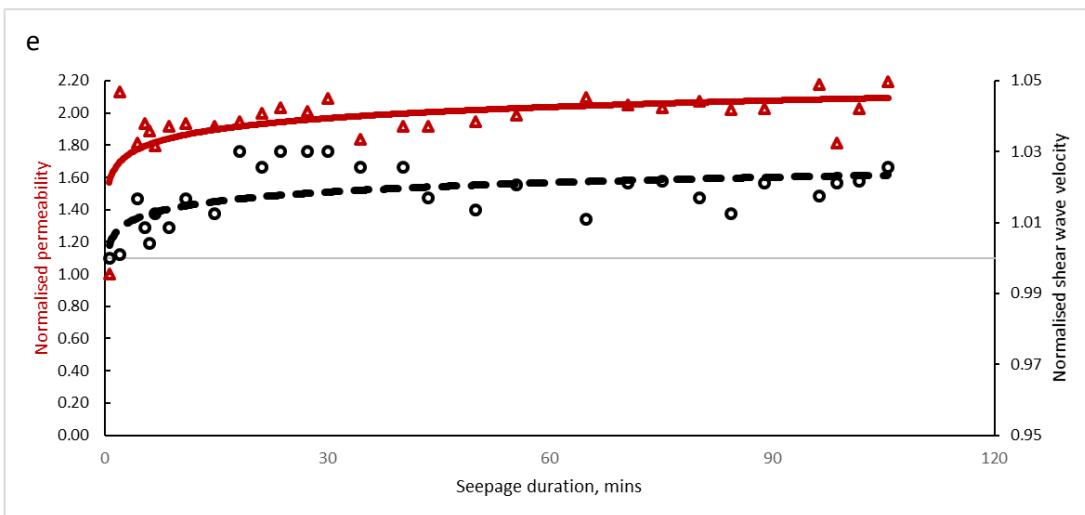
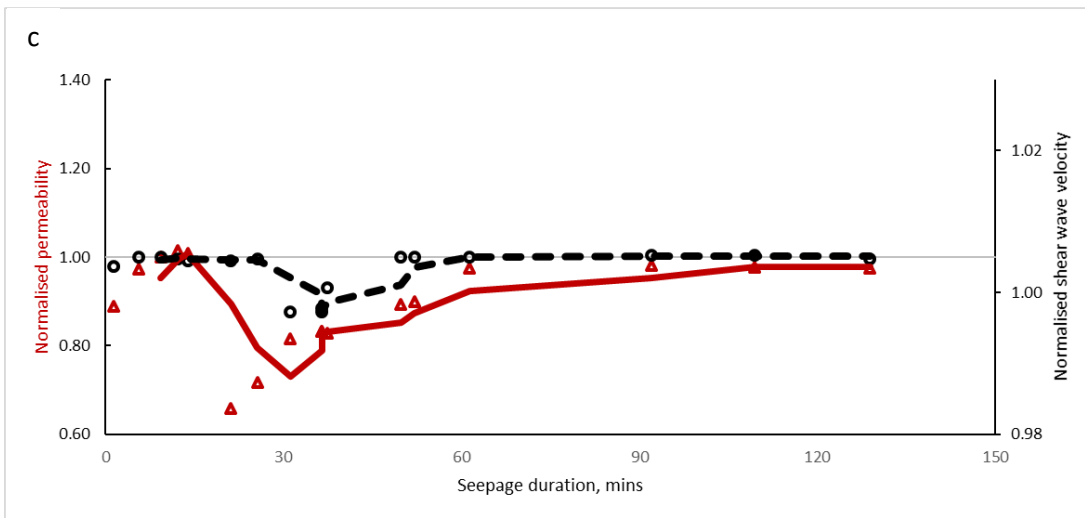
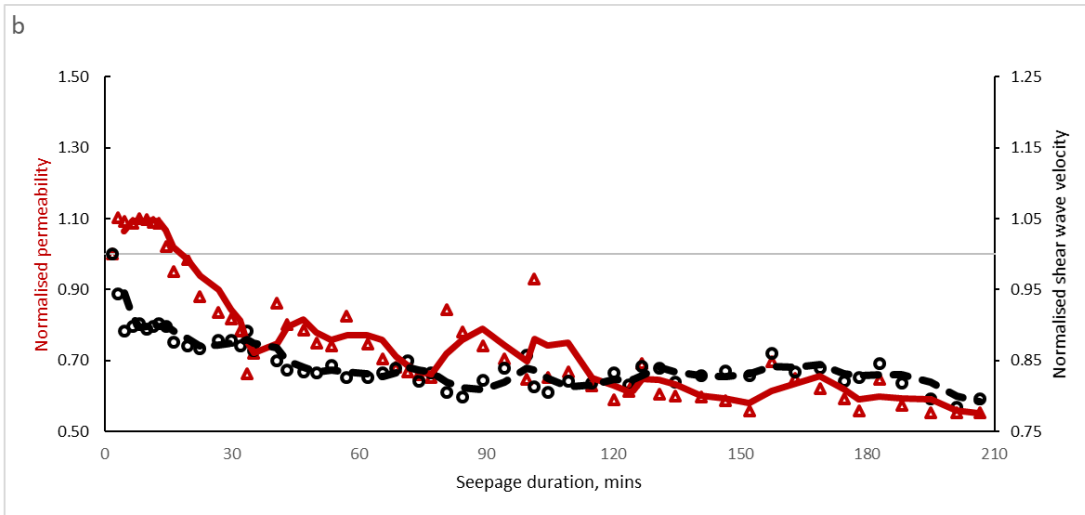


Figure 14: Observed Vs and K over time during seepage for tests a) 30D, b) 30C, c) 15D, d) 30H, e) 30B and f) 15A. d-f are continued over page. Values are normalised by the initial value for the respective property. Trend lines on A-D are three point moving averages and are logarithmic on graphs E and F.

Chapter 3



--- ○ Shear wave velocity
— △ Permeability

3.3.3 Drained shear strength and stiffness

During post seepage drained shearing, a negative correlation was observed between the amount of material removed from samples during seepage and the peak friction angle (ϕ) in samples with 15% and 30% fines content; increased amounts of material removed from samples caused reductions in friction angle (Figure 15). Samples primarily displayed strain hardening behaviour during shear (Figure 16). Samples primarily displayed strain hardening behaviour during shear (Figure 16). At low strains, <1%, strain softening was temporarily observed in the majority of samples prior to the resumption of strain hardening behaviour. Prior to this initial strain softening, samples had higher stiffness, before reloading with lower stiffness (Figure 16). Samples comprising 15% fines were sheared over a smaller axial strain range than those with 30% fines content as bender elements were mounted using silicone sealant during these tests, whereas liquid latex was used to seal bender element insertions during tests containing 30% fines content. Due to failure of the bond between the silicone sealant and the latex membrane during shear induced sample deformation, samples were compromised by confining pressure water. At this point, shearing was halted and further testing on the sample was not possible.

3.3.4 Permeability change

Permeability changes were greatest during initial seepage, with changes decreasing later in tests. Permeability changes often occurred in tandem with V_s changes; the synchronicity of permeability- V_s change was more pronounced during the initial seepage period. Absolute values of permeability change varied over three orders of magnitude between tests, with both positive and negative changes observed. Median relative permeability changes of +5% and -33.5% were recorded for 15% and 30% fines, respectively. Permeability reduction was more common in tests with 30% fines than tests with 15% fines (Table 8).

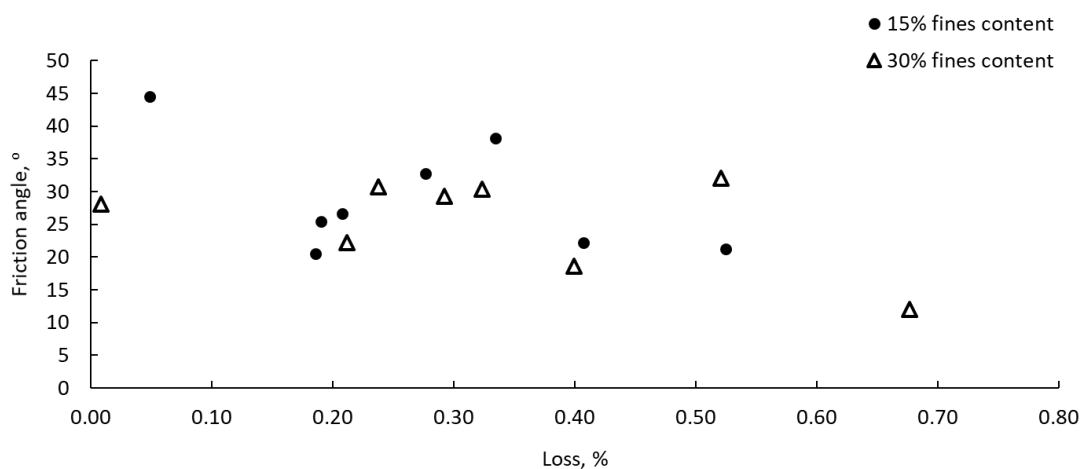


Figure 15: Friction angle change with percentage of material washed out from samples.

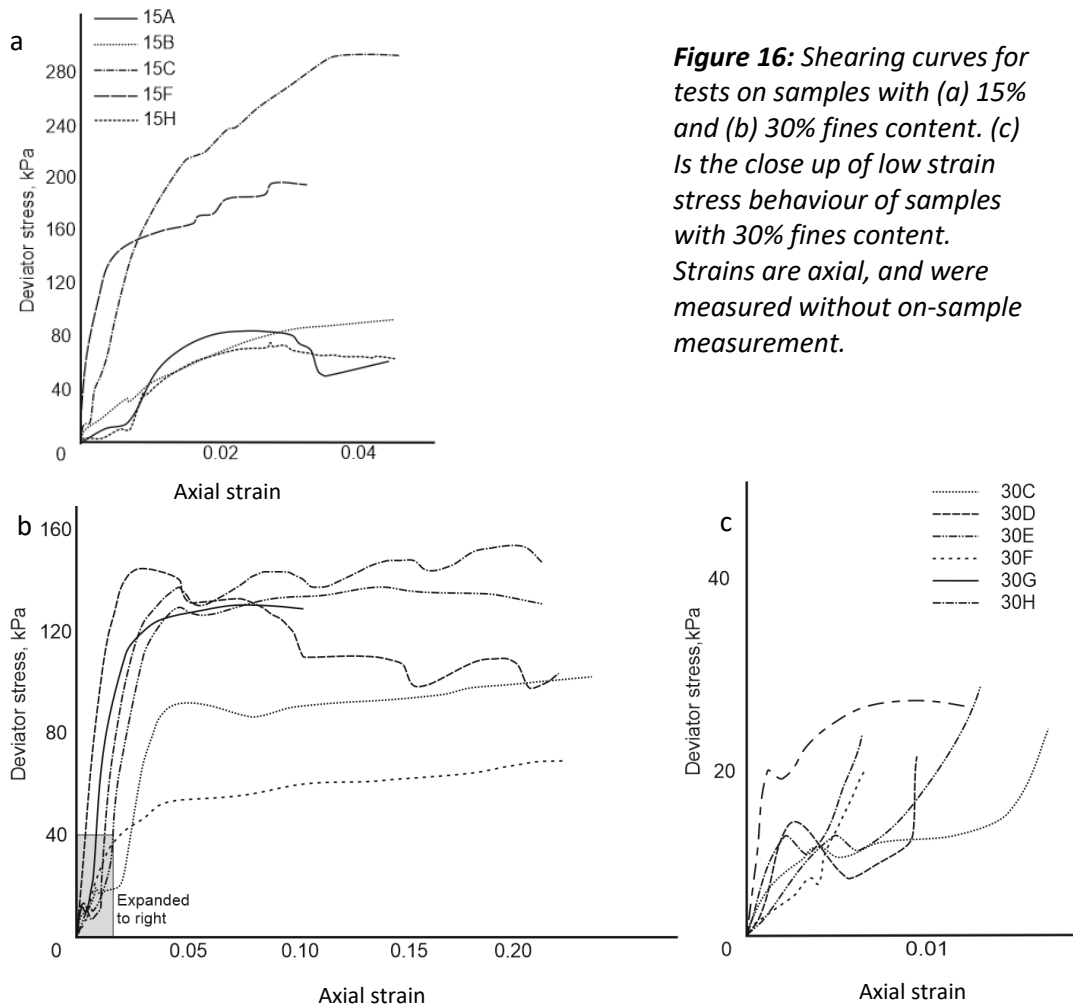


Figure 16: Shearing curves for tests on samples with (a) 15% and (b) 30% fines content. (c) Is the close up of low strain stress behaviour of samples with 30% fines content. Strains are axial, and were measured without on-sample measurement.

3.3.5 Evidence of particle migration

Three main patterns of concordant permeability and shear wave velocity changes were observed during seepage tests (Figure 14): i) V_s increases and permeability decreases (e.g. test 30D); ii) V_s decreases and permeability decreases (e.g. 30C); iii) V_s increases and permeability increases (e.g. 30B). Continuous increase or decrease in permeability and shear wave velocity during seepage was more commonly observed in samples containing 30% fines than those containing 15% fines; samples containing 15% fines were more likely to display shorter duration variations in permeability and shear wave velocity. Two styles of seepage front were observed in samples separated after seepage: a relatively uniform front across the width of samples and concentrated seepage along a flow pathway (Figure 17).

3.4 Discussion

Changes in material structure caused by the redistribution and removal of fine particles are thought to be the primary cause of V_s and permeability changes I measured. The movement of particles results in the blocking and opening of flow pathways, potentially representing the onset of macropore development and subsequent piping, causing localised changes in effective stress, density, moisture content and stiffness. V_s and K change synchronously in the majority of samples (e.g. Figure 14d, 14f), indicating the presence of a consistent cause of property change. Two methods of particle redistribution are thought to cause V_s and K changes: i) migration of fine particles downwards through, and out of, samples; and ii) redistribution of fine particles from void spaces to interparticle contacts (Chang and Zhang, 2013b, Alramahi et al., 2010) (Figure 18).

Proportionally large early changes in V_s and K , and reducing rates of loss with increased seepage volume, indicate that the majority of particle movement and loss occurred during early seepage. Rapid property alteration during initial stages of seepage may be related to the movement of initially poorly constrained fine particles, which do not form part of a sample's force chain, through flow pathways and/or to constrictions between coarser grained particles. The lack of volume change in samples during seepage suggests that suffusive particle migration was occurring during seepage and that the redistribution of fine particles, as opposed to soil skeletal collapse, caused property alterations. If suffusion occurred in concentrated areas, it may allowed for the movement of larger particles due to

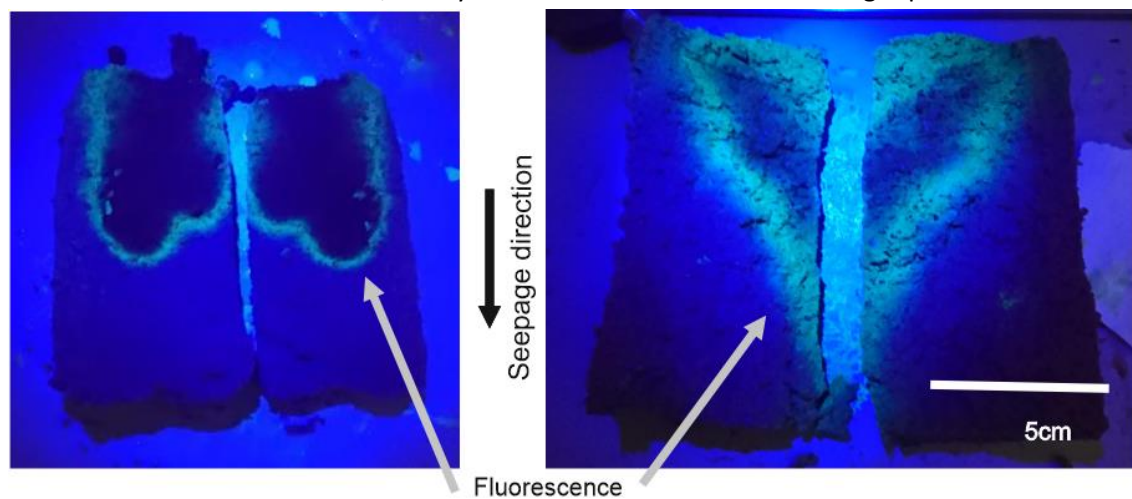


Figure 17: Seepage front development inside samples shown by fluorescence migration; samples were halved post-seepage and imaged using UV light. Fluorescence was initially located at the top of samples, before migrating downwards during seepage. a) Seepage development across the width of samples. b) Concentrated seepage development along a preferential seepage plane.

the initial loss of supporting fine particles. The extensive movement of larger particles in addition to fine particles may have led to the onset of macropore and pipe development.

S-wave velocity increases are thought to be caused by a greater amount of fine particles entering the V_s measurement zone than were removed (Figure 18), and by the redistribution of fine-grained particles to coarse-grained particle contacts, when deposition allows for fine-grained particles to accommodate stress transfer (Alramahi et al., 2010, Salgado et al., 2000). A net loss of fine particles from the V_s measurement zone reduces grain interlocking and increases the void ratio and soil moisture content, reducing sample density, stiffness and measured V_s (Figure 18). V_s measurements were point measurements taken in the middle of samples; particle migration outside of this point did not directly affect V_s measurements. Hence, V_s variations are not directly comparable with particle loss. Localised effective stress changes caused by particle migration may also affect V_s measurements (Salgado et al., 2000).

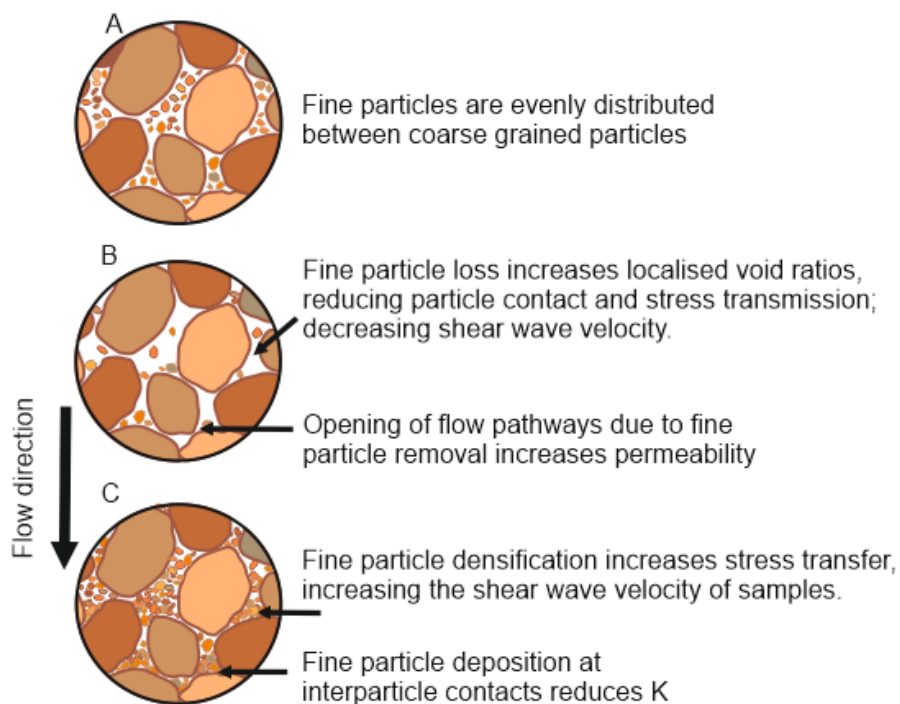


Figure 18: Conceptual model of change in fine particle distribution and soil structure caused by seepage.

A: Prior to seepage.

B: Zones of fine particle loss which are thought to cause reduced V_s and increased K .

C: Zones of fine particle deposition which are thought to have higher V_s and lower K . The enlargement of pores by fine particle migration can allow for the migration of coarser particles and piping initiation.

Chapter 3

Permeability reductions may have developed in samples where a permeability barrier forms due to the deposition of mobilised particles (Ke and Takahashi, 2014). Samples with continuous increases in K indicate that constrictions, causing particle deposition within the sample, were not present in the zones of samples with the lowest permeability. With prolonged duration, observed K reductions were greater. This finding is consistent with internal instability observed by Chang and Zhang (2011); fine particles are deposited within basal pore spaces and clog them during later stage seepage. Relative changes in V_s and K can be used to understand the movement of fine particles within samples. Concordant decreases in V_s and K indicate that there is a net removal of fine particles from the V_s measurement zone and an increase in fine particles in the permeability limiting zone. Increases in V_s and decreases in K indicate that there is densification of the V_s measurement zone. Testing programmes with bender elements at multiple locations, with constant washout mass monitoring, would be needed to define the full nature of particle movement and acoustic velocity changes at higher resolution.

Reducing sediment loss with increased seepage is consistent with multi-stage internal erosion development described by Chang and Zhang (2013b). As seepage volume, not duration, is thought to be the primary driver of particle loss I suggest that $\text{g m}^{-2}\text{L}^{-1}$ should be used when assessing particle loss rate from samples, not $\text{g m}^{-2}\text{s}^{-1}$. The decreasing rate of permeability and stiffness change with test progression suggests that the movement of material is focused, although not solely present, in the earlier stages of seepage. This is supported by the visual evidence of outflow water colour becoming paler with test progression. Testing with full continuous monitoring of washed out material is needed to better define the seepage volume–washout relationship. Preferential selection of fine material, below $125\ \mu\text{m}$, mobilised in samples, shown by the increased mass of washed out finer-grained material, is consistent with grain sizes which the instability criteria (Table 6) denote as unstable.

Variable amounts of particle loss between tests prevented repeat shear testing on a given material, therefore peak friction angle was obtained for each sample using the assumption of zero cohesion. Variability in sample structure may also alter the development of permeability and shear wave velocity changes. Localised sections of samples with higher densities or finer grain sizes may prohibit the movement of fine particles, thus reducing the rates of change in permeability and shear wave velocity observed. The migration of fine particles forms a differential soil structure across samples, resulting in localised behaviour changes. The reduction of angle of friction values with increased particle removal is thought

to have been caused by the migration of fine particles, creating an overall loosening of the soil structure. Samples predominantly displayed strain hardening behaviour during drained shearing (Figure 16). Low strain, <1%, strain softening is thought to be caused by particle redeposition and intra sample variability. Prior to early stage strain softening, the stiffness of samples is higher than post strain softening. This is consistent with the behaviour that the initial stress response is representative of a denser, stiffer, material; following this failure, strain hardening resumed with a lower stiffness and represented the looser, weaker, material (Ke and Takahashi, 2015). Angle of friction values are representative of mass failure through less dense, looser zones. Strain softening was not observed in test 30G, undertaken without seepage. Multiple cycles of strain hardening and softening are observed in some samples (e.g. 30B); each successive cycle has lower stiffness than the previous one, suggesting that multiple zones of loose and dense material form during seepage.

While previous research has shown strength reductions and contraction increases following larger amounts of internal erosion development (Sato and Kuwano, 2016, Zhang and Cheuk, 2014), no clear pattern was present in my findings. It may be that the proportionally smaller amounts of particle movement and loss which developed during seepage in these tests did not cause strength changes as large as those observed in previous studies, preventing an obvious trend developing. Absolute V_s changes in the order of 10% were smaller than V_s reductions recorded by Truong et al. (2010) and Kelly et al. (2012). However, in comparison to the amount of material removed from samples, V_s changes measured in this work (up to ~1% of initial sample mass) are greater than those recorded by Truong et al. (2010) and Kelly et al. (2012). This suggests that small alterations in material structure through material movement, redeposition and loss (not just full removal of fine particles) can produce significant shear wave velocity, stiffness and permeability changes in soils. My data show that temporal changes in stiffness and critical velocity of slopes and earthworks need to be considered following events such as flooding along embankments that accelerate seepage through slopes, given that flooding events which cause seepage and particle migration have been recorded as causes of slope failure (Polemio and Lollino, 2011).

3.4.1 Implications for transportation embankments

Upscaling of laboratory experiments to full embankments remains challenging. However, there are implications for earthworks that should be considered:

1) The formation of flow lines and flow pathways due to particle movement within samples is a possible process by which piping may initiate. Engineers responsible for the management of such geotechnical assets should consider inspection of embankments following exposure to significant flood events. Such inspections may utilise walkover surveys or visual inspections to look for evidence of loss of fines, subsidence or evident seepage. However, a lack of visible external alteration does not preclude the potential for material property alteration.

2) The observation that a better correlation exists with flow volume rather than flow duration suggests that short lived, high intensity events may cause greater property changes. Models of climate change suggesting increased intensity of events may require increased inspection rates.

3) Geophysical methods using surface waves as non-invasive means of investigation may need careful planning in order to capture changes over the embankment. Methods that involve averaging wave velocities over significant volumes of the asset or parallel to the direction of seepage may fail to detect movement of particles and associated material property changes.

3.5 Conclusions

Horizontal bender element measurements were used to measure changes in granular soil permeability and stiffness caused by seepage flow in a triaxial setting. I found that a total of 1% of material removal was related to changes in S-wave velocity and permeability of up to 20%. Increased fine particle loss from samples was shown to cause reduced friction angle. In post seepage shearing, samples were shown to primarily display strain hardening behaviour. However, a dual stiffness was observed – which I attributed to the formation of dense zones of soil caused by fine particle deposition at interparticle contacts. Net permeability reductions over the duration of the experiments were observed in the majority of samples. These changes show the significant potential for seepage through slopes caused by flooding, or other causes, to move earthworks and slopes towards instability. Material property changes and loss were found to be greatest during initial seepage phases. There was no significant difference in the magnitude of property changes observed between samples with 15% and 30% fine particles; samples with greater fines contents displayed more gradual behaviour changes. V_s change appears to be a suitable proxy to monitor changes in sample permeability when subjected to seepage flow and when particle migration develops during internal erosion. However, with a single V_s

monitoring point, V_s measurements are unable to fully quantify the direction, magnitude and causes of mass scale changes in behaviour. I therefore recommend further testing with a higher resolution array of bender elements to allow full quantification of sample behaviour during seepage.

3.6 References

- ALRAMAHI, B., ALSHIBLI, K. A. & FRATTA, D. 2010. Effect of Fine Particle Migration on the Small-Strain Stiffness of Unsaturated Soils. *Journal of Geotechnical and Geoenvironmental Engineering*, 136, 620-628.
- BENNETT, E. H. 1884. Court of Appeal. Whalley v. Lancashire and Yorkshire Railway Co. *The American Law Register (1852-1891)*, 32, 633-640.
- BERGAMO, P., DASHWOOD, B., UHLEMANN, S., SWIFT, R., CHAMBERS, J. E., GUNN, D. A. & DONOHUE, S. 2016. Time-lapse monitoring of climate effects on earthworks using surface waves. *Geophysics*, 81, EN1-EN15.
- BONELLI, S., MAROT, D., TERNAT, F. & BENAHMED, N. 2007a. Assessment of the risk of internal erosion of water retaining structures: dams, dykes and levees.
- BRITISH STANDARDS INSTITUTION 2018. Geotechnical investigation and testing - Laboratory testing of soil. In: COMMITTEE, S. P. A. S. (ed.) *Part 9*. BSI Standards Limited,.
- CHANG, D. & ZHANG, L. 2011. A Stress-controlled Erosion Apparatus for Studying Internal Erosion in Soils. *Geotechnical Testing Journal*, 34, 579-589.
- CHANG, D. S. & ZHANG, L. M. 2013b. Extended internal stability criteria for soils under seepage. *Soils and Foundations*, 53, 569-583.
- FANNIN, R. J. & MOFFAT, R. 2006. Observations on internal stability of cohesionless soils. *Géotechnique*, 56, 497-500.
- FANNIN, R. J. & SLANGEN, P. 2014. On the distinct phenomena of suffusion and suffosion. *Géotechnique Letters*, 4, 289-294.
- FIELD, C. B., BARROS, V., STOCKER, T. F. & DAHE, Q. 2012. *Managing the risks of extreme events and disasters to advance climate change adaptation: special report of the intergovernmental panel on climate change*, Cambridge University Press.
- GUNN, D. A. Embankment stiffness characterisation using MASW and CSW methods. Proc. 11th Int. Conf. Railway Engineering,, 2011 London, .
- GUNN, D. A., CHAMBERS, J. E., DASHWOOD, B. E., LACINSKA, A., DIJKSTRA, T., UHLEMANN, S., SWIFT, R., KIRKHAM, M., MILODOWSKI, A., WRAGG, J. & DONOHUE, S. 2018. Deterioration model and condition monitoring of aged railway embankment using non-invasive geophysics. *Construction and Building Materials*, 170, 668-678.
- HORIKOSHI, K. & TAKAHASHI, A. 2015. Suffusion-induced change in spatial distribution of fine fractions in embankment subjected to seepage flow. *Soils and Foundations*, 55, 1293-1304.
- ICOLD 2017. Bulletin 164 Internal Erosion of Existing Dams, Levees and Dikes, and their Foundations. Paris: International Commission on Large Dams.
- INDRARATNA, B., NGUYEN, V. T. & RUJIKIATKAMJORN, C. 2011. Assessing the potential of internal erosion and suffusion of granular soils. *Journal of Geotechnical and Geoenvironmental Engineering*, 137, 550-554.
- JOHNSTON, I., MURPHY, W. & HOLDEN, J. 2021. A review of floodwater impacts on the stability of transportation embankments. *Earth-Science Reviews*, 215, 103553.
- KE, L. & TAKAHASHI, A. 2014. Experimental investigations on suffusion characteristics and its mechanical consequences on saturated cohesionless soil. *Soils and Foundations*, 54, 713-730.

- KELLY, D., MCDOUGALL, J. & BARRETO, D. Effect of particle loss on soil behaviour. Proc., 6th Int. Conf. on Scour and Erosion, Publications SHF, Paris, 2012. 639-646.
- KENNEY, T. & LAU, D. 1985. Internal stability of granular filters. *Canadian Geotechnical Journal*, 22, 215-225.
- KENNEY, T. C. & LAU, D. 1986. Internal stability of granular filters: Reply. *Canadian Geotechnical Journal*, 23, 420-423.
- KEZDI, A. 1979. *Soil Physics*, Amsterdam, Elsevier.
- KWAN, W. S. & MOHTAR, C. E. 2018b. A review on sand sample reconstitution methods and procedures for undrained simple shear test. *International Journal of Geotechnical Engineering*, 14, 851-859.
- LUO, Y.-L., QIAO, L., LIU, X.-X., ZHAN, M.-L. & SHENG, J.-C. 2013. Hydro-mechanical experiments on suffusion under long-term large hydraulic heads. *Natural Hazards*, 65, 1361-1377.
- MOSSA, M. 2007. The floods in Bari: What history should have taught. *Journal of Hydraulic Research*, 45, 579-594.
- PAREKH, M. L. 2016. *Advancing internal erosion monitoring using seismic methods in field and laboratory studies*. Colorado School of Mines. Arthur Lakes Library.
- PENNINGTON, D., NASH, D. & LINGS, M. 1997. Anisotropy of G₀ shear stiffness in Gault Clay. *Géotechnique*, 47, 391-398.
- PLANÈS, T., MOONEY, M. A., RITTGERS, J. B. R., PAREKH, M. L., BEHM, M. & SNIEDER, R. 2016. Time-lapse monitoring of internal erosion in earthen dams and levees using ambient seismic noise. *Géotechnique*, 66, 301-312.
- POLEMIO, M. & LOLLINO, P. 2011. Failure of infrastructure embankments induced by flooding and seepage: a neglected source of hazard. *Natural Hazards and Earth System Sciences*, 11, 3383.
- SALGADO, R., BANDINI, P. & KARIM, A. 2000. Shear Strength and Stiffness of Silty Sand. *Journal of Geotechnical and Geoenvironmental Engineering*, 126, 451-462.
- SATO, M. & KUWANO, R. 2016. Effects of internal erosion on mechanical properties evaluated by triaxial compression tests. *Japanese Geotechnical Society Special Publication*, 2, 1056-1059.
- TABARI, H. 2020. Climate change impact on flood and extreme precipitation increases with water availability. *Scientific Reports*, 10, 13768.
- TRUONG, Q. H., EOM, Y. H. & LEE, J. S. 2010. Stiffness characteristics of soluble mixtures. *Géotechnique*, 60, 293-297.
- TSUBAKI, R., KAWAHARA, Y. & UEDA, Y. 2017. Railway embankment failure due to ballast layer breach caused by inundation flows. *Natural Hazards*, 87, 717-738.
- USBR 2015. *Best Practices in Dam And Levee Safety Risk Analysis*. 4 ed.
- WAN, C. F. & FELL, R. 2008. Assessing the Potential of Internal Instability and Suffusion in Embankment Dams and Their Foundations. *Journal of Geotechnical and Geoenvironmental Engineering*, 134, 401-407.
- YAMASHITA, S., FUJIWARA, T., KAWAGUCHI, T., MIKAMI, T., NAKATA, Y. & SHIBUYA, S. 2007. International parallel test on the measurement of G_{max} using bender elements. *Organized by Technical Committee*, 29.
- YAMASHITA, S., KAWAGUCHI, T., NAKATA, Y., MIKAMI, T., FUJIWARA, T. & SHIBUYA, S. 2009. Interpretation of International Parallel Test on the Measurement of G_{max} Using Bender Elements. *Soils and Foundations*, 49, 631-650.
- ZHANG, L. & CHEUK, J. 2014. Mechanical consequences of internal soil erosion AU - Chang, Dongsheng. *HKIE Transactions*, 21, 198-208.

Chapter 4

Redistribution of particles following seepage in model embankments constructed of granular soils.

Chapter summary

The flooding of infrastructure embankments has the potential to cause lasting destabilisation through seepage-driven internal erosion development. In order to understand the effects of such erosion on slope behaviour it is imperative to identify where in slopes material alteration most commonly occurs. Laboratory testing on scale models of transportation embankments was undertaken to identify the locations within slopes where material movement, and likely property alteration, caused by seepage through slopes develops. Changes in material properties were found to most commonly occur along the base of slopes and in regions of slopes adjacent to water inflow. Slope toes were found to have a greater proportion of fine material than elsewhere, with the mean grain size of the slope toe region 4.5% smaller and the coefficient of curvature 9% higher than the main slope body, suggesting the development of a low permeability region towards the slope toe. The source zone for material deposited at the toe of slopes was the section of slopes adjacent to water inflow and the base of slopes away from the toe, shown by a coarsening of sediment in these zones. Material alteration following flooding was best identified using a combination of coefficient of curvature and mean grain size data. My results have implications for the stability of earthworks during and after flood events, and for the design of earthwork inspection and maintenance regimes.

4.1 Introduction

Transport embankment failures following flooding are relatively common globally (e.g. Polemio and Lollino, 2011, Tsubaki et al., 2017). These embankments are often not designed for water impoundment, yet large volumes of ponding can develop when linear earthworks are constructed along the base of slopes and on floodplains (e.g. Mossa, 2007, Bennett, 1884). Sometimes these slopes fail in the aftermath of flood events (e.g. USBR, 2015). However, for slopes which remain intact after an individual flood event, there is evidence that flooding and cyclic wetting–drying leads to long-term weakening (Stirling et al., 2021, Johnston et al., 2021, Menan Hasnayn et al., 2017). Understanding the lasting alterations in material properties caused by flood-induced processes in sections of slope which are affected by flooding is key to developing an understanding of the potential changes in slope stability and for developing techniques for increasing the flood resilience of slopes. This is especially important given the effects of climate change on widespread increases in rainfall and flooding which are expected to occur (Field et al., 2012) and given that more infrastructure is likely to be developed to support the world’s burgeoning population.

Floodwater impoundment behind transportation embankments can cause acute destabilisation through processes including saturation and pore pressure increase, loading and rapid draw down (Johnston et al., 2021). In addition, seepage-induced internal erosion, scour and cyclic wetting-drying (ASCE, 2011, Stirling et al., 2021) cause lasting alterations to slope stability through changes to slope structure and changes in material properties including strength, stiffness and permeability (Chang and Zhang, 2011, Ke and Takahashi, 2012). Internal erosion processes, including suffusion and piping, cause the movement of fine particles through slopes. The locations of fine particle loss and accretion are key to determining locations of material property change in slopes after flood recession. Internal erosion of slopes develops in response to flood ponding when there is a hydraulic gradient and sufficient associated water flow within soils and sediments, creating fine particle migration (Wan and Fell, 2008).

Previous studies which assessed the effects of flooding on model slopes used spherical silica beads with a bimodal distribution to identify the predominant locations of slope property changes. Fine particle movement, measured using average grain size reductions, was found to be predominantly below the phreatic line and towards the base and toe of slopes, under the effects of seepage and gravity (Horikoshi and Takahashi, 2015). The bimodal grain size distribution of materials used in tests of model slopes with silica grains does not allow for

the full development of processes occurring in full scale slopes comprised of normally graded materials, thus results may not be consistent with graded materials. The fining identified by Horikoshi and Takahashi (2015) in lower portions of slopes constructed of silica grains is consistent with observations from seepage flow tests undertaken using permeameters and triaxial apparatus which found fining to occur towards the seepage outflow (e.g. Ke and Takahashi, 2014, Chang and Zhang, 2011). Triaxial testing has also shown reductions in soil strength behaviour (e.g. Sato and Kuwano, 2016, Luo et al., 2013) and stiffness (Aramahi et al., 2010, Kelly et al., 2012) following internal erosion development in soils. Given that these small-scale laboratory tests show how the migration of particles causes property alterations, it is important to understand how this behaviour occurs in up-scaled scenarios.

In addition to average grain size and fines distribution change, it is important to consider the effects of seepage on material indices including coefficient of curvature (C_c) and coefficient of uniformity (C_u) (Equations 3.1 and 3.2) in addition to the effects of particle migration on average grain size. C_u and C_c are commonly used to determine the gradation and engineering suitability of soils. UIC 719R, the high-speed rail embankment material specification given by the International Union of Railways, requires $1 < C_c < 3$ and $C_u > 6$:

Using a laboratory model of a slope, I aim to increase understanding of where particle movement and fines redistribution is likely to occur in slopes constructed of materials representing those used in embankment construction when subjected to flood simulation loading. Additionally, I assess how seepage and particle movement cause spatially distributed changes in the values of the key material grading parameters, C_c and C_u .

4.2 Methods

Model slopes, replicating a truncated embankment cross section, were constructed (Figure 19) using material comprising well-graded silts-gravels which met grain size criteria stipulated in UIC719R. Model slopes were used to enable higher durations of seepage through slopes, representing longer term flood conditions in comparison to sampling full-scale embankments where particle migration would likely take longer to develop. Materials with a realistic grain size distribution and properties representing embankment specifications were used to create a more accurate model of fines behaviour, especially in the slope toe region, with the acceptance that this may cause more inter-test variability.

4.2.1 Equipment design and slope structure

In total, five slopes (denoted A-E) were constructed. Each slope was constructed in a transparent Perspex box, to allow for observation of slope behaviour during seepage. Slopes were designed to represent one side of an embankment and were 170 mm high, 400 mm long and up to 480 mm wide. Slope dimensions were selected to create a slope angle commensurate with full-scale embankments. Slopes were split into two sections, a flat topped section representing an embankment crest at the head of the slope and a frontal slope section with a slope angle of $\sim 33^\circ$. Wooden basal supports were installed to prevent basal sliding between the Perspex box and soil material in slopes A-C (Table 9); these were not used in slopes D and E to ensure there was no disruption to fluid flow along the base of slopes. Longitudinal supports ran continuously across the full width of slopes, whereas spikes were discontinuous. A fluid reservoir was located behind a permeable Perspex sheet divider at the back of the slope. Seepage into the back of the slope occurred through a

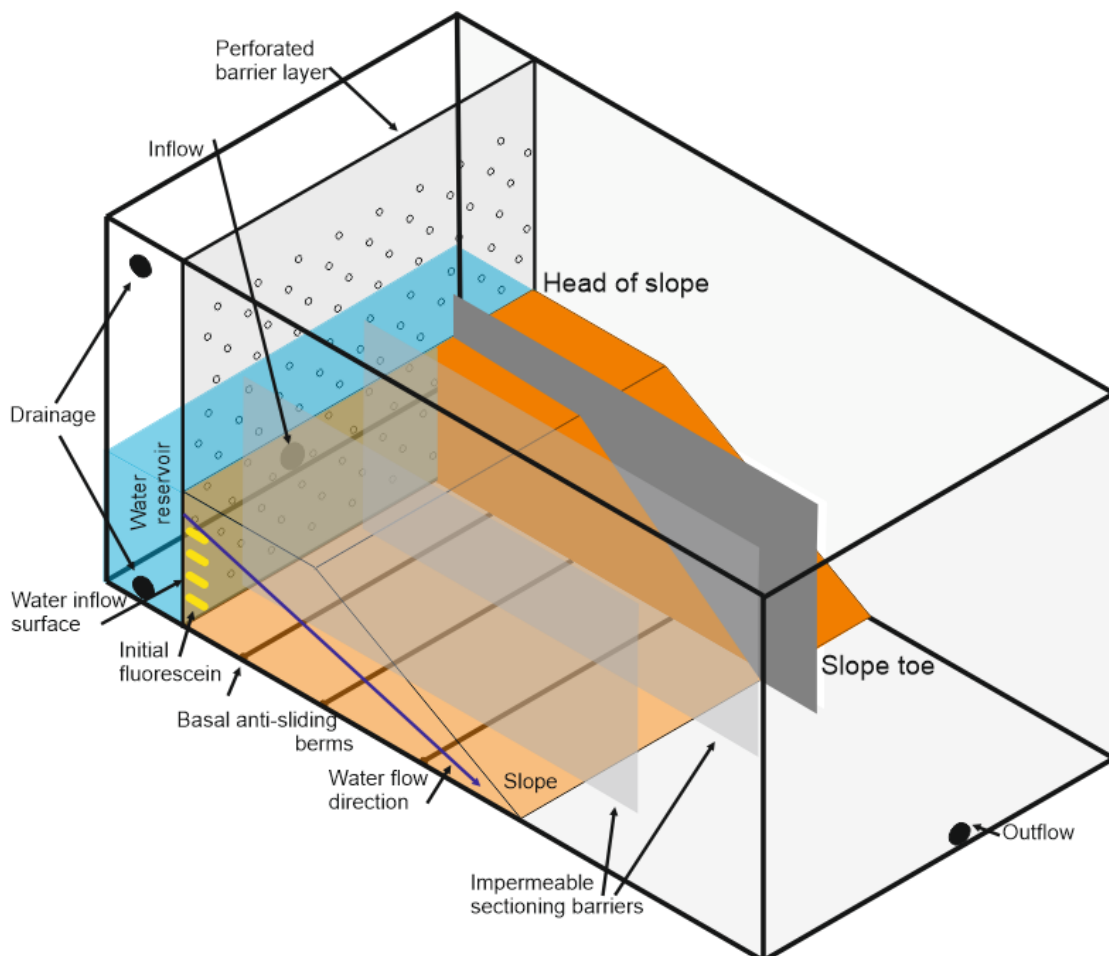


Figure 19: Experiment design schematic for testing undertaken in Chapter 4.

series of holes with a grid spacing of 50 mm and 4 mm diameter, to represent infiltration of water during a flood event.

For each test a slope was constructed using moist compaction with lifts of 25 mm between compactions; slopes were constructed with a target density of 1550 kg m^{-3} (Table 9). Moist compaction was utilised to prevent fines separation during the construction processes (Kwan and Mohtar, 2018a). The development of seepage through slopes was established via the use of fluorescein powder which was inserted at multiple depths at the head of slopes during compaction and used to track fluid and particle movement. The development of fluorescence across the length of a model slope showed that seepage was developing through a slope. Throughout the duration of tests, the fluorescein response weakened due to dilution from additional seepage water inflow and was not consistently visible towards the toe of the slopes. Water which seeped through the slope drained via a drainage hole in the Perspex beyond the slope base. In tests C and D barriers were inserted into the slope parallel to flow to allow for the effects of different durations of seepage to be monitored for the same slope (Figure 19). In test C, barriers were installed during seepage; transect *C(i)* underwent the least seepage at 135 minutes, with each additional transect undergoing an additional 135 minutes of seepage. In test D barriers were inserted prior to seepage initiation; transect *D (i)* underwent no seepage and is a control section.

Table 9: Slope design properties. Slope density was not recorded for slope A due to procedural error.

Slope	Mean slope density, kg m^{-3}	Seepage duration, mins	Hydraulic gradient, i	Sampling	Slope structure
A	----	85	3	Nine samples per transect; three transects	Longitudinal basal supports
B	1483	246	1	10 samples per transect; three transects	Basal spikes
C	1532	552	1	10 samples per transect; four transects	Three slope dividers Basal spikes
D	1578	145	3	10 samples per transect; two transects	Three slope dividers
E	1517	374	1	24 samples from a single transect	Single narrow slice

4.2.2 Slope material

Granular soils were constructed to form a material with the desired grain size distribution and properties. Soils used in this chapter were produced by mixing two bulk soils with a known grain size distribution, in comparison to soils used in Chapter three which were produced by addition of specific masses of soil at each grain size. The greater mass of soil required to produce slopes in this chapter necessitated the differences in sample preparation method. Soils with a fine material content of 15% were used during testing, where fines are defined as grains $<125 \mu\text{m}$. Soil gradation curves are shown in Figure 20. Material stability was assessed using the stability criteria (Table 10) prescribed by Kenney and Lau (1985) which dictate that soils with a h/f value > 1.3 are stable and a h/f value of 1-1.3 indicates a soil in transition between stability and instability, where f is the weight fraction finer than grain size d and h is the weight fraction between grain size d and $4d$. The use of well graded soils means that slopes better represent more modern embankments, specifically those designed with floodwater retention in mind.

4.2.3 Testing processes

Following slope construction, a hydraulic head was applied to the back of the slope. Tap water was used to fill the water reservoir and took approximately 1 minute. Total seepage durations and head values used are displayed in Table 9. All tests were planned to run for a total of 480 minutes (8 hours) of seepage time. In tests where slope failure occurred, seepage was halted at the onset of failure to preserve the remaining slope material. A constant head was used during seepage. A hydraulic gradient of 1 was used on slopes B, C and E, and a hydraulic gradient of 3 was used on slopes A and D to accelerate particle movement; higher hydraulic gradients were not used in all tests due to the potential for uplift pressures to cause instability.

Table 10: Slope material stability criteria. Materials with h/f values >1.3 are considered stable.

Slope	C_c	C_u	Kenny – Lau h/f ratios (1985)
A	6.8	1.3	2.4
B	9.9	1.1	2.1
C	7.5	0.9	1.8
D	6.5	1.0	1.7
E	5.8	1.1	1.5

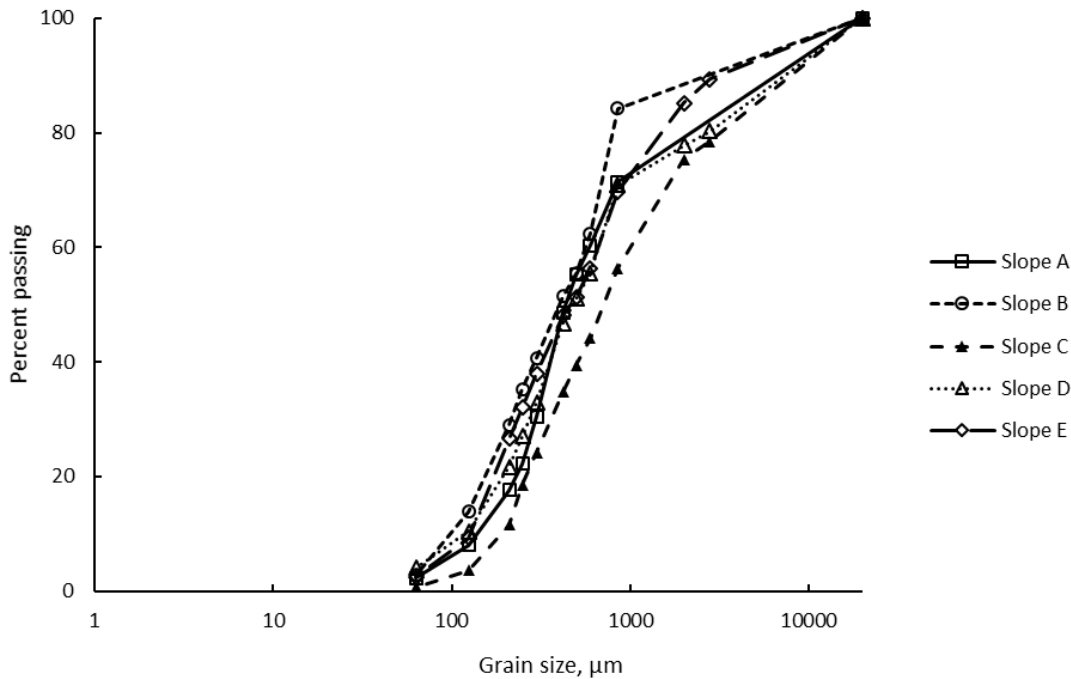


Figure 20: Grainsize distribution of material used during slope construction.

Samples were taken from the slope immediately following seepage and draining. In slopes A-D, 10 samples were taken from each section of the slope, making a total of 30 or 40 samples per slope. In slope E, 24 samples were taken from an individual slope section to obtain higher resolution results. Slope D was split to contain two sections - a control section which comprised a transect of the slope sampled without undergoing seepage, and a second section of slope which was sampled after undergoing seepage. After drying, the grain size distribution was measured for each sample by sieving using 12 size grading bands. C_u , C_c and average grain size values were calculated for each sample; average grain size for each sample was taken as the geometric mean, after Shirazi and Boersma (1984). A small amount of mass at higher grain sizes can have a disproportionately large effect on the results if an arithmetic mean value is taken. Fines were non-plastic so fines loss during sieving through fine particle conglomeration or fine particle attachment to coarser particles is thought to be minimal; this was confirmed by microscope analysis of the sieved particles.

4.3 Results

Here I assumed that areas where mean grain size is smaller coincide with locations where fine particles accumulated, or coarse particles eroded, while locations with larger mean grain size indicate that fine particles were removed, or coarse particles deposited, in that section of a slope. Grain size distribution (Figure 21) and C_c (Figure 22) data suggest that the predominant locations of change in material properties occurred along the base and the sections of slopes adjacent to the water inflow. Although these patterns were seen

across all slopes, they were most clearly observed in test E which had a higher sampling resolution (Figure 21E, 22E). Grain size distribution across each slope can be split into two broad categories. In the first, as measured in slope E and transects of slope A, B and C, higher mean grain size values were measured along the section of the slope adjacent to water inflow and along the base of the slope, with finer mean grain sizes at the toe of the slope (Figure 21). In the second category, the toe of the slope and the section of the slope adjacent to water inflow had higher grain sizes with lower mean grain size measured along the base of the slope – as seen in slope transects B-i and D-ii (Figure 21).

The average grain size of the slope toe region was 4.5% smaller across all non-control slope transects than in the slope body (Fig. 23a); indicating that fine particle accumulation had occurred in the toe region. The 4.5% change in grainsize in the slope toe region is greater than the 3% variability seen between all data points. Across all slopes, average grainsize behaviour was not as well defined in the upper right sections of slopes, which was thought to be above the phreatic surface. In slopes D and E, the mean grain size for each sampling layer (geometric mean of each horizontal layer) shows that the top half of the slope had a constant average grain size and in the bottom sampling sections the average grain size increased (Figure 24). Increases of 17.5% were observed in the lowest layer in transect *D-ii* and 12.5% across the lowest two sampling layers in transect *E-i*. This pattern was not observed in the control transect of slope D (*D-i*), which had a maximum measurement range of 3.7% between sampling layers; as transect *D-i* was sampled without undergoing seepage this suggests the variance observed was due to slope inhomogeneity. Accounting for the inherent inhomogeneity from slope construction, increases of 13.7% and 9.7% are thought to have developed due to seepage induced particle migration in transects *D-i* and *E-i*, respectively. Although the base of slopes predominately showed higher mean grain sizes than sampled layers above, indicating that fine particles had been removed, at the toe of slopes mean grain sizes were predominantly lower relative to values along the base of the slope (e.g. transect B-iii).

Distinct C_c patterns were observed in tests C, D and E (Figure 22). In slope transects B-i, B-ii, C-iv D-ii and E-i low C_c values were observed in the basal slope layer relative to higher sampling layers, with the exception of the slope toe. In slope C, along the slope section adjacent to water inflow, C_c values were lowest following the initial stage of seepage (transect C-i), and C_c values increased with further seepage. Along the base of the slope, C_c values predominantly decreased with time — with the exception of the slope toe region (Figure 23). Normalised average C_c values for all tests showed distinctly higher C_c values in

the slope toe region (Figure 23b). Higher C_c values recorded at the toe of the slope indicate that the material became better graded, consistent with fine particle deposition. Areas with lower C_c values indicate that the slope forming materials were more poorly graded. Across all tests, distinct spatial or temporal behavioural trends were not observed in C_u data.

In slope C, after the first stage of seepage, average grain size values were initially high at the head of the slope relative to the rest of the slope, with larger fines content at the slope toe. With seepage progression, the toe of the slope coarsened before fining again, while towards the head of the slope the material initially fined and then became coarser.

Temporal development of slope properties was also observed in slope D, in which there was a decrease in mean grain size in the slope area adjacent to water inflow and increase in grain size along the base and toe of the slope with time.

Little variation was observed in the properties of materials in the upper right portion of slopes. In slope A, a more defined pattern of behaviour is observed higher up the slope. Furthermore, a fine grained zone was observed in the bottom left corner and slope toe region of slope A in slices 'i' and 'ii'. In slope transect A-i, fine particle accumulation was visible at the toe of the slope after 75 minutes of seepage (Figure 25), consistent with the observed fluorescence movement through the slope and lower mean grain size values measured in this region. Fine-grained material was observed exiting the toe of slopes with seepage progression in all slopes. Fluorescence migration through slopes primarily displayed movement towards the slope toe and downwards towards the slope base from the input locations. Fluorescence migration was more obvious in the lower sections of slopes, consistent with locations of observed spatial trends in C_c and mean grain size data. In slope A, fluorescent water can be seen rising over the zone of fines deposition at the slope toe (Figure 25).

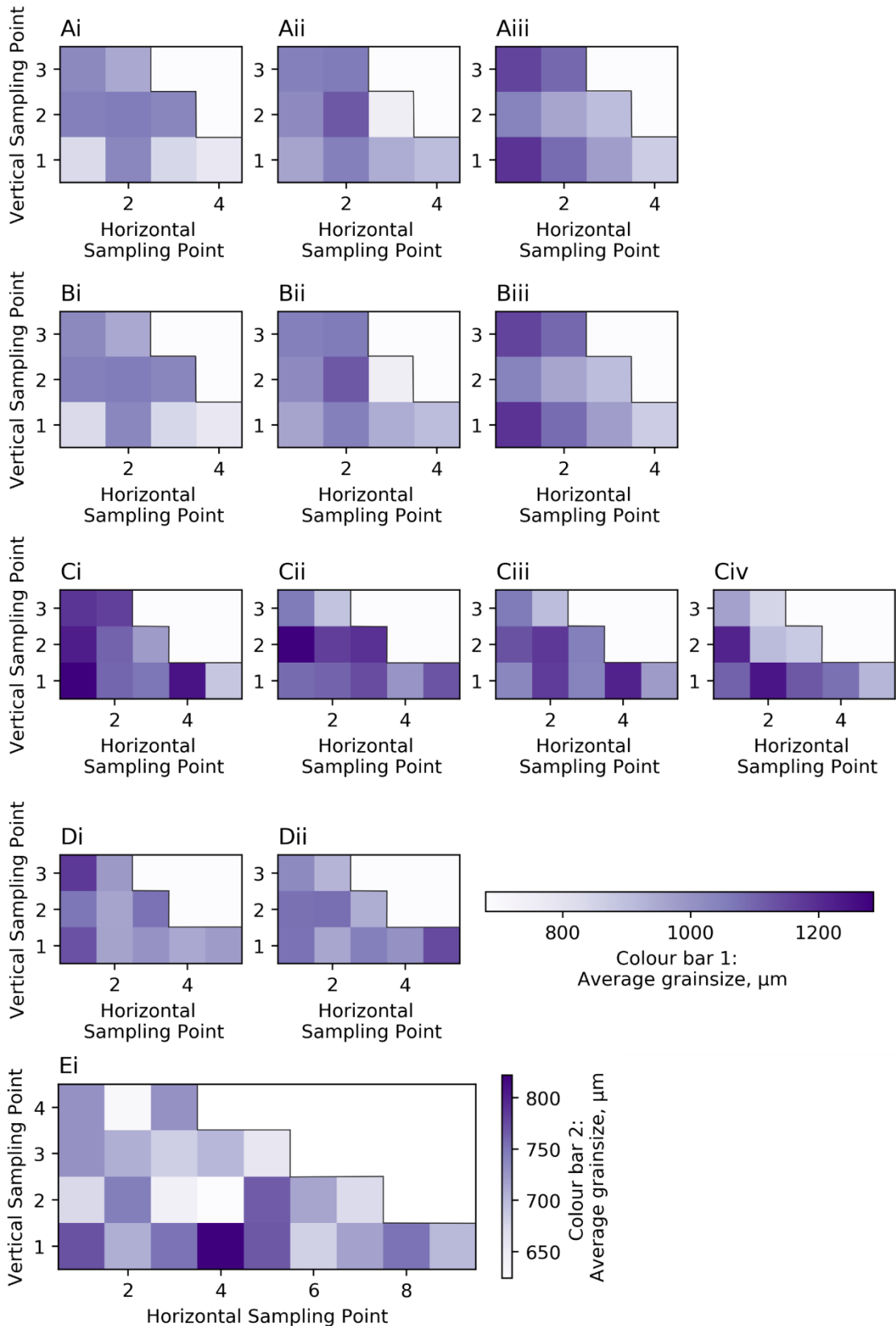


Figure 21: Geometric mean grain size values for slopes A - E. Colour bar 1 is used for slopes A - D, colour bar 2 refers to slope E. Lowest mean grain sizes are observed in the bottom rear portion of the slope. In slope C, transect (i) underwent the shortest duration of seepage. Transect D (i) was a control transect and underwent no seepage.

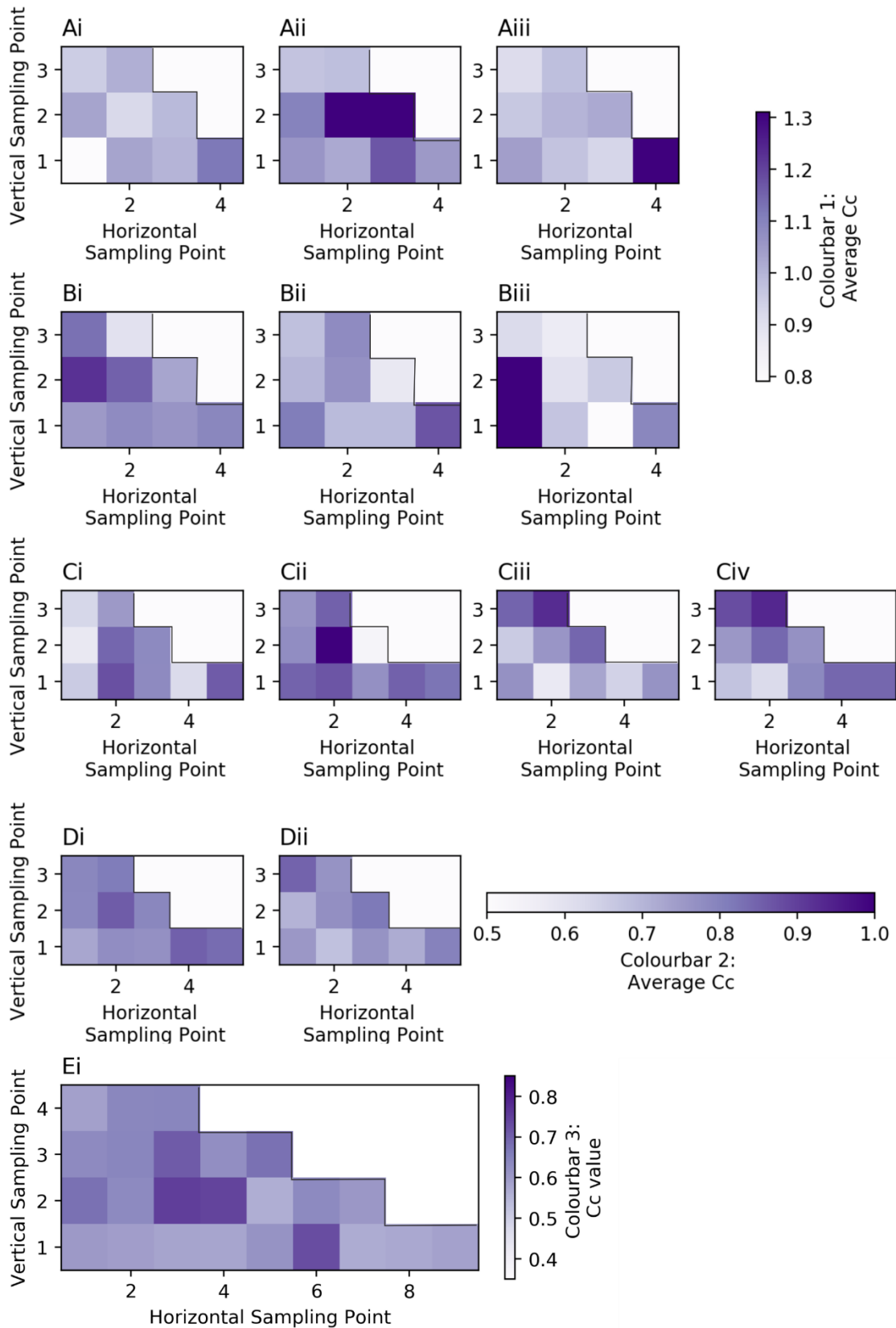


Figure 22: Mean C_c value for each sampling point in slopes A - E. In slopes C, transect (i) underwent the shortest duration of seepage. Transect D (i) was a control transect and underwent no seepage. Colour bar 1 refers to slope A, colour bar 2 to slopes B - D and colour bar 3 to slope E.

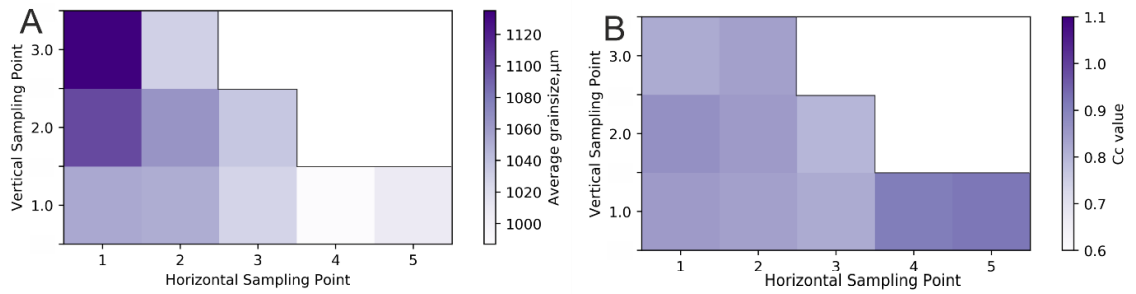


Figure 23: a) mean grain size and b) normalised mean C_c values at each sampling point for all transects of slopes A-D, excluding the control transect Di which did not undergo seepage. Average grain size values for each sampling cell show the mean of the geometric mean grain size of each transect. C_c values were normalised by the average C_c value of all samples in slopes A-D combined.

Debris flow failures initiated in the upper sections of slopes A, B and D. In slope C, a rotational failure initiated in the middle of the slope. These tests were halted at this point to preserve the remaining material for sampling. Material altered by failure was not sampled.

4.4 Discussion

Observed spatial patterns in mean grain size and C_c data are consistent with the migration of fine particles, driven by water inflow at the back of the slope, from the rear of the slope towards the slope toe with movement primarily occurring along the basal region of the samples. This is shown by mean grain size and C_c data and is broadly consistent with previous model slope tests which used bi-modal silica as a soil substitute (Horikoshi and Takahasi, 2015). I found highest mean grain sizes were most commonly measured along the

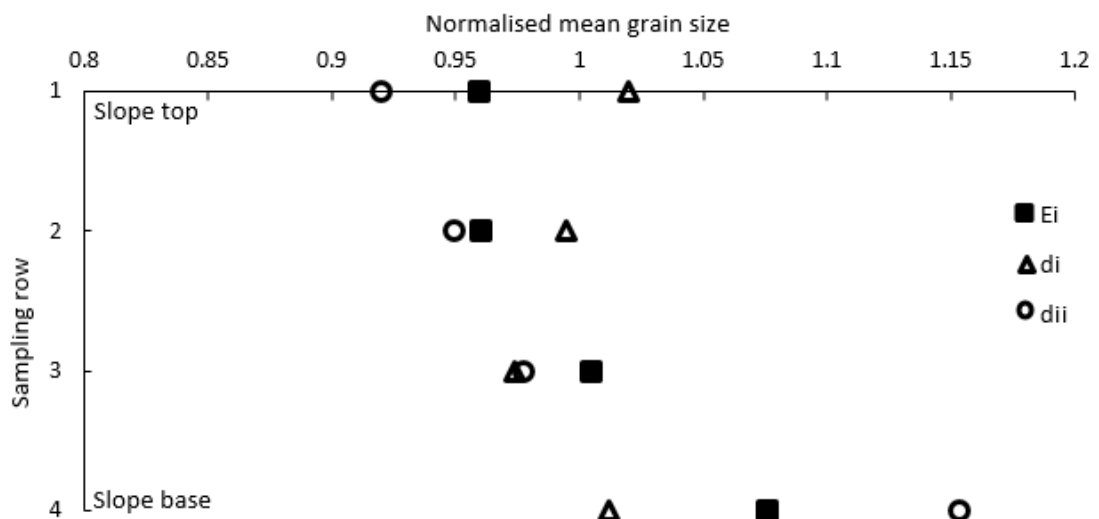


Figure 24: Normalised mean grain size for each horizontal layer in slopes D and E. Transect ‘D-i’, measured without seepage, does not show geometric mean grain size variations between each vertical layer in comparison to transect D-ii, measured following seepage. Values normalised by the geometric mean grain size of each transect.

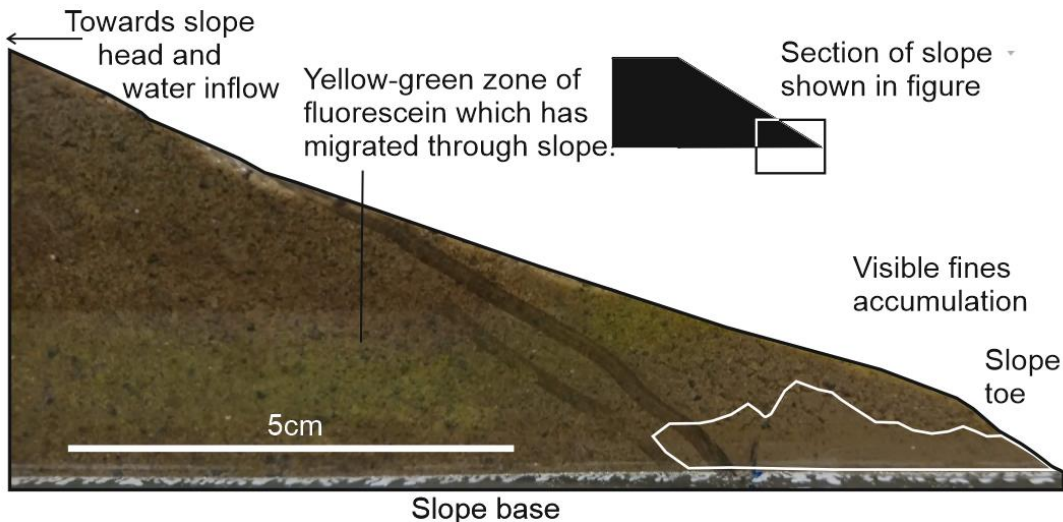


Figure 25: Fine particle accumulation at the toe of slope 'A'. Fluorescein migration is also evident, with a fluorescent zone visible above the zone with fine particle deposition.

base and at the rear of the slope, suggesting that fine particle removal occurred from those areas. Low average grain sizes were most commonly found in the toe of the slope, consistent with fine particle deposition in this area. Higher C_c values, suggesting a better graded soil, at the toe of the slope also support the suggestion that there was migration of fine particles towards the slope toe, with the source regions being the back of the slope and slope base. The deposition of fine particles in the downstream section, specifically the toe region of the slope, has the potential effect of reducing permeability (Chang and Zhang, 2013a) and increasing pore water pressures; these changes have the potential to reduce slope stability when applied to larger embankments. Fluorescein flow over the top of the fine particle accumulation zone in the slope toe (Figure 25) suggests the development of an area of lower permeability.

In some tests, higher mean grain size values were observed in the slope toe region than the remainder of the slope base, e.g. in transects *D-ii* and *C-ii*. This is thought to be due to shorter durations of seepage in these tests and the removal of mobilised loose fine particles from the slope toe during early seepage — but without enough seepage volume to cause additional fine particles washed out from the back of the slope to be moved into the terminal slope sections. Loose particle migration at the onset of seepage, followed by coarser particles and macropore development, is consistent with the expected behaviour of unstable granular soils (Chang and Zhang, 2013b). In addition to the aforementioned seepage-driven directional movement of fine particles, the development of zones with locally increased grain sizes along the base of slope A is thought to have been caused by deposition of fine particles behind impermeable berms and the removal of such particles from in front of them. Higher mean grain sizes in the slope regions closest to water

inflow and in the basal sections of slopes, e.g. slope *E*, (Figures 21, 23a) suggest that the majority of fine particles deposited in the toe or washed out of slopes are sourced from these regions.

The localised movement and redistribution of fine particles initially located in inter-granular zones to constrictions at interparticle contacts, under the effects of seepage, is thought to have a significant effect on the mechanical behaviour of slopes (Alramahi et al., 2010). Although the particles mobilised are not removed from the slope during this localised redistribution, the restructuring of the soil alters the material behaviour. As particles are not removed from the slope during localised redistribution, average grain size, C_c or C_u will be consistent with pre-seepage values for each sampling location. The permeability reductions associated with the movements of fine particles from head to toe of slopes and accumulation of fine particles at interparticle contacts are potential causative factors for the formation of failure events observed during the latter stages of flow during testing. If extrapolated to larger-scale slopes, as found in infrastructure earthworks, these changes have the potential to cause long-term degradation of slopes and associated destabilisation; material changes may not be observable without intrusive investigation. Although the authors are not aware of studies on full scale embankments assessing the effects of flooding on particle migration, evidence of sediment removal from slopes is available (e.g. Bernatek-Jakiel and Poesen, 2018).

Although the laboratory model used in the testing is thought to be a good proxy for assessing the potential for changes in full-scale embankment properties caused by water impoundment and seepage throughflow, boundary effects may have altered the primary flow pathway. Additionally, the impermeable basal layer prevented the movement of water and fine particles out of the slope base. The permeability barrier formed by the soil-box base contact may exacerbate the role of basal flow in these tests, making them more representative of scenarios where embankments overlie impermeable soils or bedrock. However, it is evident from the primary trends in C_c and mean grain size data that the majority of property alteration is likely to occur in these lower slope regions. Due to the time-dependent nature of the effects of seepage on slopes, it is difficult to specify the exact property changes that would develop in full-scale embankments after a specific flooding event as it may be dependent on factors including the head of water, previous slope alteration and duration of the specific flooding process in question (Johnston et al., 2021). I found that, during initial seepage, fine particles are lost from the slope toe region, before being re-deposited as particle migration occurs from upstream sections of a slope.

Geometric mean grain size and C_c were found to display the most obvious patterns of material behaviour following seepage; no distinct spatial or temporal pattern was observed in C_u data. Based on these results, C_c and geometric mean grain size change are thought to be the most reliable measure for assessing changes in the behaviour of materials following seepage development. It is thought that C_u values are not consistently altered by the migration of fine particles as the movement of fine particles has more effect on D_{10} and D_{30} than on D_{60} . The patterns of material alteration, likely caused by the redistribution of fine particles, identified in this testing suggest that funding should be invested to examine the scale of slope alteration following flooding in full-scale embankment slopes.

4.5 Conclusion

Seepage through scale model slopes caused material property differences along the slope profile relative to the control slope where no differences were observed across the slope profile. The spatial differences were observed in geometric mean grain size and C_c data. Larger mean grain sizes were primarily observed at the base and back of slopes, suggesting that fine particle loss occurred. Smaller mean grain sizes were most commonly found at the toe of slopes, suggesting fine particle deposition occurs in these areas. The movement of fine particles appeared to be time dependent. Initial short durations of seepage may remove fine particles from some areas, e.g. the slope toe, before additional seepage causes deposition of fine particles sourced from upstream sections of slopes. Reduction in average grain size, and associated fine particle deposition, at the toe of slopes has the potential to reduce overall slope permeability and may cause slope destabilisation. This potential for slope destabilisation suggests the need for investment in larger-scale analysis of embankment slopes affected by flooding.

4.6 References

- ALRAMAHI, B., ALSHIBLI, K. A. & FRATTA, D. 2010. Effect of Fine Particle Migration on the Small-Strain Stiffness of Unsaturated Soils. *Journal of Geotechnical and Geoenvironmental Engineering*, 136, 620-628.
- ASCE 2011. Earthen Embankment Breaching. *Journal of Hydraulic Engineering*, 137, 1549-1564.
- BENNETT, E. H. 1884. Court of Appeal. Whalley v. Lancashire and Yorkshire Railway Co. *The American Law Register (1852-1891)*, 32, 633-640.
- BERNATEK-JAKIEL, A. & POESEN, J. 2018. Subsurface erosion by soil piping: significance and research needs. *Earth-Science Reviews*, 185, 1107-1128.
- CHANG, D. & ZHANG, L. 2011. A Stress-controlled Erosion Apparatus for Studying Internal Erosion in Soils. *Geotechnical Testing Journal*, 34, 579-589.
- CHANG, D. S. & ZHANG, L. M. 2013a. Critical Hydraulic Gradients of Internal Erosion under Complex Stress States. *Journal of Geotechnical and Geoenvironmental Engineering*, 139, 1454-1467.

- CHANG, D. S. & ZHANG, L. M. 2013b. Extended internal stability criteria for soils under seepage. *Soils and Foundations*, 53, 569-583.
- FIELD, C. B., BARROS, V., STOCKER, T. F. & DAHE, Q. 2012. *Managing the risks of extreme events and disasters to advance climate change adaptation: special report of the intergovernmental panel on climate change*, Cambridge University Press.
- HORIKOSHI, K. & TAKAHASHI, A. 2015. Suffusion-induced change in spatial distribution of fine fractions in embankment subjected to seepage flow. *Soils and Foundations*, 55, 1293-1304.
- JOHNSTON, I., MURPHY, W. & HOLDEN, J. 2021. A review of floodwater impacts on the stability of transportation embankments. *Earth-Science Reviews*, 215, 103553.
- KE, L. & TAKAHASHI, A. 2012. Strength reduction of cohesionless soil due to internal erosion induced by one-dimensional upward seepage flow. *Soils and Foundations*, 52, 698-711.
- KE, L. & TAKAHASHI, A. 2014. Experimental investigations on suffusion characteristics and its mechanical consequences on saturated cohesionless soil. *Soils and Foundations*, 54, 713-730.
- KELLY, D., MCDOUGALL, J. & BARRETO, D. Effect of particle loss on soil behaviour. Proc., 6th Int. Conf. on Scour and Erosion, Publications SHF, Paris, 2012. 639-646.
- KENNEY, T. & LAU, D. 1985. Internal stability of granular filters. *Canadian Geotechnical Journal*, 22, 215-225.
- KWAN, W. S. & MOHTAR, C. E. 2018a. A review on sand sample reconstitution methods and procedures for undrained simple shear test. *International Journal of Geotechnical Engineering*, 14, 1-9.
- LUO, Y.-L., QIAO, L., LIU, X.-X., ZHAN, M.-L. & SHENG, J.-C. 2013. Hydro-mechanical experiments on suffusion under long-term large hydraulic heads. *Natural Hazards*, 65, 1361-1377.
- MENAN HASNAYN, M., JOHN MCCARTER, W., WOODWARD, P. K., CONNOLLY, D. P. & STARRS, G. 2017. Railway subgrade performance during flooding and the post-flooding (recovery) period. *Transportation Geotechnics*, 11, 57-68.
- MOSSA, M. 2007. The floods in Bari: What history should have taught. *Journal of Hydraulic Research*, 45, 579-594.
- POLEMIO, M. & LOLLINO, P. 2011. Failure of infrastructure embankments induced by flooding and seepage: a neglected source of hazard. *Natural Hazards and Earth System Sciences*, 11, 3383.
- SATO, M. & KUWANO, R. 2016. Effects of internal erosion on mechanical properties evaluated by triaxial compression tests. *Japanese Geotechnical Society Special Publication*, 2, 1056-1059.
- STIRLING, R. A., TOLL, D. G., GLENDINNING, S., HELM, P. R., YILDIZ, A., HUGHES, P. N. & ASQUITH, J. D. 2021. Weather-driven deterioration processes affecting the performance of embankment slopes. *Géotechnique*, 71, 957-969.
- TSUBAKI, R., KAWAHARA, Y. & UEDA, Y. 2017. Railway embankment failure due to ballast layer breach caused by inundation flows. *Natural Hazards*, 87, 717-738.
- USBR 2015. Best Practices in Dam And Levee Safety Risk Analysis. 4 ed.
- WAN, C. F. & FELL, R. 2008. Assessing the Potential of Internal Instability and Suffusion in Embankment Dams and Their Foundations. *Journal of Geotechnical and Geoenvironmental Engineering*, 134, 401-407.

Chapter 5

The effects of flood induced material alteration on embankment displacement due to dynamic loading

Chapter summary

The results of microscale analysis of the effects of fine particle migration on material properties, and of up-scaled laboratory testing of the effects of seepage and fine particle migration on slope structure presented in chapters 3 and 4 were used to define material properties and slope structure in finite element method (FEM) models. The aim of this modelling was to investigate the effects of the measured material changes and slope alterations on the dynamic response of embankments under live loading scenarios, in comparison to embankment slopes with a uniform material structure. The background to live rail loading induced displacements, model structure and model results are presented. These are then discussed with consideration of the effects of material change on embankment performance. Reductions in material density and stiffness are found to cause increases in vibration following live loading, as are increases in the proportion of a slope where material alteration has occurred. Areas of slopes with increases in density and stiffness are found to have a smaller effect on increasing displacement. Increased slope vibrations have the potential to cause embankment damage, especially if they occur during flood conditions.

5.1 Introduction

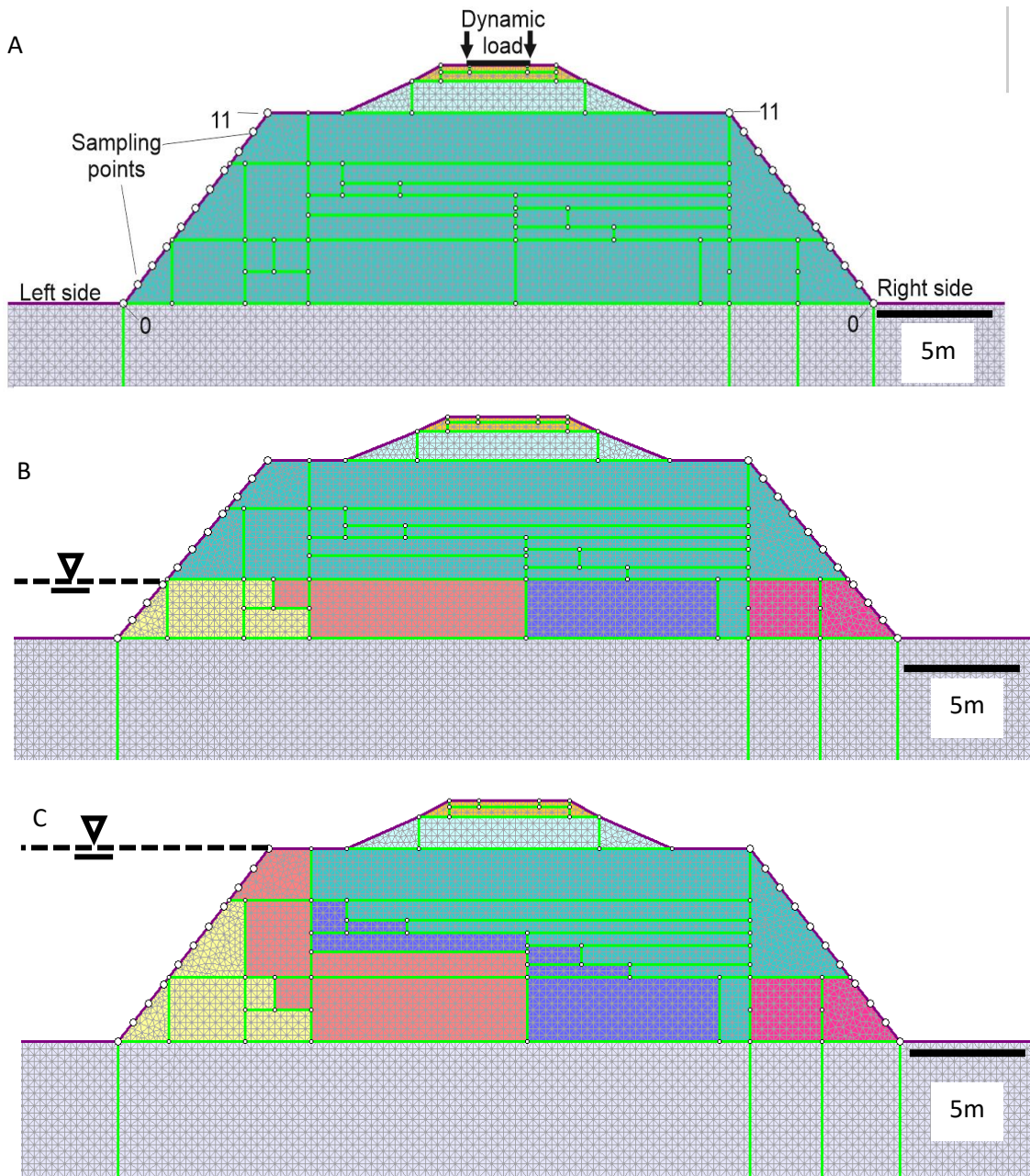
The long-term destabilisation of embankments poses potential risks to the safe operation of infrastructure. Weakening of slopes has been recorded as a result of processes including wetting-drying cycles (Stirling et al., 2021) and flooding (Polemio and Lollino, 2011). These processes may alter material properties including strength, stiffness, and permeability (Chang and Zhang, 2011, Alramahi et al., 2010, Ke and Takahashi, 2012). Slope weakening may cause immediate failure (e.g. Bisantino et al., 2016). However, an understudied area of potential hazard is the effect of slope material alteration on the dynamic response of slopes during live loading.

Live loading of embankments caused by trains has the potential to cause significant ground vibration development, both within and external to the rail infrastructure (Olivier et al., 2016, Connolly et al., 2015). Increases in train speeds caused by high-speed rail development have the potential to create more damaging vibrations, with potential to cause annoyance to humans, building damage and degradation of rail and earthwork safety (Paolucci et al., 2003, Nelson and Saurenman, 1983, Bian et al., 2016). Rail-induced vibrations are more problematic in areas with soft soils (Madshus and Kaynia, 2000). The majority of potential harmful effects are caused by vibrations in the 0 - 10 Hz frequency range (Paolucci et al., 2003); vibrations above 60 Hz, which are primarily caused by train-track-embankment interaction rather than vehicle passage and train speed, contain small amounts of power in comparison to lower frequency vibrations (Nelson and Saurenman, 1983, Connolly et al., 2014).

Research into understanding railway-induced vibrations in embankments has previously been undertaken via field measurement of embankment response to live loading. Measurement of high-speed train passage shows that the majority of wave power is in the frequency range of 0 - 50 Hz (Degrande and Lombaert, 2000) and that the frequency of excitation due to train passage, as opposed to rail or ground excitation, is in the range of 2 - 50 Hz (Connolly et al., 2014). Numerical modelling to understand the effects of embankment composition on vibration development has primarily been undertaken using boundary element and finite element models. 3D finite element method (FEM) model analysis has shown that stiffer embankments decrease vibrations away from rail tracks, whereas softer embankments cause increased displacement within rail embankments due to 'trapping' of wave energy in the embankment body (Connolly et al., 2013). Peak particle velocity alteration due to variation in embankment stiffness was also identified by Kouroussis et al. (2016) using FEM, who found that five-fold increases and decreases in the

Young's Modulus of embankment materials caused significant respective reductions and increases in peak particle velocity. A five times change in Young's Modulus is a significantly greater property range than found in soils; at a constant confining pressure, Salgado et al. (2000) reported Young's Modulus increases of a maximum factor of two due to changes in the fines content of sands. In laboratory testing reported in Chapter 3, Young's Modulus increases and decreases of up to 35% of initial values were observed following seepage, when calculated using the assumption of uniform material loss in samples. When soil stiffness is significantly reduced, train velocity can become greater than the critical velocity of the ground, causing significant excess vibrations (Kouroussis et al., 2016, Madshus and Kaynia, 2000). In addition to defining displacements caused by train loading, comparative 2D FEM models have also been used to calculate the effects of changes to rail structures on vibration levels (Andersen and Jones, 2006). Boundary element modelling, which in certain circumstances is more computationally efficient than FEM, has also been used, either alone or in conjunction with FEM, to assess ground vibrations from train loading (e.g. Sheng et al., 2006), with the limitation of not assessing internal slope behaviour.

Studies considering the effects of differential embankment material change caused by long-term destabilisation processes have not been identified. These changes have the potential to increase the amount of vibration in and away from embankments, and cause differential vibrations across slopes to develop. Of principle interest in this chapter is considering how flood-induced embankment material alteration identified from the results in Chapters 3 and 4 may cause changes to a slope's response to dynamic loading when live loading occurs, taking into account both property changes and locations of material changes. Consideration was made of both differences in the dynamic response between unaltered and altered materials, and the potential for the development of differential displacement across a single altered slope. A modelling approach was taken for two primary reasons. Firstly, the modelling approach provides an ability to assess multiple different scenarios in a controlled manner. Secondly, the approach avoids the difficulty of accessing and testing in field environments on embankments with known conditions — the difficulties of which were exacerbated by access limitations enforced by COVID-19 restrictions. The aim of this chapter is to understand the degree to which flood-induced alteration may cause changes in displacement behaviour on embankment slopes caused by dynamic loading.



Ground Ballast Embankment 1 Embankment 3 Embankment 5 Embankment 5
 Subgrade Load slab Embankment 2 Embankment 4 Embankment 5

Figure 26: Locations of material zones used in the altered models. a) Uniform model b) Basal alteration (BO-AM) c) Large scale embankment alteration (FS-AM). The same material regions and mesh were applied to all three models. The ground below the model continued uniformly to a depth of 40 m. Material properties are defined in Table 1. In B and C theoretical water table level is indicated by black dashed lines. Sampling point location descriptions and dynamic load inputs are labelled in A, and the same sampling points and load locations were used in all models. Sampling points were numbered 0-11 left and right, with 0 at the base of the embankment body on each side. Sampling points had a 0.5 m horizontal spacing.

5.2 Methods

5.2.1 Modelling structure

Models were created using the finite element method modelling software RS2, from Rocscience, which allows for dynamic 2D plane-stress and plane-strain analysis. Dynamic finite element modelling was used due to the ability to couple complex material property geometries and defined dynamic loading with relative computational efficiency. RS2 was used as the program is capable of creating non-grid aligned slope and material boundaries, and to produce flexible meshing of more complex shapes. 2D plane strain models, which calculate stress-strain changes in the x-y plane, but do not account for changes in the z plane, and use the assumption of infinitely uniform material properties in the z plane, were preferred over more computationally expensive 3D models. Full 3D models take multiple orders of magnitude longer to run than 2D models (Andersen and Jones, 2006). The primary limitation of the 2D dynamic models is that they do not account for the directional progression of a wave front and potential interaction of the rail loading and ground waves along the length an embankment which occurs in the un-modelled z plane. The magnitude of particle displacement in the un-modelled z orientation and modelled x orientation, parallel and perpendicular to embankment length, respectively, are comparable (Connolly et al., 2014).

2D models were created representing a granular embankment overlying a uniform substratum. Three models were assessed; all three models were identical apart from material properties within the embankment (Figure 26, Table 11). Firstly, a model with uniform material properties throughout the embankment section was used, designed to represent the simplified condition of an unaltered embankment, henceforth referred to as the 'uniform model' (Figure 26a). Secondly, model BO-AM with material alteration only along the basal portion of the slope (Figure 26b), and thirdly model FS-AM, with material alteration through a larger portion of the embankment (Figure 26c). The altered material properties were allocated to create a slope with conditions representing the migration of fine particles through an embankment body, caused by flooding-induced seepage. The model with a larger degree of alteration represents a condition where there is a higher floodwater level and more extensive seepage than the model with basal material property changes only. Material properties used in the models are shown in Table 11.

Table 11: Material properties used in the models. Properties for the load slab, ballast and subgrade were taken from Connolly et al. (2013). Poisson's Ratio, which varies from roughly 0.15-0.45 in soils (Olivier et al., 2016, Suwal and Kuwano, 2012) was set at a constant 0.3 for the embankment body.

Material number	Unit weight, kNm ⁻³	Young's Modulus, MPa	Poisson's Ratio
1. Rail load slab	79	210	0.25
2. Ballast	18	80	0.35
3. Subgrade	21	120	0.35
4. Substrata	17.3	15	0.3
5. Embankment 1	16	25	0.3
6. Embankment 2	16.5	30	0.3
7. Embankment 3	17	35	0.3
8. Embankment 4	17.5	45	0.3
9. Embankment 5	18	55	0.3

5.2.2 Model design

The models were meshed with three noded triangular elements with two degrees of freedom per node, in the vertical and horizontal orientations. A uniform mesh, with element length of 0.2 m, was used within the model with the exception of irregularly shaped triangular material regions, which necessitated non-uniform meshing. All materials were modelled as isotropic and linearly elastic. All models created used the same model design, including material boundaries and mesh, with the only alterations between models the material properties within the embankment body (Table 11). The locations of material alterations in the altered models BO-AM and FS-AM (Figure 26) were based on the results from laboratory testing presented in Chapter 4 and wider literature (e.g. Horikoshi and Takahashi, 2015); the theoretical flood head was located on the left side of the modelled embankment. The magnitude of property alteration was based on changes in material properties described in Chapter 3, in addition to wider literature (Chang and Zhang, 2011, Alramahi et al., 2010). The locations of material zones are shown in Figure 26 and properties of individual material zones displayed in Table 11. The slope model used had steeper embankment batters, approximately 50°, than is commonly found in transportation embankments, where slope angle is commonly lower than 30°. Though the presence of steeper embankment sides makes the model less realistic, as it is greater than the angle of

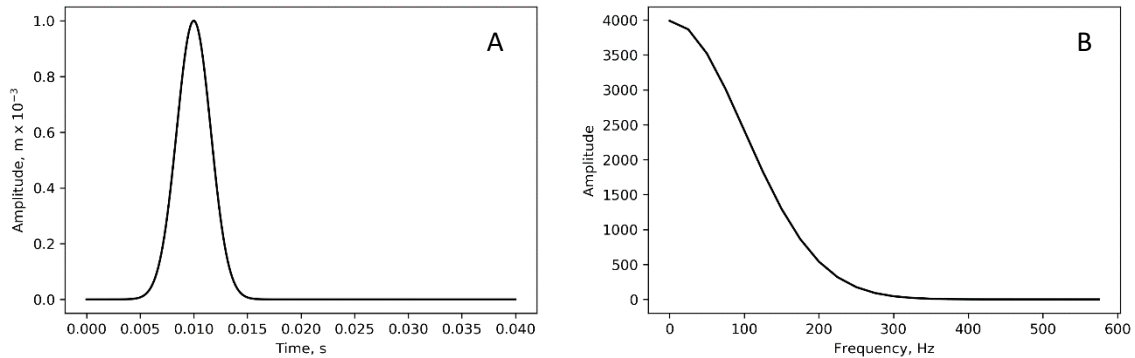


Figure 27: *Dynamic load Gaussian wave content. a) Time domain b) Frequency domain, calculated using a Fast Fourier transform.*

repose for many soils, the primarily reason for having steep slopes was due to the meshing requirements of the model. To create a more accurate model, it was necessary to have as close an amount of uniformly spaced nodes on each side of each meshing region as possible; the discrepancy between the number of elements on base and side of the meshing zones would have increased with low angled slope batters. There is potential that the steeper angle of the slope better altered the wave reflection behaviour, potentially increasing the amount of displacement within the embankment in comparison to a slope with lower angles.

The broad principle used during assignment of material properties was that the theoretical loss of fine particles from near the flood head inflow is represented by a decrease in density and stiffness, whilst the base of the outflow side of the slope has an increased density and stiffness, due to the theoretical deposition of fine particles. A dynamic load was applied to the centre of the embankment across a slab, not to rail heads. The horizontal and vertical dynamic responses of the slope were measured at a number of sampling points with half metre spacing along the embankment batters (Figure 26).

Dynamic loading of the models used a displacement defined Gaussian wave pulse (Figure 27), applied to a stiff slab representing a rail-sleeper system. A Gaussian wave allowed for the effects of a range of frequencies to be considered; a displacement defined load was used to represent the loading caused by a train wheel-rail interface (Connolly et al., 2013). The applied displacement amplitude of 1mm (Figure 27a) is similar to displacements caused by train passage over high quality subgrades, which were measured in the range of 0.5mm – 2mm depending on train type (Murray, 2015). Using a Gaussian wave pulse has the additional benefit of providing a simpler source than a dynamic input representing a train-loading event. To ensure accurate displacement calculation, a minimum element length : wavelength ratio of 1 : 5 was considered valid (Papadakis and Stavroulakis, 2018), resulting

in output frequencies of up to 70 Hz being considered accurate based on the lowest velocity material modelled. Higher frequency waves contain shorter wavelengths, thus reducing the element length : wavelength ratio. Results for higher frequency waves therefore contain larger errors and become unreliable. The models were run with a time step of 1×10^{-5} seconds. The models were produced with absorbing boundaries, in addition to large basal boundary distances, to limit the effects of reflected waves which exit the embankment on altering displacements measured in the embankment slope.

Results from the models are presented in a comparative fashion as ‘transfers’ which compare, across a range of frequencies, the response signals of the uniform and altered models’ outputs at given x-y coordinates along the embankment boundaries. Transfers are presented for particle displacement in the horizontal ‘x’ and vertical ‘y’ orientations. Measurements were taken every 0.5 metres along each embankment batter.

5.2.3 Transfer functions

The transfer functions presented divide the displacement outputs for two sets of data, specifically they show the ratio of two signals evaluated in the frequency domain. Frequency domain data was calculated by applying a Fourier Transform to the time series model output data. Two different types of transfer are reported. Firstly, results from opposite sides of the embankment from the same model run show the differential change in displacement across the slope caused by differential material alteration. Secondly, a comparison of change at the same sampling points between the uniform model and each of the altered models, showing the effects of different degrees of material change on displacement behaviour. Descriptions of the contents of each of the transfer functions presented are given in

Table 12.

If a transfer value > 1 was produced, then a larger amplitude response magnitude was recorded. If a transfer value of 1 was produced, the two datasets had the same output at the given point. If a transfer value < 1 was produced, a decrease in displacement was observed (Figure 28, Table 12). Transfer values are presented on logarithmic scales; a transfer value of 0.2 represents a 5 times decreased amplitude response while a transfer value of 5 represents a 5 times increase in magnitude response. As the transfer functions represent the differences between the two models, the initial model displacement values do not represent realistic values for a train-loading scenario. As the models were identical apart from the material properties, any differences in the outputs were caused by the

differential material properties used, not from other factors such as meshing. In Figures 30-36, transfer values are presented chromatically on the 'z' axis. An increase in signal amplitude, a transfer value > 1, is shown in red and a decrease in signal amplitude, a transfer value < 1, in blue.

Table 12: Detail of the contents of transfer functions presented in results.

Group description	Model description	Figure
Transfer value shows how the same sampling point changes behaviour between the unaltered and altered model. Transfer value = altered model / uniform model.	Compares horizontal displacement data for uniform and altered model results for left hand embankment batter	30b, 33b
	Compares horizontal displacement data for uniform and altered model results for right hand embankment batter	31b, 34b
Deeper red – altered model had a higher displacement at this location and frequency. Deeper blue – uniform model had a higher displacement at this frequency.	Compares vertical displacement data for uniform and altered model results for left hand embankment batter	30a, 33a
	Compares vertical displacement data for uniform and altered model results for right hand embankment batter	31a, 34a
Transfer shows differential behaviour between sampling points at the same height on opposite sides of the slope. Transfer value = right batter / left batter. Deeper red – the right hand side of the model had a higher vibration than the left at this sampling height and frequency. Deeper blue – the left hand side of the model had a higher vibration at this frequency and location.	Compares the horizontal displacement data for the left and right embankment batters in the altered models.	32a, 35b
	Compares the vertical displacement data for the left and right embankment batters in the altered models.	32b, 35a
	Compares the horizontal displacement data for the left and right embankment batters in the uniform models.	36b
	Compares the vertical displacement data for the left and right embankment batters in the uniform models.	36a

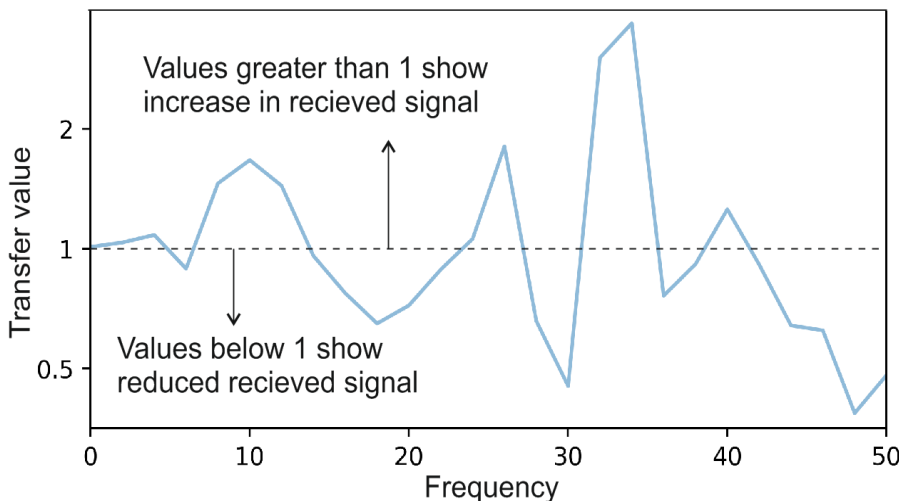


Figure 28: Example transfer graph for an individual sampling point. The transfer value represents a change in signal amplitude between two datasets and is calculated for each frequency.

5.3 Results

5.3.1 Displacement – frequency relationship

The Fourier transform of the recorded signals (Figure 29) shows that the measured vertical displacement predominantly had power in the frequency range of 0-10 Hz. The displacement magnitude was smaller in the horizontal orientation than in the vertical orientation (Figure 29) and retained a higher proportion of its initial power over a larger frequency range.

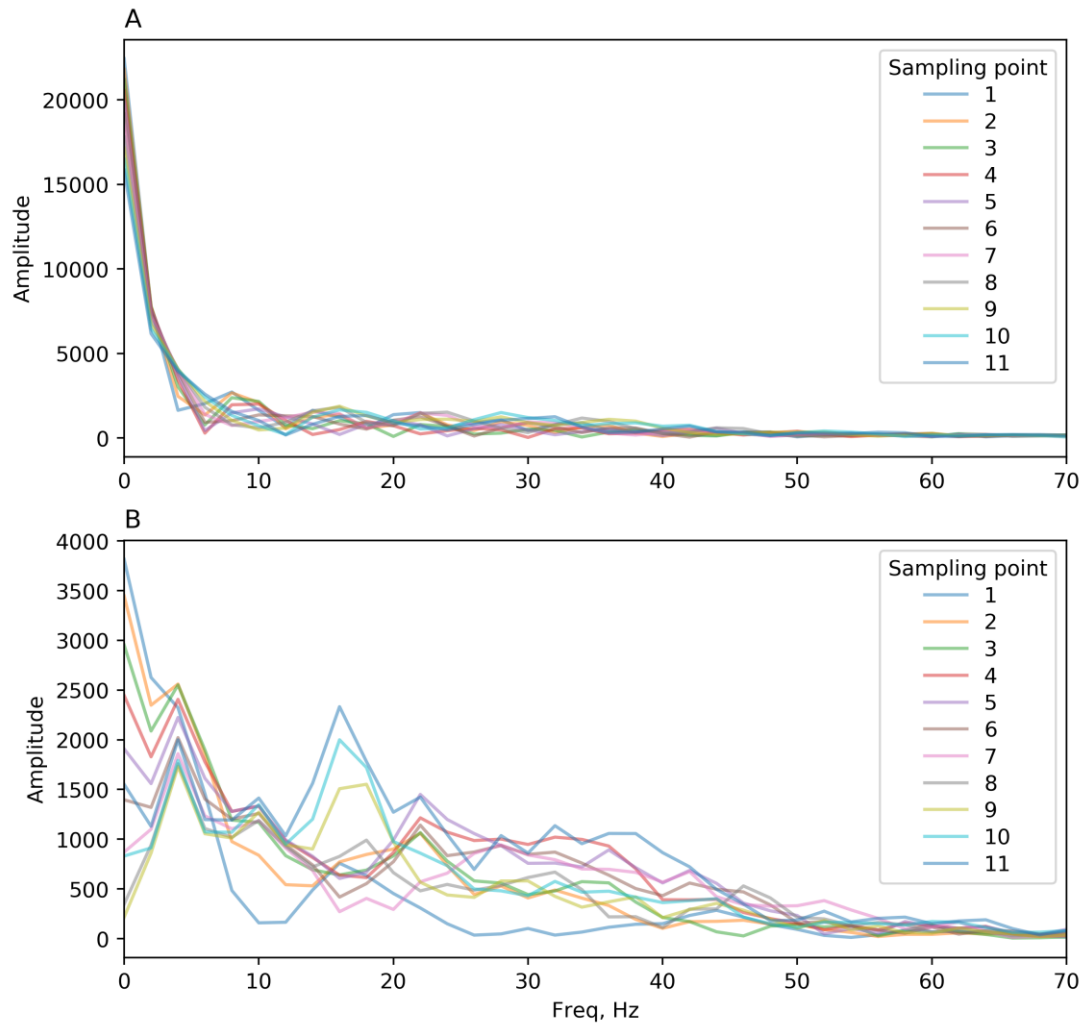


Figure 29: Fourier transform of displacement signal, displaying power – frequency relationship for all sampling points on the left hand slope face for the uniform model (the right hand slope face and altered model displayed displacements of a comparable amplitude). a) Vertical displacement b) Horizontal displacement.

5.3.2 Base only altered model (BO-AM)

5.3.2.1 Left slope batter

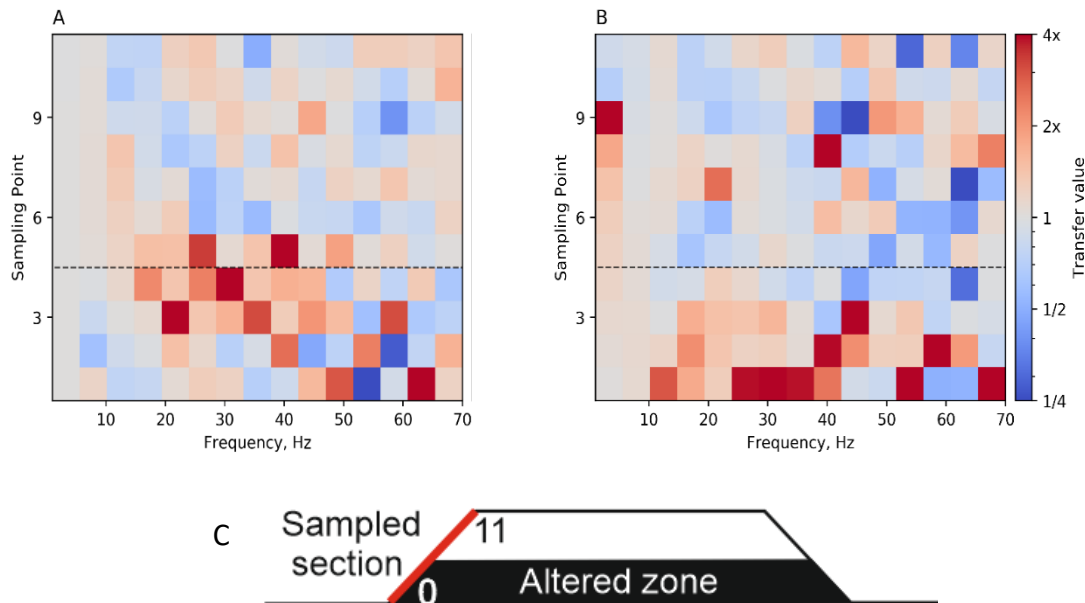


Figure 30: Transfer functions for the BO-AM left embankment batter for a) Vertical displacement and b) horizontal displacement. The horizontal dashed black line across the plot denote points at which material boundaries were present on the slope face. c) The red line denotes the location of sampling points, with the black area the section of the slope where material alteration was modelled.

If there was no effect of the material properties on displacement behaviour of the slope then the transfer values comparing the uniform and altered models should uniformly be equal to 1. As the transfer values presented are not solely equal to 1, there is an effect of material property change on slope behaviour.

Increased displacement in the BO-AM, in comparison to the unaltered model, was present in the lower sections of the slope (Figure 30), across the full range of frequencies, with increased amplification at higher frequencies. Alteration of vertical displacement was more pronounced than horizontal displacement, with higher amplitude alteration recorded over an increased range of frequencies and to a greater height in the slope. Displacement amplification was recorded above the zone of material alteration in the vertical displacement data, a trait less frequently observed in horizontal displacement data. At the lowest frequencies, where the highest amounts of absolute wave power were observed, there was a smaller degree of amplification of horizontal displacement and a decreased displacement response in the vertical displacement data. The zones of increased displacement in the BO-AM are consistent with the regions of lower material density and stiffness.

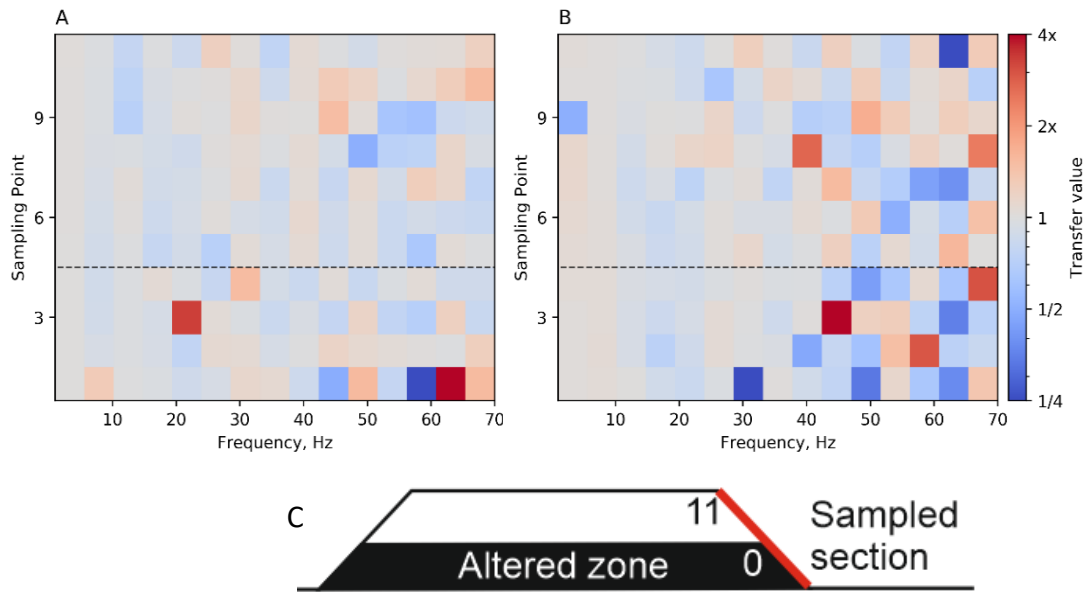


Figure 31: Transfer functions for the BO-AM right hand embankment batter, for a) Vertical displacement and b) horizontal displacement. The horizontal dashed black line across the plot denote points at which material boundaries were present on the slope face. c) The red line denotes the location of samling points, with the black area the section of the slope where material alteraion was modelled.

5.3.2.2 Right slope batter

There was, overall, a smaller amount of change in the right-hand embankment batter (Figure 31) than the left-hand embankment batter, in comparison to the unaltered model. The degree of horizontal displacement change was greater than vertical displacement. Reductions in displacement were predominantly seen in the horizontal displacement data below sampling point 4, with exceptions at 45 and 60 Hz, with larger magnitudes of change observed at higher frequencies.

5.3.2.3 Differential displacement alteration

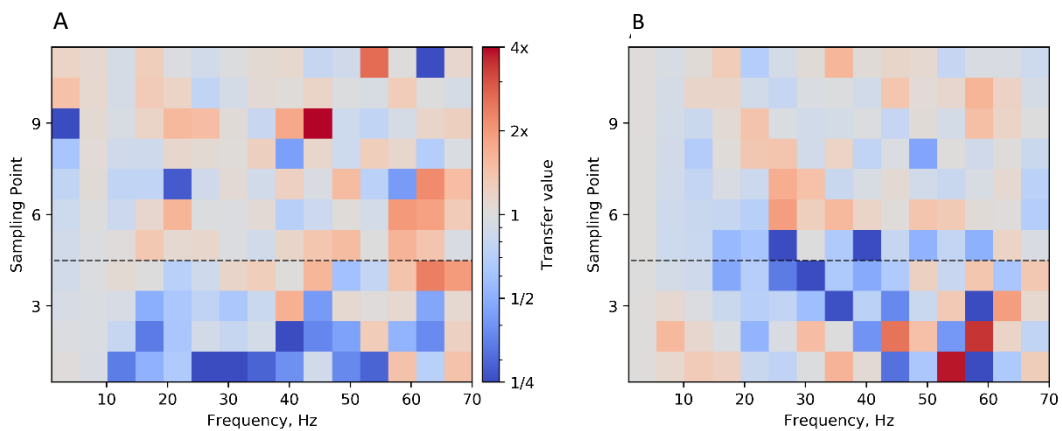


Figure 32: Transfer functions for the BO-AM showing differential change between the right and left sides of the embankment, for a) Horizontal displacement and b) Vertical displacement. The horizontal dashed black line across the plot denote points at which material boundaries were present on the slope face.

In the BO-AM, notably higher horizontal displacement was observed in the base of the slope, below sampling point 4, on the left-hand embankment batter than the right-hand embankment batter (Figure 32). The highest intensity of reduction was in the frequency range 20-50 Hz. This is consistent with there being a lower-density, less stiff, material in the basal region on the left hand side of the slope. On the left side of the slope the reduction in vertical displacement was less well defined than the reduction in horizontal displacement, with reduction being over a lower frequency range and slightly higher in the slope.

5.3.3 Full slope altered model (FS-AM)

5.3.3.1 Left embankment batter

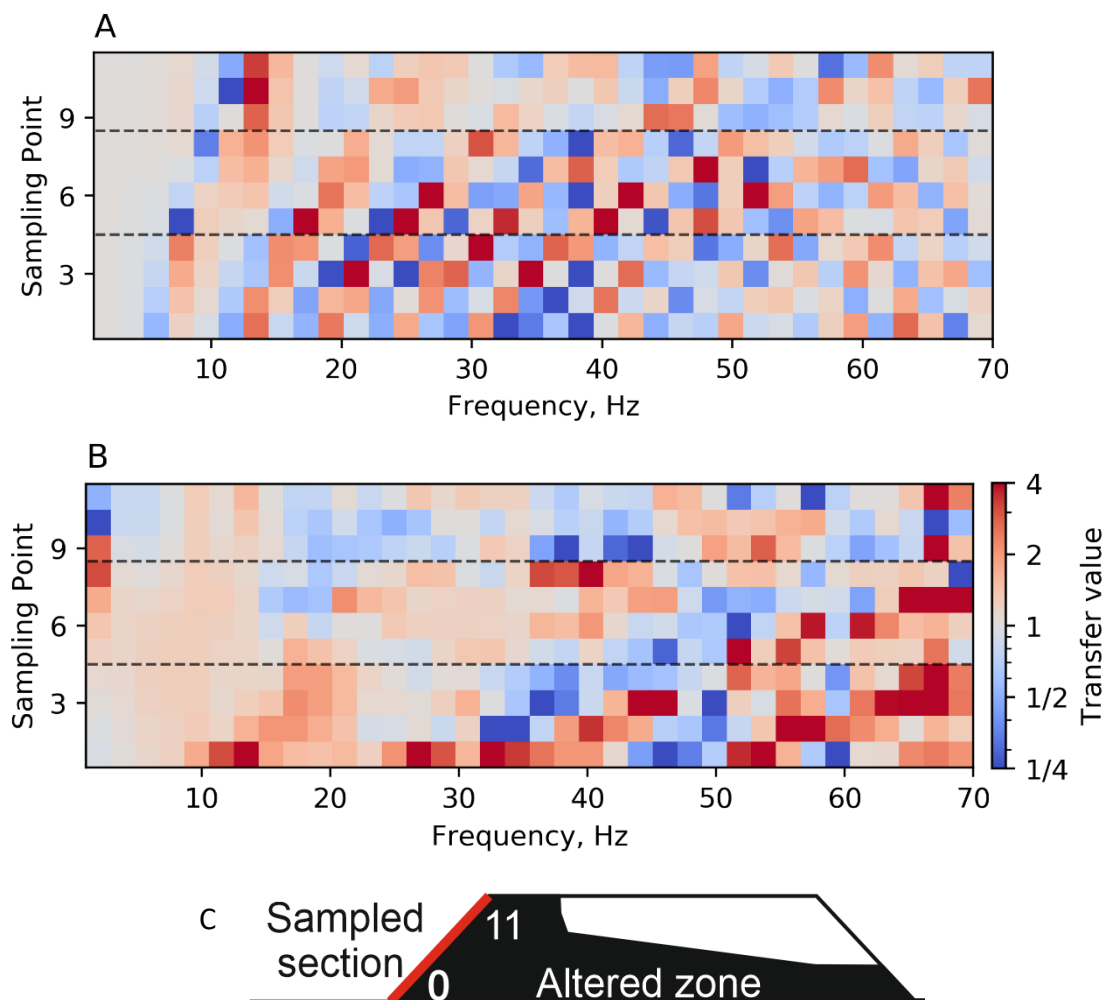


Figure 33: Transfer functions for the FS-AM left embankment batter for a) Vertical displacement and b) horizontal displacement. The horizontal dashed black lines across the plot denote points at which material boundaries were present on the slope face. c) The red line denotes the location of sampling points, with the black area the section of the slope where material alteration was modelled.

On the left-hand side of the FS-AM model slope, zones of predominantly increased signal response in the horizontal direction were observed (Figure 31), in comparison to the unaltered model, with the effect most notable below 20 Hz and above 50 Hz (Figure 33b). The increase in signal response was larger in the lower sections of the slope, below sampling point 5, and had a higher magnitude of change at higher frequencies. Alteration predominantly occurring towards the base of the slope is consistent with the widest areas of material alteration and least dense regions of the slope. As the displacement amplitude of the output wave decayed towards higher frequencies (Figure 29), the effects of signal amplification on slope performance would be reduced in areas with high frequency response alteration.

On the left-hand side of the FS-AM slope (Figure 33a), a small vertical displacement reduction was present in the altered model in the lowest frequencies, up to approximately

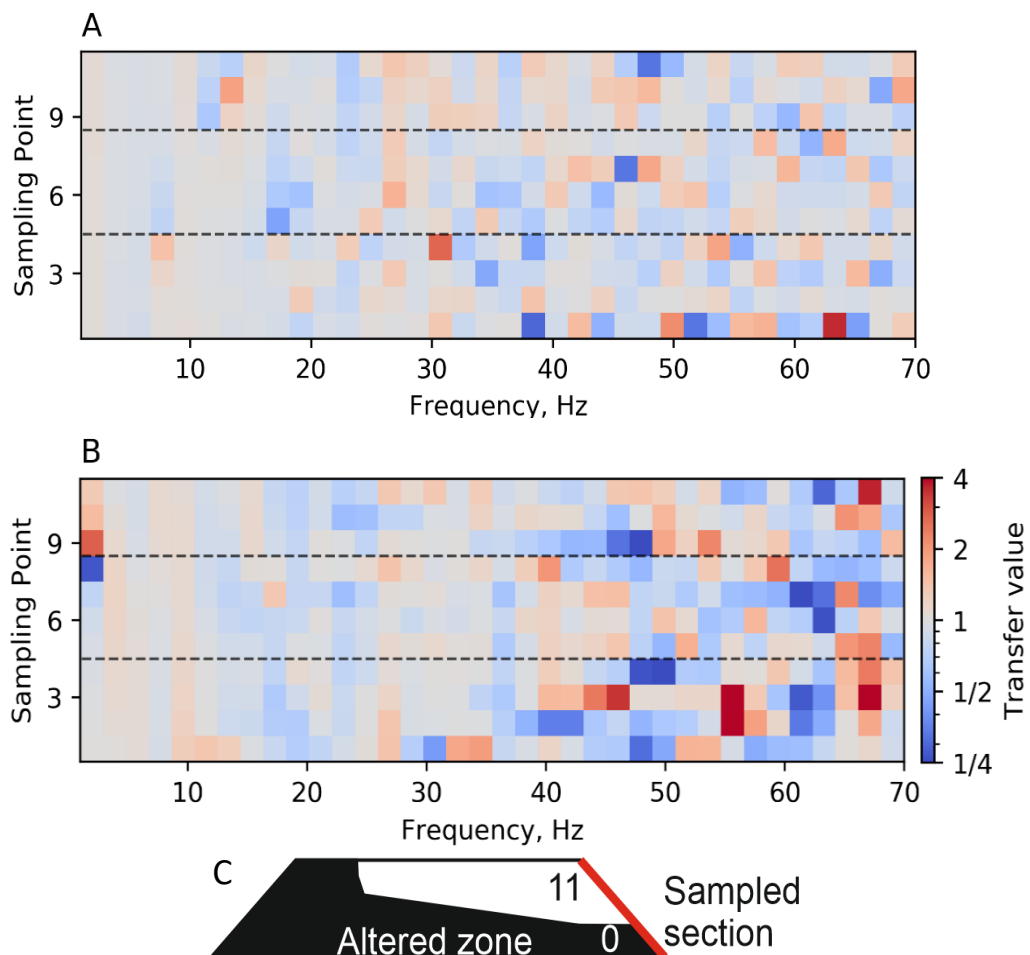


Figure 34: Transfer functions for the FS-AM right embankment batter for a) Vertical displacement and b) horizontal displacement. The horizontal dashed black lines across the plot denote points at which material boundaries were present on the slope face. c) The red line denotes the location of sampling points, with the black area the section of the slope where material alteration was modelled.

5 Hz, at the base of the slope and from 0-10 Hz towards the crest of the slope, in comparison to the unaltered model. The magnitude of signal change was greater towards the base of the slope, where material was more significantly altered. From 10-50 Hz, a series of banded displacement increases and decreases were observed in the transfer function value, with the inter-peak frequency range increasing towards the crest of the slope. Furthermore, the frequencies at which the banding initiates increase towards the slope crest. Above approximately 55 Hz, the banded nature of the frequency change continues, however the transfer function values became closer to unity (Figure 33a) and a secondary banding is present transverse to the primary structure.

5.3.3.2 Right embankment batter

On the right-hand side of the modelled slopes, there was little change in the vertical signal response between the unaltered and FS-AM model, with greater magnitude changes observed towards the base of the slope, below sampling point 5 (Figure 34a). There was little change in the horizontal displacement below 45 Hz; at higher frequencies larger changes in displacement were observed, with the greatest differences being towards the base of the slope (Figure 34b). There were notably lower relative differences between the altered and unaltered models in the frequency ranges which have higher power (Figure 29); larger absolute variation is needed between models if there is higher wave power in the uniform model to produce an equal transfer value.

Smaller changes in vertical displacement between the unaltered models and both altered models were observed on the right-hand side of the slope than on the left side. This is consistent with more widespread material alteration on the left side of the slope and more concentrated towards the base on the right-hand side of the slope.

5.3.3.3 Differential changes

The rhythmic changes observed in the vertical displacement data for the left-hand embankment batter (Figure 33a) were also observed in a similar fashion in the differential displacement between the two sides of the FS-AM slope (Figure 35a). There were comparatively minor variations in the right side of the FS-AM slope and rhythmic behaviour was not observed. The differences in horizontal displacement between the left and right sides of the FS-AM slope were more pronounced. There was a general increase in the amount of vibration recorded on the left-hand embankment batter in comparison to the right-hand embankment batter on the FS-AM slope (Figure 35b). Increased displacement is observed on the right-hand batter towards the top of the FS-AM slope, and from 30–35 Hz towards the base of the slope.

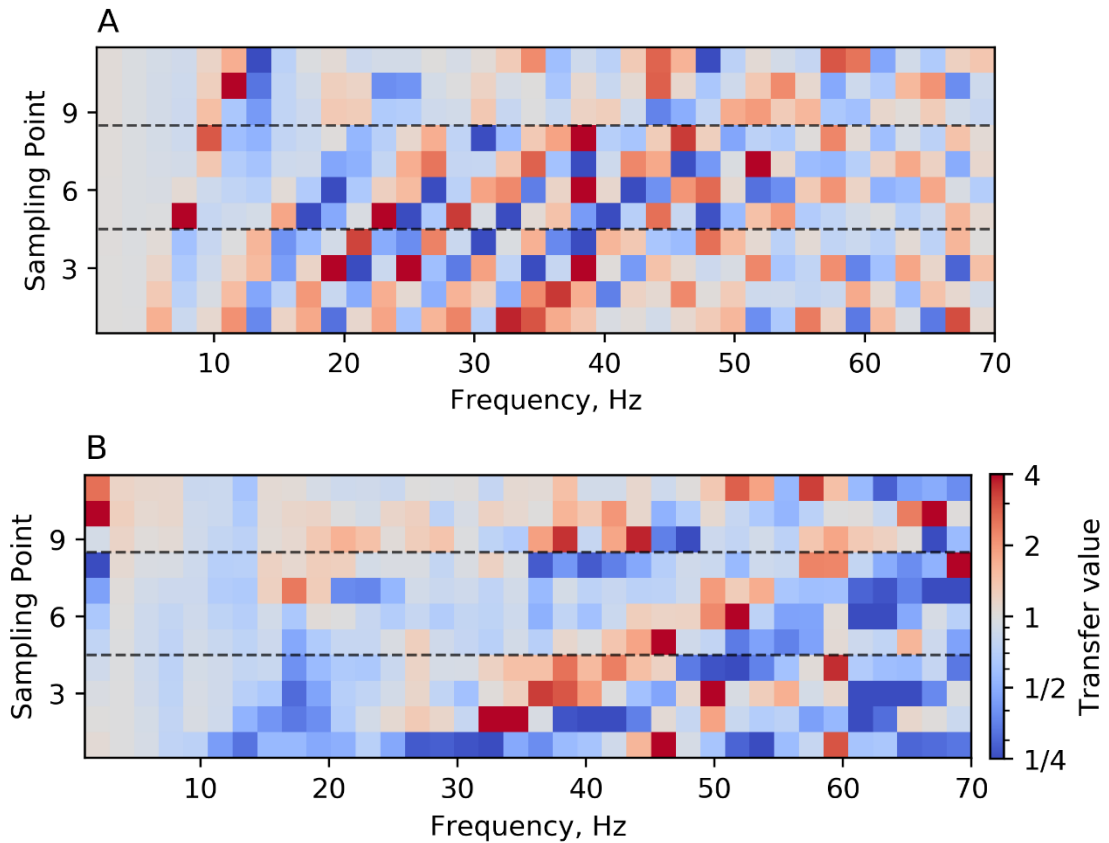


Figure 35: Transfer functions for the FS-AM showing differential change between the right and left sides of the embankment, for a) Vertical displacement and b) Horizontal displacement. The horizontal dashed black line across the plot denote points at which material boundaries were present on the slope face.

On the whole, relative changes in vertical particle displacements, those measured in the 'y' orientation, between the unaltered model and the FS-AM were of a lower magnitude than in the horizontal 'x' orientation. Although the changes in vertical displacement between the uniform and altered models are smaller than in the horizontal direction, the absolute magnitude of displacement was greater (Figure 29).

5.3.4 Uniform model

Theoretically, displacement values should be the same on both sides of the uniform slope, yet differences were present. At low frequencies, variations between the left and right of the uniform slope were not evident (Figure 36). Noticeable differences between the left and right sides of the uniform slope initiated at 20 Hz, and became more prominent above 50 Hz, more so in the horizontal displacement data. The 50 Hz increase coincides with the significantly reduced wave power observed (Figure 29).

5.3.5 Basal alteration – full slope alteration comparison

The changes observed for the BO-AM and FS-AM models were broadly comparable, with increases in displacement on the left-hand embankment batter which were of greater

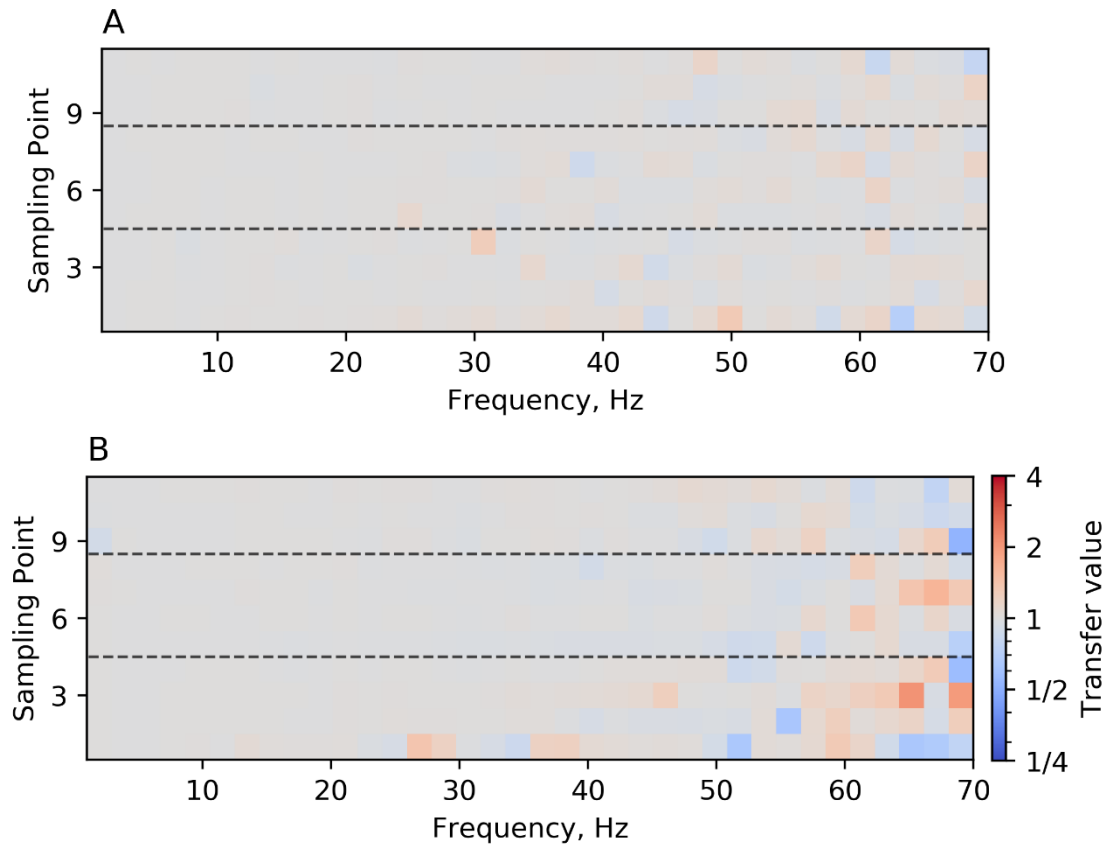


Figure 36: Transfer functions for the uniform model showing differential change between the right and left sides of the embankment, for a) vertical displacement and b) horizontal displacement. Black dashed lines represent the point mesh changes met the slope boundary.

magnitude towards the base of the slope, where a greater reduction in material density and stiffness is present. Reductions in displacement towards the base of the right-hand side of the slope were also observed, which is consistent with the regions of highest material density.

A key difference in displacement behaviour between the two models is that the changes identified occur over a greater proportion of the FS-AM slope, which is to be expected given that there is a greater amount of material alteration. The second difference between the behaviour of the two slopes is the presence of a banded alteration on the left-hand side of the uniform model in the vertical displacement data.

5.4 Discussion

Reduced displacement in sections of embankments constructed of stiffer materials, and increased displacement in slopes constructed of less dense materials, is consistent with observations from previous studies, which showed higher displacements in embankments composed of rarer materials (Olivier et al., 2016, Connolly et al., 2013). Larger displacement

variations observed on the left side than the right side of the FS-AM model are likely due to there being a larger area of material alteration. The relationship between material alteration area and displacement behaviour is also observed between the BO-AM and FS-AM models; more localised regions of displacement change which occurred in the BO-AM, and with lower magnitudes of change, are consistent with the smaller zones of material alterations present in the model.

The banding observed in the vertical displacement data of the left side of the FS-AM is likely due to superposition of waves reflected off internal material boundaries. This is thought to have developed at higher frequencies towards the top of the slope due to the narrowing of the altered material zone (Figure 26c), meaning that reflections occurred at higher frequencies. This effect is likely to develop to a lesser degree in real embankments, as in real embankments material alteration will probably occur not with discrete boundaries, but with continuous gradation between zones of higher and lower material stiffness and density — which would cause refraction to develop.

Displacement alteration between the altered and uniform models occurred across the measured frequency range. Larger displacements were predominantly recorded in the frequency ranges of 0- 20 Hz and 50-70 Hz in both the BO-AM and FS-AM models. During train loading of rail embankments, displacements from 0-20 Hz are primarily caused by vehicle passage. In the range 40-70 Hz displacements are caused by soil excitation and track deflection mechanisms, such as rail bending and wheel-track interaction (Connolly et al., 2014). Reduced train speeds will therefore reduce the effects of increased vibrations.

The fact that displacement changes become more noticeable in higher frequencies across the majority of models - including the left and right sides of the theoretically uniform unaltered model, especially above 50 Hz - was potentially due to wave reflections from slope faces and embankment-ground contact. The decreases in wave power in these higher frequency ranges are also potentially a cause of alteration; due to the smaller absolute values, smaller variations are needed to cause a larger comparative change. The majority of the wave power being recorded in the range of 0-50 Hz is consistent with observed field vibrations from high-speed trains recorded by Olivier et al. (2016). Alternatively, the non-uniform mesh towards the slope edges and differences in meshing zones on the two sides of the model may cause minor changes to the model behaviour. The non-uniform mesh, coupled with the reduced wavelength : element length ratio at higher frequencies,

is also a potential explanation of the greater discrepancies between the two models at higher frequencies.

In addition to the generic negative effects of high train vibrations – including annoyance to humans and potential building damage (Connolly et al., 2016) – the stability of earthworks may also be affected. There is the potential that increased vibration could accelerate the removal of fines from an embankment body during a flood event, as has been recorded in large-scale dynamic loading of physical models (Jiang et al., 2015). This has the potential to cause a two-fold destabilisation scenario: directly reducing soil strength through particle loss and increasing loading due to reduced contact between track bed and embankment – in combination, these factors enhance the potential for failure. Fines removal coupled with increased vibration loading also has the potential to cause increased settlement (Bian et al., 2016, Dong et al., 2018), and may even result in liquefaction in situations where there are high pore pressures – such as during flooding (Pando et al., 2001).

5.5 Conclusion

Finite element modelling of rail embankments altered by internal erosion processes, which may result from flooding, shows that there is potential for increases and decreases in vibration to develop, depending on the material alterations which have occurred. Areas of reduced density and stiffness, representing areas of particle removal, show increases in displacement. Regions of increased material density show relatively smaller increases in displacement. Areas of slopes with larger volumes of altered materials, and with materials which have experienced a higher degree of alteration, resulting from longer alteration periods, are shown to have larger magnitude displacement alterations. Increased vibrations have the potential to cause localised material removal and excess loading if live loading of slopes occurred during flooding.

5.6 References

- ALRAMAHI, B., ALSHIBLI, K. A. & FRATTA, D. 2010. Effect of Fine Particle Migration on the Small-Strain Stiffness of Unsaturated Soils. *Journal of Geotechnical and Geoenvironmental Engineering*, 136, 620-628.
- ANDERSEN, L. & JONES, C. J. C. 2006. Coupled boundary and finite element analysis of vibration from railway tunnels—a comparison of two- and three-dimensional models. *Journal of Sound and Vibration*, 293, 611-625.
- BIAN, X., JIANG, H. & CHEN, Y. 2016. Preliminary Testing on High-speed Railway Substructure Due to Water Level Changes. *Procedia Engineering*, 143, 769-781.
- BISANTINO, T., PIZZO, V., POLEMIO, M. & GENTILE, F. 2016. Analysis of the flooding event of October 22-23, 2005 in a small basin in the province of Bari (Southern Italy). *Journal of Agricultural Engineering*, 47, 8.

- CHANG, D. & ZHANG, L. 2011. A Stress-controlled Erosion Apparatus for Studying Internal Erosion in Soils. *Geotechnical Testing Journal*, 34, 579-589.
- CONNOLLY, D., GIANNOPOULOS, A. & FORDE, M. C. 2013. Numerical modelling of ground borne vibrations from high speed rail lines on embankments. *Soil Dynamics and Earthquake Engineering*, 46, 13-19.
- CONNOLLY, D. P., KOUROUSSIS, G., LAGHROUCHE, O., HO, C. L. & FORDE, M. C. 2015. Benchmarking railway vibrations – Track, vehicle, ground and building effects. *Construction and Building Materials*, 92, 64-81.
- CONNOLLY, D. P., KOUROUSSIS, G., WOODWARD, P. K., ALVES COSTA, P., VERLINDEN, O. & FORDE, M. C. 2014. Field testing and analysis of high speed rail vibrations. *Soil Dynamics and Earthquake Engineering*, 67, 102-118.
- CONNOLLY, D. P., MARECKI, G. P., KOUROUSSIS, G., THALASSINAKIS, I. & WOODWARD, P. K. 2016. The growth of railway ground vibration problems — A review. *Science of The Total Environment*, 568, 1276-1282.
- DEGRANDE, G. & LOMBAERT, G. High-speed train induced free field vibrations: in situ measurements and numerical modelling. Proceedings of the international workshop wave, 2000. 29-41.
- DONG, K., CONNOLLY, D. P., LAGHROUCHE, O., WOODWARD, P. K. & ALVES COSTA, P. 2018. The stiffening of soft soils on railway lines. *Transportation Geotechnics*, 17, 178-191.
- HORIKOSHI, K. & TAKAHASHI, A. 2015. Suffusion-induced change in spatial distribution of fine fractions in embankment subjected to seepage flow. *Soils and Foundations*, 55, 1293-1304.
- JIANG, H., BIAN, X., CHEN, Y. & HAN, J. 2015. Impact of Water Level Rise on the Behaviors of Railway Track Structure and Substructure. *Transportation Research Record: Journal of the Transportation Research Board*, 2476, 15-22.
- KE, L. & TAKAHASHI, A. 2012. Strength reduction of cohesionless soil due to internal erosion induced by one-dimensional upward seepage flow. *Soils and Foundations*, 52, 698-711.
- KOUROUSSIS, G., CONNOLLY, D. P., OLIVIER, B., LAGHROUCHE, O. & COSTA, P. A. 2016. Railway cuttings and embankments: Experimental and numerical studies of ground vibration. *Science of The Total Environment*, 557-558, 110-122.
- MADSHUS, C. & KAYNIA, A. M. 2000. High-speed railway lines on soft ground: Dynamic behaviour at critical train speed. *Journal of Sound and Vibration*, 231, 689-701.
- MURRAY, C. A., TAKE, W.A. AND HOULT, N.A., 2015. Measurement of vertical and longitudinal rail displacements using digital image correlation. *Canadian Geotechnical Journal*, 52, 141-151.
- NELSON, J. T. & SAURENMAN, H. J. 1983. State-of-the-Art Review : Prediction and Control of Groundborne Noise and Vibration from Rail Transit Trains.
- OLIVIER, B., CONNOLLY, D. P., ALVES COSTA, P. & KOUROUSSIS, G. 2016. The effect of embankment on high speed rail ground vibrations. *International Journal of Rail Transportation*, 4, 229-246.
- PANDO, M. A., OLGUN, C. G., MARTIN, I. & JAMES, R. 2001. Liquefaction Potential of Railway Embankments. *International Conferences On Recent Advances In Geotechnical Earthquake Engineering And Soil Dynamics*. San Diego, California.
- PAOLUCCI, R., MAFFEIS, A., SCANDELLA, L., STUPAZZINI, M. & VANINI, M. 2003. Numerical prediction of low-frequency ground vibrations induced by high-speed trains at Ledsgaard, Sweden. *Soil Dynamics and Earthquake Engineering*, 23, 425-433.
- PAPADAKIS, N. M. & STAVROULAKIS, G. E. Effect of Mesh Size for Modeling Impulse Responses of Acoustic Spaces via Finite Element Method in the Time Domain. Proceedings of the Euronoise, 2018.

- POLEMIO, M. & LOLLINO, P. 2011. Failure of infrastructure embankments induced by flooding and seepage: a neglected source of hazard. *Natural Hazards and Earth System Sciences*, 11, 3383.
- SALGADO, R., BANDINI, P. & KARIM, A. 2000. Shear Strength and Stiffness of Silty Sand. *Journal of Geotechnical and Geoenvironmental Engineering*, 126, 451-462.
- SHENG, X., JONES, C. J. C. & THOMPSON, D. J. 2006. Prediction of ground vibration from trains using the wavenumber finite and boundary element methods. *Journal of Sound and Vibration*, 293, 575-586.
- STIRLING, R. A., TOLL, D. G., GLENDINNING, S., HELM, P. R., YILDIZ, A., HUGHES, P. N. & ASQUITH, J. D. 2021. Weather-driven deterioration processes affecting the performance of embankment slopes. *Géotechnique*, 71, 957-969.
- SUWAL, L. P. & KUWANO, R. 2012. Poisson's ratio evaluation on silty and clayey sands on laboratory specimens by flat disk shaped piezo-ceramic transducer. *Bulletin of ERS*, 45, 141-158.

Chapter 6

Synthesis and conclusions

Chapter summary

In this chapter, the results and findings from Chapters 2 to 5 are discussed in the context of the wider literature. In this framework, the separate research strands are summarised and drawn together in order to provide answers to the initial research questions and objectives identified in Chapter 1. The implications of the results for railway embankments are then identified, as are links to wider research fields. The limitations of the work conducted are reviewed. This chapter concludes with the identification of areas for further research that could be developed and a summary of the overarching conclusions.

Key findings include:

- The identification and classification of four types of flood which impact rail embankments. These are: overtopping, top of slope, offset head and basal floods.
- The term 'washout' should be reserved to describe the effect of a process and post failure geomorphological condition, and should not be used as a type of failure in and of itself.
- Along with immediate failure, there is the potential for flooding to cause lasting weakening of slopes. One of the potential weakening mechanisms is the redistribution of fine particles caused by seepage induced internal erosion.
- Internal erosion processes, namely suffusion, have the potential to cause alterations in material strength, stiffness and permeability. This effect may be differential across an embankment.
- The movement of fine particles, driven by differential flood head and caused by seepage processes, is primarily located along the base of slopes and along the water inflow surface. Fine particles are lost from the water inflow and deposited at the opposing slope base.
- Flooding induced material alteration has the potential to modify slope vibration caused by dynamic loading, with increases in displacement in regions of particle loss.

6.1 Overarching questions and objectives

6.1.1 *How do floods cause slope failure and lasting slope condition alteration to develop in transportation infrastructure?*

The processes which cause slope failure depend on the type of flood which occurs. A classification of four types of flood was produced in this work: offset head, overtopping, above slope, and basal floods. The main causes of destabilisation can be grouped as the effects of slope saturation and pore water pressure increases, scour and, in situations where offset head develops across a slope, internal erosion. Each of the identified flood types causes different slope processes to develop, as summarised in Table 13. The effects of these destabilisation processes may be amplified by the increased stresses caused by live loading, such as during the Barrow upon Soar and Acquaviva failures (Polemio and Lollino, 2011, RAIB, 2013a).

6.1.2 *To compile reports of global flood-induced embankment failures in order to identify (i) types of flood which affect embankments and (ii) flood-induced processes which promote slope destabilisation.*

Reports of flood-induced failures were collated from a range of global sources. Events were primarily identified through published research literature, news sources and online videos. More detailed assessment of UK data was possible due to input from industry and asset management agencies, primarily Network Rail and Highways England. Larger and more impactful events are better represented in the identified failure records as they are more likely to have been reported in open literature, whereas small failure events — even if multiple small failures occur during the same event — are less likely to have been recorded or only recorded as a single event. The under-reporting of the true number of slope failures which occurred following a major flooding event is typified by the widespread November 2021 floods in British Columbia, Canada (NASA, 2021), where it is difficult to obtain a detailed understanding of specific failure events due to the scale of flooding and infrastructure damage.

To mitigate this issue, the novel approach of assessing the number of flood events which cause failure, rather than the discrete number of failures, was utilised, with the benefit of quantifying the types of flood which may be hazardous. However, only recording the number of floods may mask the scale of a problem; a single flood event which causes scores of small failures may be classified in the same manner as an event which causes one large failure. From the recorded failures, three main destabilisation processes were

Table 13: Summary of destabilisation process development caused by each of the four identified flood types.

Flood type	Internal erosion	Scour	Saturation and pore water pressure
Offset head flood	Yes, if slopes are comprised of materials susceptible to internal erosion development.	Scour of slope sides when flowing floodwater is present	Yes, due to water infiltration into slope. Rapid drawdown effects may also develop following floodwater recession.
Overtopping flood	Yes, if slopes are comprised of materials susceptible to internal erosion development. Altered material may be removed due to crest erosion.	Scour of slope crest due to flow across slope.	Increases in water pressure in slope due to water infiltration. Rapid drawdown effects may also develop following floodwater recession
Above slope flood	Yes, but only in situations where there is a large flood head.	Scour down slope, due to water flowing over slope crest.	Yes, due to water percolation into slopes
Basal flood	No, as significant head differential does not occur.	Scour of base of slopes when water flowing	Increased water level in slopes due to reduced ability for water egress.

identified: internal erosion, scour, and wetting from development – all of which may be amplified by live loading processes. Although flooding causes wetting-drying cycles in soils, which have been shown to cause material deterioration (Stirling et al., 2021), internal erosion in the form of piping or suffusion/suffosion is likely to directly cause long-term slope destabilisation in materials comprised of susceptible materials. There is a differing propensity for lasting changes in material properties to develop depending on the flood type in question.

The lack of significant head development during basal floods means it is probable basal floods are of low susceptibility to causing lasting alteration from internal erosion. During basal flooding, the predominant failure trigger that is likely to develop is live loading of a slope weakened by pore pressure development, as seen during the Barrow upon Soar failure (RAIB, 2013a). Slopes affected by offset head floods have a higher susceptibility to alteration from internal erosion than basal floods as the prolonged presence of a differential head has an enhanced potential to cause particle migration. Alteration from internal erosion development in overtopping and above slope floods may occur, but the extent of this is likely to be site-specific and dependent on the extent of overtopping. Overtopping floods inherently initiate as offset head floods, however the development of crest erosion of slopes due to water overtopping is likely to erode altered material.

Furthermore, once overtopping develops, internal erosion is less likely to occur as there is no head differential across a slope. Top of slope floods have the potential to cause internal erosion development, but the presence of sufficient water head to drive significant particle migration is unlikely to develop during top of slope floods.

6.1.3 *To understand the magnitude of material property alteration caused by specific flood-induced processes, with a focus on the effects of seepage and internal erosion on strength, stiffness and permeability.*

Embankments which are composed of materials vulnerable to internal erosion and affected by flooding, which produces a differential head across the slope, are most likely to be subject to changes in material properties following flooding. From laboratory testing presented in Chapters 3 and 4, changes were measured in strength, permeability, shear wave velocity, average grainsize, C_c and material density following seepage. However, as the test apparatus did not permit constant monitoring of material loss or density at a given point in samples, it was not possible to calculate stiffness changes.

During triaxial seepage tests the highest shear wave velocity change recorded was a 19% increase, in test 30C (Chapter 3), with positive and negative V_s changes in the range of 0-7% of initial values recorded during all other tests. V_s changes were attributed to the removal and deposition of fine particles in the shear wave measurement zone. Test length permeability changes ranged from +120% to -90% of initial values. Permeability reductions potentially occurred due to the localised blocking of flow pathways, as has been observed during previous internal erosion testing (Chang and Zhang, 2013a). Decreased angle of friction values after seepage were found to occur following increased amounts of particle removal from samples. At low strains, <1%, strain hardening–softening cycles were observed during shear and smaller stiffnesses were observed during re-hardening (Figure 16). Friction angle reduction was likely due to the development of looser zones within samples where fine particles had been eroded; the associated development of sample heterogeneity due to particle erosion and deposition was also the likely cause of strain softening development at low strains. Across all model slopes, 4.5% reductions in mean grainsize and 9% increases in mean C_c were recorded in the slope toe region (Chapter 4).

Although it was identified that shear wave velocity change monitoring can be used to detect the development of internal erosion, the relationships between permeability and shear wave velocity changes due to particle migration were harder to define. The primary reason for this is that permeability was measured as a full sample value, controlled by the

least permeable section of a sample, whereas shear wave velocity measurements were measured as a point value, controlled by the behaviour of the material between the two bender element probes. As strength reductions are thought to be caused, in part, by the loss of fine particles it may be possible to identify these via measured reductions in shear wave velocity. Particle migration through and out of samples, which was found to increase with increased seepage volume, was identified as the overall control on material property changes during internal erosion. Due to measurement of material loss at a given time point in the triaxial tests undertaken (Chapter 3), it is difficult to assess the specific relationship between washout mass and material property change.

Higher temporal resolution measurement of material removal from samples would not inherently relate to changes in material behaviour, as localised particle deposition and removal within a sample would not be shown by full sample material loss measurement. Localised material movement is thought to control property change. Using shorter samples may help to resolve this, as there would be a more direct relationship between the mass of material removed from samples and the changes in properties, however using short samples would have the limitation of having only a small length of material within which to develop erosion and deposition.

6.1.4 *To identify the sections of slopes where changes in material properties are most likely to occur due to flood-induced seepage, and to evaluate the best material parameters to identify change.*

From scale model testing of slopes constructed with realistic soils (Chapter 4), it is clear that the primary regions of slopes which are affected by flood-induced seepage are regions nearest to water inflow and the base of the slope; similar particle distribution observations have been recorded during previous studies (Horikoshi and Takahashi, 2015). Fine particles were primarily removed from the area near the water inflow surface and deposited at the opposing slope toe. Little change was identified in the upper parts of slopes. At a given sampling point, geometric mean grain size and C_c were both found to be suitable for measuring changes in slope structure. In full-scale slopes, this is likely to mean that particle loss occurs near the water retaining slope face.

While changes in grain size and C_c could have been caused by fine particle or coarse particle movement, when coupled with the grain size of washed out material collected during triaxial tests (Chapter 3) and fine particle accumulation observed at the toe of slopes during model slope tests (Figure 25) reported in Chapter 4, it is likely that fine particle

migration is the cause of change. Reductions in geometric mean grain sizes are thought to be caused by relative increases in the amount of fine particles at a given point, while increases in geometric mean grain size are thought to be caused by fine particle erosion at a given point. Increases in C_c in areas of fine particle deposition are caused by the material becoming better graded in these regions. The development of grain migration in larger-scale slopes may be observable by measuring shear wave velocity changes, as identified during triaxial testing (Chapter 3). Although changes in slope properties were observed in decimetre-scale slopes and samples in a laboratory setting (Chapter 4), it is not clear whether the observed relationships will upscale to full-scale environments nor whether the same process relationships would be observed in decametre-scale slopes.

6.1.5 *To identify the consequence of flood-induced property alterations in embankments, focusing on identifying the significance of changes in the magnitude of slope vibrations.*

The numerical modelling research described in Chapter 5 showed that the alteration of material within embankments was found to change the dynamic response of slopes when a live load is applied. Larger-amplitude dynamic particle displacements were consistently recorded in areas of slopes which represented areas of fine particle loss, through decreases in material density and stiffness. Areas with increased density were found to have less significant responses to loading. The magnitude of dynamic particle displacement change in slopes was found to be affected by both the size of the altered region and the degree of material alteration.

Scour caused by basal flooding may cause slope failure or, if not remediated, lasting reductions in factor of safety due to alteration of the slope stress distribution. As differential head does not develop, there is thought to be a small risk of flood-induced particle migration causing lasting changes in slope properties, however wetting-drying cycles may weaken slopes in the long term (Stirling et al., 2021). It is likely that the small heads which develop in above slope floods do not induce significant material alteration. Offset head flooding forms a hydraulic gradient across a slope, potentially causing seepage and inducing particle migration. This may reduce slope strength and potentially cause a permeability barrier to form, meaning future loading events act on a slope with a pre-weakened structure (Figure 5). Overtopping floods may cause the same lasting destabilisation due to the potential for scour and differential head development, however in many cases material is removed during overtopping scour – meaning that there is little

material left to be destabilised.

6.2 Scaling

The issues of scale effects must be addressed. The fundamental results of modified triaxial testing, with particle movement through and out of samples during seepage, were replicated in the decimetre-scale tests which show particle movement from water inflow to water outflow. Due to the imposition of COVID-19 restrictions, it has not been possible to assess how long this movement would take to develop, and the conditions needed for it to develop, in full-scale embankments with sizes in the order of decametres during this study.

As fine particle migration occurs through suspension in pore fluid, migration of fine particles from water inflow to the opposing slope toe would be expected to take longer to develop in larger slopes, potentially over the period of multiple flood events, compared to slopes modelled during this work, assuming there is a comparable flow velocity through the full-scale and modelled slopes. A comparable flow velocity between laboratory testing and full-scale slopes would occur if the hydraulic gradients and material permeabilities were similar between the two settings. If short-term flooding occurred on decametre-scale embankments over periods comparable to those used during laboratory testing, fine particle deposition may be expected to occur within the slope body rather than towards the slope toe, when seepage flow could no longer suspend the eroded particles. Permeability barriers, which form in areas of fine particle deposition (Chang and Zhang, 2011), may then form in interim sections of slopes. Non-toe deposition may also occur if fine particles are constricted at inter-grain contacts within a slope body. The development of permeability barriers has the potential to cause increases in pore water pressures in slopes, reducing slope strength. In situations where slope body deposition occurs there is potential for slope stability and alterations to the effects of dynamic loading in regions away from the slope toe. As the numerical modelling work recorded in Chapter 5 focused on situations with material alteration at the base and toe of slopes, the behavioural changes may differ from the results presented if material alteration occurs in different parts of a slope. The larger scale of embankments compared to laboratory tests means that there is the possibility that material heterogeneity development will behave differently to that observed following seepage in laboratory environments. In laboratory settings, seepage and particle migration is limited to a small cross sectional area without the potential for flow to bypass zones of

low permeability; in decametre scale slopes seepage may be able to laterally bypass areas of particle deposition and low permeability zones.

Particle migration differences between larger-scale embankments and those observed during the laboratory testing undertaken in this study would have ramifications for the locations of strength and stiffness changes which occur in the areas of fine particle loss and deposition. Without movement of particles across a whole slope, material property changes would occur in different places from those measured during laboratory testing and then modelled in Chapter 5.

Sampling of large-scale model embankments which had been subjected to flooding could be used to understand the migration of fine particles through a large embankment, including the timescales of full slope migration and regions of deposition. This would allow for assessment of slopes with known construction properties and known seepage durations, providing a fuller understanding of how slope development occurs during seepage. An alternative would be the sampling of existing embankments which have been subjected to flood conditions. This would allow for an understanding of a wider swathe of destabilisation conditions, but with the compromise of an incomplete understanding of applied flood loading conditions, material conditions or other material alteration which may have been applied. Centrifuge modelling has been undertaken on samples to investigate the effects of scale on internal erosion initiation, primarily studying the critical hydraulic gradients needed to initiate internal erosion (e.g. Ovalle-Villamil and Sasanakul, 2021, Marot et al., 2012). Reductions in the critical hydraulic gradient needed to initiate internal erosion were found to decrease with increasing scale model height (Ovalle-Villamil and Sasanakul, 2021, Marot et al., 2012). This suggests that there may be earlier initiation of internal erosion within decametre-scale slopes, however the centrifuge modelling research identified does not consider the locations of particle movement within slopes.

6.3 Monitoring and measurement

As fine particle migration is shown to cause differential changes in the average grain size of soils in different sections of slopes, intrusive investigation and sampling could be undertaken to assess how these properties have altered in slopes following flooding.

However, intrusive investigation only measures localised material changes and it may still be difficult to present a detailed assessment of slope change due to the density of sampling points required. An alternative is the possibility of using seismic geophysical testing to measure differences in ground response prior to and post an event, and to identify

development of differential changes across embankments. As shown in triaxial testing on a small scale with bender elements, shear wave velocity alterations would be detected if material movement had occurred; these variations may also be related to changes in other material properties, such as permeability, stiffness, and strength. If seismic testing was undertaken, it would have to take into account the orientation of potential seepage flow and transient alteration effects, such as the degree of soil saturation (Gunn et al., 2018, Bergamo et al., 2016). An alternative method of monitoring the migration of fine particles through slopes is live monitoring of acoustic signals produced by grain migration, as has been used to monitor landslide deposit development (Yang et al., 2022). Live acoustic monitoring has potential to show the magnitude and location of particle movement, however it may be difficult to correlate acoustic noise and locations of property change within slopes as it would be necessary to identify whether particle erosion or deposition had occurred.

6.4 Applications

6.4.1 Application to industry

Flooding events have been identified as causing embankment failure and have the potential to induce material alteration across a range of settings. Chapter 2 demonstrated that there is a need for the transport infrastructure industry to make advances in the description and recording of failures which occur, in order to provide an improved understanding of failures. A specific recommendation is that the term ‘washout’ should be reserved for describing a post-failure geomorphic condition, and should not be used to describe the process of failure or used as a failure type. Without a clear understanding of the causes and types of failure which occur, it is difficult to create tools to identify the most problematic areas and to tackle the pressing issues of an ageing and deteriorating asset base.

This work shows that flooding events can cause failure of rail embankments, however the action needed will depend on flood types. Even small amounts of flooding at the base of slopes, which can cause failure when live loading occurs (RAIB, 2013a, Independent, 2018), may require stability assessment or speed restrictions. The need for assessment of the effects of live loading on slope stability will depend on factors including slope composition, flood type and soil moisture conditions of the slope.

There is a need to assess the condition of embankments which do not undergo shear failure when there is evidence of seepage into or through a slope following flooding, as there is potential that slope properties will have been detrimentally changed. In situations where

embankments have been affected by flooding, it is suggested that inspections should consider the potential for lasting slope alteration and destabilisation, as a slope's condition may have changed from before a flooding event. Although intrusive sampling may be required, it may be possible to use seismic geophysical methods to determine whether lasting slope condition change has occurred during a flood event, as demonstrated during laboratory testing in Chapter 3. Furthermore, walkover surveys may provide evidence of material removal from slopes. Unless there is specific evidence of slope destabilisation, it is not suggested that a full-scale embankment inspection should take place after every flood.

6.4.2 Application to wider fields

While the focus of this project has been on rail infrastructure, the processes identified are present in a wide swathe of natural and anthropogenic environments. Landslide dams, reservoir embankments, flood embankments and levees, and tailing dams, are examples of systems that may undergo similar material property changes over time when subject to flood head development. There is potential for application of seismic methods to monitor the deterioration of these environments. Relationships between shear wave velocity, particle migration, strength and permeability change could be used to help monitor slope condition and understand whether slopes may fail.

The monitoring of micro-seismic noise due to particle movement is a research field which has received recent attention (e.g. Yang et al., 2022). This technique could be adapted to use seismic wave monitoring to assess changes in the condition of a slope between construction and a present time point, or to monitor the changes in conditions of natural slopes such as landslide dams — which are often comprised of materials susceptible to internal erosion processes due to the mix of large and small clasts and lack of material compaction (Meyer et al., 1994). Although it may not be possible to quantify the absolute values of material property changes with time, the direction of change may be defined — for example densification or rarefaction of a slope may indicate the development of a permeability barrier or material weakening.

6.5 Limitations and further research

6.5.1 Limitations

The major limitation of the flood-induced failure review, presented in Chapter 2, was data accessibility. Information on smaller and less consequential failures is not commonly recorded in open literature, meaning that they are likely to be under-represented in the failures identified. This may be remedied with full access to datasets held by infrastructure

operators, however such access to these was not available during this work. Furthermore, the lack of recording of smaller flood events means that it is difficult to assess the full scale of slope weakening during previous flooding events.

A second limitation of this research is the spatial and temporal resolution of sampling during triaxial seepage tests, reported in Chapter 3, and tests on model slopes, reported in Chapter 4. As the experimental equipment used in Chapter 3 only allowed for the mass of material removed from samples to be measured at the end of testing, it was not possible to identify the relationship between material removal, permeability and shear wave velocity change. Furthermore, as shear wave velocity was only measured at a single point it was not possible to fully quantify the differential changes across a sample during an individual seepage test and relate these to full sample measurements of permeability. Monitoring of property development within samples is possible, for example using X-ray CT scanning to measure internal density change during tests (Watanabe et al., 2012), however this was not available during the testing reported in this thesis. An increased density of slope sampling points during testing reported in Chapter 4 would have allowed for a more complete understanding of particle migration. As discussed in section 6.2, one of the major limitations of applying laboratory results to full-scale embankment slopes is the effects of scaling, and the potential for process behaviour to change at larger scales.

6.5.2 Further research

The principal focus of further research should be on developing an understanding of the conditions required to cause changes in slope properties, and understanding how changes develop in full-scale embankments. Key questions include:

- How long does it take for detectable and important changes in material properties to develop in full-scale slopes subject to different degrees of flooding?
- Is the behaviour following a single larger flood event the same as that following multiple repeat flooding events?
- After what duration of flooding, and with what degree of material alteration, is the change in material properties sufficiently deleterious to cause infrastructure slope destabilisation?
- Are the locations of material erosion and deposition the same in full-scale slopes as they were in the upscaling tests undertaken in the laboratory and described in Chapter 4; do these changes have the potential to form a permeability barrier in different parts of a slope?

Further work assessing how material properties change due to internal erosion will allow for an increased understanding of the effects of seepage on the stability of slopes. The further development of non-intrusive methods for monitoring material alteration in embankments over time would be advantageous. Although seismic velocity has been shown in principle to identify fine particle migration due to internal erosion, and these measurements have been related to changes in permeability across small-scale samples, for larger-scale measurement and a fuller understanding of these relationships to be achieved, testing needs to be undertaken with a wider array of monitoring systems and on larger scales.

6.6 Summary

Flooding has been identified as a cause of landslides in transportation embankments, with four types of flood classified: overtopping, top of slope, offset head and basal floods. However, decoupling the effects of rainfall and flooding on the activation of landslides presents an inherently challenging problem; in all but the most exceptional circumstances flooding is a direct result of rainfall, and similar processes can develop in both situations. The difficulty in assessing the effects of flooding is also stymied by the lack of systematic reporting and recording of embankment failures. In addition, information on floods which affect slopes but do not cause failure is sparse. These factors make it difficult to fully quantify the prevalence and impact of the different flood types. Tentatively, offset head floods are identified as most commonly causing failure, however this may be due to the under-reporting of less consequential events caused by other types of flood. Therefore, it is recommended that recording of flood-induced failure events should be improved. Specifically, the term 'washout' should be reserved to describe the effect of a process and post-failure geomorphological condition, not used to describe a type of failure in and of itself.

Along with immediate failure, flooding can cause lasting weakening of slopes. One of the mechanisms involved is the redistribution of fine particles caused by internal erosion. These internal erosion processes, namely suffusion, have the potential to cause alterations in material strength, stiffness and permeability. This effect may be differential across an embankment and may not leave an externally observable change in embankment condition. The movement of fine particles during internal erosion, driven by differential flood head and caused by seepage processes, primarily develops along the base of slopes and along the water inflow surface. Fine particles are thought to be sourced from areas near to water inflow and deposited at the opposing slope base. It is therefore probable that there are decreases in strength, stiffness and permeability towards water inflow locations and increases in these properties at the base of slopes on the outflow side. The changes in material properties caused by flooding have the potential to modify slope vibration caused by dynamic loading, with increases in displacement in regions of particle loss, and may cause future destabilisation events to act on pre-weakened structures.

6.7 References

- BERGAMO, P., DASHWOOD, B., UHLEMANN, S., SWIFT, R., CHAMBERS, J. E., GUNN, D. A. & DONOHUE, S. 2016. Time-lapse monitoring of climate effects on earthworks using surface waves. *Geophysics*, 81, EN1-EN15.
- CHANG, D. & ZHANG, L. 2011. A Stress-controlled Erosion Apparatus for Studying Internal Erosion in Soils. *Geotechnical Testing Journal*, 34, 579-589.
- CHANG, D. S. & ZHANG, L. M. 2013a. Critical Hydraulic Gradients of Internal Erosion under Complex Stress States. *Journal of Geotechnical and Geoenvironmental Engineering*, 139, 1454-1467.
- GUNN, D. A., CHAMBERS, J. E., DASHWOOD, B. E., LACINSKA, A., DIJKSTRA, T., UHLEMANN, S., SWIFT, R., KIRKHAM, M., MILODOWSKI, A., WRAGG, J. & DONOHUE, S. 2018. Deterioration model and condition monitoring of aged railway embankment using non-invasive geophysics. *Construction and Building Materials*, 170, 668-678.
- HORIKOSHI, K. & TAKAHASHI, A. 2015. Suffusion-induced change in spatial distribution of fine fractions in embankment subjected to seepage flow. *Soils and Foundations*, 55, 1293-1304.
- INDEPENDENT. 2018. *Crude oil pours into river after train derails in US* [Online]. Available: <https://www.independent.co.uk/news/world/americas/oil-spill-train-derailment-water-contamination-iowa-rock-river-doon-a8413626.html> [Accessed 2019].
- MAROT, D., LE, V. D., GARNIER, J., THOREL, L. & AUDRAIN, P. 2012. Study of scale effect in an internal erosion mechanism: centrifuge model and energy analysis. *European Journal of Environmental and Civil Engineering*, 16, 1-19.
- MEYER, W., SCHUSTER, R. L. & SABOL, M. A. 1994. Potential for Seepage Erosion of Landslide Dam. *Journal of Geotechnical Engineering*, 120, 1211-1229.
- NASA. 2021. *Pacific Northwest Flooding and Landslides November 2021* [Online]. Available: <https://appliedsciences.nasa.gov/what-we-do/disasters/disasters-activations/pacific-northwest-flooding-and-landslides-november-2021> [Accessed 2022].
- OVALLE-VILLAMIL, W. & SASANAKUL, I. 2021. Assessment of centrifuge modelling of internal erosion induced by upward flow conditions. *International Journal of Physical Modelling in Geotechnics*, 21, 251-267.
- POLEMIO, M. & LOLLINO, P. 2011. Failure of infrastructure embankments induced by flooding and seepage: a neglected source of hazard. *Natural Hazards and Earth System Sciences*, 11, 3383.
- RAIB 2013a. Derailment of a freight train at Barrow upon Soar, Leicestershire. *Rail Accident Report*. Rail Accident Investigation Branch, Department for Transport.
- STIRLING, R. A., TOLL, D. G., GLENDINNING, S., HELM, P. R., YILDIZ, A., HUGHES, P. N. & ASQUITH, J. D. 2021. Weather-driven deterioration processes affecting the performance of embankment slopes. *Géotechnique*, 71, 957-969.
- WATANABE, Y., LENOIR, N., OTANI, J. & NAKAI, T. 2012. Displacement in sand under triaxial compression by tracking soil particles on X-ray CT data. *Soils and Foundations*, 52, 312-320.
- YANG, Y., CHEN, G., MENG, X., BIAN, S., CHONG, Y., SHI, W., JIANG, W., JIN, J., LI, C., MU, X. & YUE, D. 2022. Analysis of the microseismicity characteristics in landslide dam failure flume tests: implications for early warning and dynamics inversion. *Landslides*, 19, 789–808.

Full document reference list

- ABERNETHY, B. & RUTHERFURD, I. D. 2000. The effect of riparian tree roots on the mass-stability of riverbanks. *Earth Surface Processes and Landforms*, 25, 921-937.
- AL-RIFFAI, M. & NISTOR, I. Influence of seepage on the erodibility of overtopped noncohesive embankments. Proceedings of the 21st Canadian Hydrotechnical Conference, 2013.
- ALONSO, E. E. & PINYOL, N. M. 2016. Numerical analysis of rapid drawdown: Applications in real cases. *Water Science and Engineering*, 9, 175-182.
- ALRAMAHI, B., ALSHIBLI, K. A. & FRATTA, D. 2010. Effect of Fine Particle Migration on the Small-Strain Stiffness of Unsaturated Soils. *Journal of Geotechnical and Geoenvironmental Engineering*, 136, 620-628.
- ANDERSEN, L. & JONES, C. J. C. 2006. Coupled boundary and finite element analysis of vibration from railway tunnels—a comparison of two- and three-dimensional models. *Journal of Sound and Vibration*, 293, 611-625.
- ANSARY, A. M. M. S. A. S. M. A. 1998. Damages to railway embankments during the 1998 flood in Bangladesh. *15th International Conference on Soil Mechanics and Foundation Engineering*. Istanbul.
- ASCE 2011. Earthen Embankment Breaching. *Journal of Hydraulic Engineering*, 137, 1549-1564.
- ASGHARI TABRIZI, A., ELALFY, E., ELKHOLY, M., CHAUDHRY, M. H. & IMRAN, J. 2017. Effects of compaction on embankment breach due to overtopping. *Journal of Hydraulic Research*, 55, 236-247.
- AUSTRALIAN TRANSPORT SAFETY BUREAU 2015. Derailment of freight train 9T92.
- BBC. 2020. *Corby train crash: 'Ineffective' flood system caused landslide* [Online]. Available: <https://www.bbc.co.uk/news/uk-england-northamptonshire-52807827> [Accessed].
- BEEK, V. V. A. N., BEZUIJEN, A. & SELLMEIJER, H. 2013. Backward Erosion Piping. *Erosion in Geomechanics Applied to Dams and Levees*. John Wiley And Sons, Inc.
- BELL, F. G. 2000. *Engineering properties of soils and rocks*, Oxford, Elsevier.
- BENNETT, E. H. 1884. Court of Appeal. Whalley v. Lancashire and Yorkshire Railway Co. *The American Law Register (1852-1891)*, 32, 633-640.
- BERGAMO, P., DASHWOOD, B., UHLEMANN, S., SWIFT, R., CHAMBERS, J. E., GUNN, D. A. & DONOHUE, S. 2016. Time-lapse monitoring of climate effects on earthworks using surface waves. *Geophysics*, 81, EN1-EN15.
- BERNATEK-JAKIEL, A. & POESEN, J. 2018. Subsurface erosion by soil piping: significance and research needs. *Earth-Science Reviews*, 185, 1107-1128.
- BETTES, R. & REEVE, C. E. 1995. Performance of River Flood Embankments. Ministry of Agriculture, Fisheries and Food.
- BETTS, R. A. & BROWN, K. 2021. Introduction. In: *The Third UK Climate Change Risk Assessment Technical Report* [Betts, R.A., Haward, A.B. and Pearson, K.V.(eds.)]. Prepared for the Climate Change Committee, London.
- BGS. 2012. *Rest and Be thankful (A83) landslides, 2012* [Online]. Available: <http://www.bgs.ac.uk/landslides/RABTAug2012.html> [Accessed 2018 May 2018].
- BIAN, X., JIANG, H. & CHEN, Y. 2016. Preliminary Testing on High-speed Railway Substructure Due to Water Level Changes. *Procedia Engineering*, 143, 769-781.
- BISANTINO, T., PIZZO, V., POLEMIO, M. & GENTILE, F. 2016. Analysis of the flooding event of October 22-23, 2005 in a small basin in the province of Bari (Southern Italy). *Journal of Agricultural Engineering*, 47, 8.

- BLANCKAERT, K. 2011. Hydrodynamic processes in sharp meander bends and their morphological implications. *Journal of Geophysical Research: Earth Surface*, 116, F01003.
- BLANCKAERT, K., DUARTE, A., CHEN, Q. & SCHLEISS, A. J. 2012. Flow processes near smooth and rough (concave) outer banks in curved open channels. *Journal of Geophysical Research: Earth Surface*, 117, F04020.
- BONELLI, S., MAROT, D., TERNAT, F. & BENAHMED, N. 2007a. Assessment of the risk of internal erosion of water retaining structures: dams, dykes and levees.
- BONELLI, S., MAROT, D., TERNAT, F. & BENAHMED, N. 2007b. Assessment of the risk of internal erosion of water retaining structures: dams, dykes and levees. Intermediate Report of the European Working Group of ICOLD Deutsches TalksperrrenKomitee.
- BRIGGS, K., SMETHURST, J. & POWRIE, W. 2014. Modelling the Influence of Tree Removal on Embankment Slope Hydrology. 2014 2014 Cham. Springer International Publishing, 241-246.
- BRIGGS, K. M., LOVERIDGE, F. A. & GLENDINNING, S. 2016. Failures in transport infrastructure embankments. *Engineering Geology*, 219, 107-117.
- BRITISH STANDARDS INSTITUTION 2018. Geotechnical investigation and testing - Laboratory testing of soil. In: COMMITTEE, S. P. A. S. (ed.) *Part 9*. BSI Standards Limited,.
- BROWN, A., CHAPMAN, A., JACOBS, U., GOSDEN, J. & SMITH, F. The influence of infrastructure embankments on the consequences of dam failure. 15th British Dams Society Conference, Warwick, 2008.
- BUFFINGTON, J. M. & MONTGOMERY, D. R. 1997. A systematic analysis of eight decades of incipient motion studies, with special reference to gravel - bedded rivers. *Water Resources Research*, 33, 1993-2029.
- BUNCE, C. M. 2008. *Risk estimation for railways exposed to landslides*. PhD thesis, University of Alberta.
- CHANG, D. & ZHANG, L. 2011. A Stress-controlled Erosion Apparatus for Studying Internal Erosion in Soils. *Geotechnical Testing Journal*, 34, 579-589.
- CHANG, D. S. & ZHANG, L. M. 2013a. Critical Hydraulic Gradients of Internal Erosion under Complex Stress States. *Journal of Geotechnical and Geoenvironmental Engineering*, 139, 1454-1467.
- CHANG, D. S. & ZHANG, L. M. 2013b. Extended internal stability criteria for soils under seepage. *Soils and Foundations*, 53, 569-583.
- CML. 2016. *Farnley Haugh Landslide Repair* [Online]. Available: <https://www.cml.uk.com/case-studies/farnley-haugh-landslide/> [Accessed].
- CONNOLLY, D., GIANNOPOULOS, A. & FORDE, M. C. 2013. Numerical modelling of ground borne vibrations from high speed rail lines on embankments. *Soil Dynamics and Earthquake Engineering*, 46, 13-19.
- CONNOLLY, D. P., KOUROUSSIS, G., LAGHROUCHE, O., HO, C. L. & FORDE, M. C. 2015. Benchmarking railway vibrations – Track, vehicle, ground and building effects. *Construction and Building Materials*, 92, 64-81.
- CONNOLLY, D. P., KOUROUSSIS, G., WOODWARD, P. K., ALVES COSTA, P., VERLINDEN, O. & FORDE, M. C. 2014. Field testing and analysis of high speed rail vibrations. *Soil Dynamics and Earthquake Engineering*, 67, 102-118.
- CONNOLLY, D. P., MARECKI, G. P., KOUROUSSIS, G., THALASSINAKIS, I. & WOODWARD, P. K. 2016. The growth of railway ground vibration problems — A review. *Science of The Total Environment*, 568, 1276-1282.
- COUPER, P. R. & MADDOCK, I. P. 2001. Subaerial river bank erosion processes and their interaction with other bank erosion mechanisms on the River Arrow, Warwickshire, UK. *Earth Surface Processes and Landforms*, 26, 631-646.

- CRUDEN, D. M. & VARNES, D. J. 1996. Landslide Types and Processes. *Special Report* Transportation Research Board, National Academy of Sciences.
- DAWSON, R., GOSLING, S., CHAPMAN, L., DARCH, G., WATSON, G., POWRIE, W., BELL, S., PAULSON, K., HUGHES, P. & WOOD, R. 2017. UK Climate Change Risk Assessment 2017 Evidence Report: Chapter 4, Infrastructure.
- DEGRANDE, G. & LOMBAERT, G. High-speed train induced free field vibrations: in situ measurements and numerical modelling. *Proceedings of the international workshop wave*, 2000. 29-41.
- DONG, K., CONNOLLY, D. P., LAGHROUCHE, O., WOODWARD, P. K. & ALVES COSTA, P. 2018. The stiffening of soft soils on railway lines. *Transportation Geotechnics*, 17, 178-191.
- DREWETT, Z. 2018. *Train pushed off the tracks by tonnes of mud in landslide* [Online]. Available: <http://metro.co.uk/2018/01/22/train-pushed-off-tracks-tonnes-mud-landslide-7250305/> [Accessed].
- DUGGAN, R. 2018. *Greater Anglia services will run tomorrow after engineers repair damage from landslide* [Online]. Essex Live. Available: <https://www.essexlive.news/news/greater-anglia-services-run-tomorrow-1355314> [Accessed March 2018 2018].
- DYER, M. 2004. Performance of flood embankments in England and Wales. *Proceedings of the Institution of Civil Engineers - Water Management*, 157, 177-186.
- FANNIN, R. J. & MOFFAT, R. 2006. Observations on internal stability of cohesionless soils. *Géotechnique*, 56, 497-500.
- FANNIN, R. J. & SLANGEN, P. 2014. On the distinct phenomena of suffusion and suffosion. *Géotechnique Letters*, 4, 289-294.
- FEDERAL RAILROAD ADMINISTRATION 2001-2010. Railroad Safety Statistics Annual Report. Federal Railroad Administration Office of Safety Analysis.
- FICARELLA, I. 2005. *Il day after di una catastrofe 'Bari risparmiata grazie alla cava'* [Online]. Available: <https://ricerca.repubblica.it/repubblica/archivio/repubblica/2005/10/25/il-day-after-di-una-catastrofe-bari.html> [Accessed 2020].
- FIELD, C. B., BARROS, V., STOCKER, T. F. & DAHE, Q. 2012. *Managing the risks of extreme events and disasters to advance climate change adaptation: special report of the intergovernmental panel on climate change*, Cambridge University Press.
- FOURIE, A. B. 1996. PREDICTING RAINFALL-INDUCED SLOPE INSTABILITY. *Proceedings of the Institution of Civil Engineers - Geotechnical Engineering*, 119, 211-218.
- FRANCZYK, A., DWORNIK, M. & LEŚNIAK, A. 2016. Numerical modelling of the impact of flood wave cyclicality on the stability of levees. *E3S Web Conf.*, 7, 03022.
- FREEBOROUGH, K. A., DIAZ DOCE, D., LETHBRIDGE, R., JESSAMY, G., DASHWOOD, C., PENNINGTON, C. & REEVES, H. J. 2016. Landslide hazard assessment for National Rail Network. *Procedia Engineering*, 143, 689-696.
- GIBSON, A. D., CULSHAW, M. G., DASHWOOD, C. & PENNINGTON, C. V. L. 2013. Landslide management in the UK—the problem of managing hazards in a ‘low-risk’ environment. *Landslides*, 10, 599-610.
- GILVEAR, D., DAVIES, J. & WINTERBOTTOM, S. 1994. Mechanisms of floodbank failure during large flood events on the rivers Tay and Earn, Scotland. *Quarterly Journal of Engineering Geology and Hydrogeology*, 27, 319-332.
- GUNN, D. A. Embankment stiffness characterisation using MASW and CSW methods. Proc. 11th Int. Conf. Railway Engineering,, 2011 London, .
- GUNN, D. A., CHAMBERS, J. E., DASHWOOD, B. E., LACINSKA, A., DIJKSTRA, T., UHLEMANN, S., SWIFT, R., KIRKHAM, M., MILODOWSKI, A., WRAGG, J. & DONOHUE, S. 2018. Deterioration model and condition monitoring of aged railway embankment using non-invasive geophysics. *Construction and Building Materials*, 170, 668-678.

- HAINES, A. 2020. Interim report to the Secretary of State for Transport following the derailment at Carmont, near Stonehaven. Network Rail.
- HEFLIN, C. 2011. *Plymouth Road in Ann Arbor remains closed following embankment failure; midday reopening expected* [Online]. Available: <http://www.annarbor.com/news/plymouth-road-remains-closed-following-embankment-failure-midday-reopening-expected/> [Accessed].
- HIGGINS, J. 2019. *Midwest flooding washes out hundreds of miles of roads, rail lines* [Online]. Available: https://www.upi.com/Top_News/US/2019/04/04/Midwest-flooding-washes-out-hundreds-of-miles-of-roads-rail-lines/2351554328299/ [Accessed].
- HOLDEN, M. 2019. *Steam railway CLOSED after flood damage* [Online]. Available: <https://www.railadvent.co.uk/2019/10/steam-railway-closed-after-flood-damage.html> [Accessed].
- HONG, L., OUYANG, M., PEETA, S., HE, X. & YAN, Y. 2015. Vulnerability assessment and mitigation for the Chinese railway system under floods. *Reliability Engineering & System Safety*, 137, 58-68.
- HOOKE, J. M. 1980. Magnitude and distribution of rates of river bank erosion. *Earth Surface Processes*, 5, 143-157.
- HORIKOSHI, K. & TAKAHASHI, A. 2015. Suffusion-induced change in spatial distribution of fine fractions in embankment subjected to seepage flow. *Soils and Foundations*, 55, 1293-1304.
- HUNGR, O., LEROUEIL, S. & PICARELLI, L. 2014. The Varnes classification of landslide types, an update. *Landslides*, 11, 167-194.
- HUTCHINSON, C. S. 1890. *Lancashire and Yorkshire Railway*. Whitehall, London, S.W>,: Railway Department, Board of Trade.
- ICOLD 2017. Bulletin 164 Internal Erosion of Existing Dams, Levees and Dikes, and their Foundations. Paris: International Commission on Large Dams.
- INDEPENDENT. 2018. *Crude oil pours into river after train derails in US* [Online]. Available: <https://www.independent.co.uk/news/world/americas/oil-spill-train-derailment-water-contamination-iowa-rock-river-doon-a8413626.html> [Accessed 2019].
- INDRARATNA, B., NGUYEN, V. T. & RUJIKIATKAMJORN, C. 2011. Assessing the potential of internal erosion and suffusion of granular soils. *Journal of Geotechnical and Geoenvironmental Engineering*, 137, 550-554.
- INGLES, O. & AITCHISON, G. 1969. *Soil-water disequilibrium as a cause of subsidence in natural soils and earth embankments*, Division of Soil Mechanics, CSIRO.
- JABOYEDOFF, M. & LABIOUSE, V. 2011. Preliminary estimation of rockfall runout zones. *Natural Hazards Earth System Sciences*, 11, 819–828.
- JADID, R., MONTOYA, B. M., BENNETT, V. & GABR, M. A. 2020. Effect of repeated rise and fall of water level on seepage-induced deformation and related stability analysis of Princeville levee. *Engineering Geology*, 266, 105458.
- JIA, G. W., ZHAN, T. L. T., CHEN, Y. M. & FREDLUND, D. G. 2009. Performance of a large-scale slope model subjected to rising and lowering water levels. *Engineering Geology*, 106, 92-103.
- JIAN, W., XU, Q., YANG, H. & WANG, F. 2014. Mechanism and failure process of Qianjiangping landslide in the Three Gorges Reservoir, China. *Environmental Earth Sciences*, 72, 2999-3013.
- JIANG, H., BIAN, X., CHEN, Y. & HAN, J. 2015. Impact of Water Level Rise on the Behaviors of Railway Track Structure and Substructure. *Transportation Research Record: Journal of the Transportation Research Board*, 2476, 15-22.
- JIANG, H., BIAN, X., JIANG, J. & CHEN, Y. 2016. Dynamic performance of high-speed railway formation with the rise of water table. *Engineering Geology*, 206, 18-32.

- JOHANSSON, J. & EDESKÄR, T. 2014. Effects of external water-level fluctuations on slope stability. *The Electronic journal of geotechnical engineering*, 19, 2437-2463.
- JOHNSTON, I., MURPHY, W. & HOLDEN, J. 2021. A review of floodwater impacts on the stability of transportation embankments. *Earth-Science Reviews*, 215, 103553.
- JOSEPHS, J. 2011. *Train derailed in Australia flood* [Online]. BBC. [Accessed].
- JULIAN, J. P. & TORRES, R. 2006. Hydraulic erosion of cohesive riverbanks. *Geomorphology*, 76, 193-206.
- KE, L. & TAKAHASHI, A. 2012. Strength reduction of cohesionless soil due to internal erosion induced by one-dimensional upward seepage flow. *Soils and Foundations*, 52, 698-711.
- KE, L. & TAKAHASHI, A. 2014. Experimental investigations on suffusion characteristics and its mechanical consequences on saturated cohesionless soil. *Soils and Foundations*, 54, 713-730.
- KELLER, E. A. & SWANSON, F. J. 1979. Effects of large organic material on channel form and fluvial processes. *Earth Surface Processes*, 4, 361-380.
- KELLERMANN, P., SCHÖNBERGER, C. & THIEKEN, A. H. 2016. Large-scale application of the flood damage model RAILway Infrastructure Loss (RAIL). *Nat. Hazards Earth Syst. Sci.*, 16, 2357-2371.
- KELLY, D., MCDOUGALL, J. & BARRETO, D. Effect of particle loss on soil behaviour. Proc., 6th Int. Conf. on Scour and Erosion, Publications SHF, Paris, 2012. 639-646.
- KENNEY, T. & LAU, D. 1985. Internal stability of granular filters. *Canadian Geotechnical Journal*, 22, 215-225.
- KENNEY, T. C. & LAU, D. 1986. Internal stability of granular filters: Reply. *Canadian Geotechnical Journal*, 23, 420-423.
- KEZDI, A. 1979. *Soil Physics*, Amsterdam, Elsevier.
- KOKS, E. E., ROZENBERG, J., ZORN, C., TARIVERDI, M., VOUSDOKAS, M., FRASER, S. A., HALL, J. W. & HALLEGATTE, S. 2019. A global multi-hazard risk analysis of road and railway infrastructure assets. *Nature Communications*, 10, 2677.
- KOUROUSSIS, G., CONNOLLY, D. P., OLIVIER, B., LAGHROUCHE, O. & COSTA, P. A. 2016. Railway cuttings and embankments: Experimental and numerical studies of ground vibration. *Science of The Total Environment*, 557-558, 110-122.
- KWAN, W. S. & MOHTAR, C. E. 2018a. A review on sand sample reconstitution methods and procedures for undrained simple shear test. *International Journal of Geotechnical Engineering*, 14, 1-9.
- KWAN, W. S. & MOHTAR, C. E. 2018b. A review on sand sample reconstitution methods and procedures for undrained simple shear test. *International Journal of Geotechnical Engineering*, 14, 851-859.
- LAMB, R., GARSIDE, P., PANT, R. & HALL, J. W. 2019. A Probabilistic Model of the Economic Risk to Britain's Railway Network from Bridge Scour During Floods. *Risk Analysis*, 39, 2457-2478.
- LANDERS, M. N. & MUELLER, D. S. 1996. Channel scour at bridges in the United States.
- LATO, M. J., DIEDERICHS, M. S., HUTCHINSON, D. J. & HARRAP, R. 2012. Evaluating roadside rockmasses for rockfall hazards using LiDAR data: optimizing data collection and processing protocols. *Natural Hazards*, 60, 831-864.
- LAWLER, D. 1995. The Impact of Scale on the Processes of Channel-Side Sediment Supply: A Conceptual Model. *IAHS Publications-Series of Proceedings and Reports*.
- LAWLER, D., COUPERTHWAITTE, J., BULL, L. & HARRIS, N. 1997. Bank erosion events and processes in the Upper Severn basin. *Hydrology and Earth System Sciences Discussions*, 1, 523-534.
- LAWLER, D. M. 1991. A New Technique for the Automatic Monitoring of Erosion and Deposition Rates. *Water Resources Research*, 27, 2125-2128.

- LEHTONEN, V. J., MEEHAN, C. L., LÄNSIVAARA, T. T. & MANSIKKAMÄKI, J. N. 2015. Full-scale embankment failure test under simulated train loading. *Géotechnique*, 65, 961-974.
- LI, Z., YE, W., MARENCE, M. & BRICKER, J. D. 2019. Unsteady seepage behavior of an earthfill dam during drought-flood cycles. *Geosciences*, 9, 17.
- LIANG, C., JAKSA, M. B., OSTENDORF, B. & KUO, Y. L. 2015. Influence of river level fluctuations and climate on riverbank stability. *Computers and Geotechnics*, 63, 83-98.
- LINDGREN, J., JONSSON, D. K. & CARLSSON-KANYAMA, A. 2009. Climate Adaptation of Railways: Lessons from Sweden. *European Journal of Transport and Infrastructure Research*, 9, 164-181.
- LOVERIDGE, F. A., SPINK, T. W., O'BRIEN, A. S., BRIGGS, K. M. & BUTCHER, D. 2010. The impact of climate and climate change on infrastructure slopes, with particular reference to southern England. *Quarterly Journal of Engineering Geology and Hydrogeology*, 43, 461-472.
- LUO, Y.-L., QIAO, L., LIU, X.-X., ZHAN, M.-L. & SHENG, J.-C. 2013. Hydro-mechanical experiments on suffusion under long-term large hydraulic heads. *Natural Hazards*, 65, 1361-1377.
- MADSHUS, C. & KAYNIA, A. M. 2000. High-speed railway lines on soft ground: Dynamic behaviour at critical train speed. *Journal of Sound and Vibration*, 231, 689-701.
- MAROT, D., LE, V. D., GARNIER, J., THOREL, L. & AUDRAIN, P. 2012. Study of scale effect in an internal erosion mechanism: centrifuge model and energy analysis. *European Journal of Environmental and Civil Engineering*, 16, 1-19.
- MARTO, A. & SOON, T. 2011. Short Review on Liquefaction Susceptibility. *International Journal of Engineering Research and Applications*, 2, 2115-2119.
- MENAN HASNAYN, M., JOHN MCCARTER, W., WOODWARD, P. K., CONNOLLY, D. P. & STARRS, G. 2017. Railway subgrade performance during flooding and the post-flooding (recovery) period. *Transportation Geotechnics*, 11, 57-68.
- MEYER, W., SCHUSTER, R. L. & SABOL, M. A. 1994. Potential for Seepage Erosion of Landslide Dam. *Journal of Geotechnical Engineering*, 120, 1211-1229.
- MOHAMED, M. A., SAMUELS, P., MORRIS, M. & GHATAORA, G. Improving the accuracy of prediction of breach formation through embankment dams and flood embankments. *River Flow*, 2002.
- MORGENSTERN, N. 1963. Stability Charts for Earth Slopes During Rapid Drawdown. *Géotechnique*, 13, 121-131.
- MORRIS, M., DYER, M. & SMITH, P. 2007. Management of Flood Embankments. A good practice review. Department for Environment, Food and Rural Affairs.
- MORRIS, M., HASSAN, M., KORTENHAUS, A. & VISSER, P. 2009. Breaching Processes: A state of the art review. *FLOOD site Project Report, T06-06-03*.
- MOSSA, M. 2007. The floods in Bari: What history should have taught. *Journal of Hydraulic Research*, 45, 579-594.
- MURRAY, C. A., TAKE, W.A. AND HOULT, N.A., 2015. Measurement of vertical and longitudinal rail displacements using digital image correlation. *Canadian Geotechnical Journal*, 52, 141-151.
- NASA. 2021. *Pacific Northwest Flooding and Landslides November 2021* [Online]. Available: <https://appliedsciences.nasa.gov/what-we-do/disasters/disasters-activations/pacific-northwest-flooding-and-landslides-november-2021> [Accessed 2022].
- NATIONAL WEATHER SERVICE. 2007. *Hermosa, SD, Flash Flood of August 17, 2007* [Online]. Available: <https://www.weather.gov/unr/2007-08-17> [Accessed].
- NELDER, L. M., GUNN, D. & REEVES, H. 2006. Investigation of the geotechnical properties of a Victorian Railway Embankment. *Proc. 1st Int. Conf. Railway Foundations*, 2006 2006. 34-47.

- NELSON, J. T. & SAURENMAN, H. J. 1983. State-of-the-Art Review : Prediction and Control of Groundborne Noise and Vibration from Rail Transit Trains.
- NETWORK RAIL 2014. Route Weather Resilience and Climate Change Adaptation Plans, Anglia.
- NETWORK RAIL 2016a. Task 106: JBA Overtopping (Earthworks at Flood Risk).
- NETWORK RAIL 2016b. Task 106: JBA Trust, 4 March 2016, Overtopping (Earthworks at Flood Risk).
- NETWORK RAIL 2018. Earthworks Asset Policy January 2018. Network Rail Infrastructure Ltd.
- NIÑO, Y., LOPEZ, F. & GARCIA, M. 2003. Threshold for particle entrainment into suspension. *Sedimentology*, 50, 247-263.
- NOGUCHI, T., FUJII, T. J. J. R. & REVIEW, T. 2000. Minimizing the effect of natural disasters. *Japan Railway & Transport Review*, 23, 52-59.
- O'KELLY, B. C., WARD, P. N. & RAYBOULD, M. J. 2008. Stabilisation of a progressive railway embankment slip. *Geomechanics and Geoengineering*, 3, 257-270.
- OLIVIER, B., CONNOLLY, D. P., ALVES COSTA, P. & KOUROUSSIS, G. 2016. The effect of embankment on high speed rail ground vibrations. *International Journal of Rail Transportation*, 4, 229-246.
- OUYANG, M. & TAKAHASHI, A. 2015. Influence of initial fines content on fabric of soils subjected to internal erosion. *Canadian Geotechnical Journal*, 53, 299-313.
- OVALLE-VILLAMIL, W. & SASANAKUL, I. 2021. Assessment of centrifuge modelling of internal erosion induced by upward flow conditions. *International Journal of Physical Modelling in Geotechnics*, 21, 251-267.
- PANDO, M. A., OLGUN, C. G., MARTIN, I. & JAMES, R. 2001. Liquefaction Potential of Railway Embankments. *International Conferences On Recent Advances In Geotechnical Earthquake Engineering And Soil Dynamics*. San Diego, California.
- PAOLUCCI, R., MAFFEIS, A., SCANDELLA, L., STUPAZZINI, M. & VANINI, M. 2003. Numerical prediction of low-frequency ground vibrations induced by high-speed trains at Ledsgaard, Sweden. *Soil Dynamics and Earthquake Engineering*, 23, 425-433.
- PAPADAKIS, N. M. & STAVROULAKIS, G. E. Effect of Mesh Size for Modeling Impulse Responses of Acoustic Spaces via Finite Element Method in the Time Domain. *Proceedings of the Euronoise*, 2018.
- PAPANICOLAOU, A., DEY, S., RINALDI, M. & MAZUMDAR, A. 2006. Research issues for riverine bank stability analysis in the 21st century. *Iowa City*.
- PAREKH, M. L. 2016. *Advancing internal erosion monitoring using seismic methods in field and laboratory studies*. Colorado School of Mines. Arthur Lakes Library.
- PENNINGTON, D., NASH, D. & LINGS, M. 1997. Anisotropy of G₀ shear stiffness in Gault Clay. *Géotechnique*, 47, 391-398.
- PERRY, J. 1989. A survey of slope condition on motorway earthworks in England and Wales. Wokingham, Berkshire United Kingdom Transport and Road Research Laboratory (TRRL).
- PERRY, J., PEDLEY, M., BRADY, K. & REID, M. 2003. Briefing: Embankment cuttings: condition appraisal and remedial treatment. *Proceedings of the Institution of Civil Engineers - Geotechnical Engineering*, 156, 171-175.
- PETLEY, D. 2016. *The Farnley Haugh landslide in Northumberland, northern England* [Online]. Available: <https://blogs.agu.org/landslideblog/2016/01/09/farnley-haugh-landslide-1/> [Accessed].
- PICKERT, G., WEITBRECHT, V. & BIEBERSTEIN, A. 2011. Breaching of overtopped river embankments controlled by apparent cohesion. *Journal of Hydraulic Research*, 49, 143-156.
- PINYOL, N. M., ALONSO, E. E. & OLIVELLA, S. 2008. Rapid drawdown in slopes and embankments. *Water Resources Research*, 44, W00D03.

- PLANÈS, T., MOONEY, M. A., RITTGERS, J. B. R., PAREKH, M. L., BEHM, M. & SNIEDER, R. 2016. Time-lapse monitoring of internal erosion in earthen dams and levees using ambient seismic noise. *Géotechnique*, 66, 301-312.
- POLEMIO, M. & LOLLINO, P. 2011. Failure of infrastructure embankments induced by flooding and seepage: a neglected source of hazard. *Natural Hazards and Earth System Sciences*, 11, 3383.
- POLMONT, I. R. S. O. F. D. O. E. T. G. T. L. N. 2020. *Fiona Dobie* [Online]. Available: <https://www.falkirkherald.co.uk/news/transport/images-reveal-scale-flood-damage-edinburgh-glasgow-train-line-near-polmont-2946093> [Accessed].
- PONZIANI, F., PANDOLFO, C., STELLUTI, M., BERNI, N., BROCCA, L. & MORAMARCO, T. 2012. Assessment of rainfall thresholds and soil moisture modeling for operational hydrogeological risk prevention in the Umbria region (central Italy). *Landslides*, 9, 229-237.
- POOLE, G. *CONWY VALLEY RAILWAY FLOOD REPAIRS 1994*. [Online]. Available: <http://www.6gshed.co.uk/conwyvalleyrailwayfloodrepairs.html> [Accessed].
- POSNER, A. J. & GEORGAKAKOS, K. P. 2015. Soil moisture and precipitation thresholds for real-time landslide prediction in El Salvador. *Landslides*, 12, 1179-1196.
- PRADEL, D. & RAAD, G. 1993. Effect of Permeability on Surficial Stability of Homogeneous Slopes. *Journal of Geotechnical Engineering*, 119, 315-332.
- PROSSER, I. P., HUGHES, A. O. & RUTHERFURD, I. D. 2000. Bank erosion of an incised upland channel by subaerial processes: Tasmania, Australia. 25, 1085-1101.
- PRZYLUCKI, V., HALLEGATTE, S. & TOMOZEIU, R. 2011. V. Przyluski, S. Hallegatte (SMASH-CIRED), R. Tomozeiu, C. Cacciamani (ARPA-ER) V. Pavan (ARPAER), C. Doll (Fraunhofer-ISI) (2011): —Weather trends and economy-wide impacts || Deliverable 1 within the research project WEATHER (Weather Extremes: Impacts on Transport Systems and Hazards for European Regions) European Commission, 7th framework programme. Project co-ordinator: Fraunhofer ISI. Karlsruhe, Paris, Bologna, October 2011.
- QIN, C., ZHENG, F., WELLS, R. R., XU, X., WANG, B. & ZHONG, K. 2018. A laboratory study of channel sidewall expansion in upland concentrated flows. *Soil and Tillage Research*, 178, 22-31.
- RAIB 2006a. Derailment at Oubeck North near Lancaster 4 November 2005. Rail Accident Investigation Branch.
- RAIB 2006b. Derailment near Moy, Inverness-shire on 26 November 2005. Rail Accident Investigation Branch.
- RAIB 2008. Derailment of a passenger train near Kemble, 15 January 2007. Rail Accident Investigation Branch.
- RAIB 2010. Derailment near Gillingham tunnel, Dorset, 28 November 2009. Rail Accident Investigation Branch.
- RAIB 2013a. Derailment of a freight train at Barrow upon Soar, Leicestershire. *Rail Accident Report*. Rail Accident Investigation Branch, Department for Transport.
- RAIB 2013b. RAIB Class investigation into landslips affecting Network Rail infrastructure between June 2012 and February 2013 April 2014. Rail Accident Investigation Branch.
- RAIB 2013c. Train ran onto a washed-out embankment near Knockmore, Northern Ireland 28 June 2012. Rail Accident Investigation Branch, Department for Transport.
- RAIB 2017a. Derailment due to a landslip, and subsequent collision, Watford 16 September 2016. Rail Accident Investigation Branch.
- RAIB 2017b. Report 03/2017: Trains passed over washed out track at Baildon.

- RAIL ENGINEER. 2012. *Managing Earthworks* [Online]. Rail Engineer. Available: <https://www.railengineer.uk/2012/03/16/managing-earthworks/4/> [Accessed 2018].
- RAIL ENGINEER. 2016. *The Conwy Crisis* [Online]. Available: <https://www.railengineer.uk/2016/03/18/conwy-crisis/> [Accessed 2018].
- RAILRODDER. 2011. *CN Ruel Subdivision Roadbed Failure* [Online]. Available: <https://www.youtube.com/watch?v=Pb3pZIK6UFQ> [Accessed].
- RATP. 2018. *RER B accident - Update on work in progress and traffic forecasts* [Online]. Available: <https://www.ratp.fr/groupe-ratp/newsroom/rer/accident-du-rer-b-point-sur-les-travaux-en-cours-et-previsions-de-traffic> [Accessed 14/06/2018].
- RICKARD, C. E. 2009. Floodwalls and flood embankments. *The Fluvial Design Guide*. Environment Agency.
- RIDLEY, A., MCGINNITY, B. & VAUGHAN, P. 2004. Role of pore water pressures in embankment stability. *Proceedings of the Institution of Civil Engineers - Geotechnical Engineering*, 157, 193-198.
- RINALDI, M., CASAGLI, N., DAPPORTO, S. & GARGINI, A. 2004. Monitoring and modelling of pore water pressure changes and riverbank stability during flow events. *Earth Surface Processes and Landforms*, 29, 237-254.
- ROSSETTI, M. A. 2007. Analysis of weather events on US Railroads.
- RSSB 2004. Impact of scour and flood risk on railway structures (T112).
- SALGADO, R., BANDINI, P. & KARIM, A. 2000. Shear Strength and Stiffness of Silty Sand. *Journal of Geotechnical and Geoenvironmental Engineering*, 126, 451-462.
- SATO, M. & KUWANO, R. 2016. Effects of internal erosion on mechanical properties evaluated by triaxial compression tests. *Japanese Geotechnical Society Special Publication*, 2, 1056-1059.
- SCHMOCKER, L., FRANK, P.-J. & HAGER, W. H. 2014. Overtopping dike-breach: effect of grain size distribution. *Journal of Hydraulic Research*, 52, 559-564.
- SCHMOCKER, L. & HAGER, W. H. 2012. Plane dike-breach due to overtopping: effects of sediment, dike height and discharge. *Journal of Hydraulic Research*, 50, 576-586.
- SHENG, X., JONES, C. J. C. & THOMPSON, D. J. 2006. Prediction of ground vibration from trains using the wavenumber finite and boundary element methods. *Journal of Sound and Vibration*, 293, 575-586.
- SHIRE, T. & O'SULLIVAN, C. 2013. Micromechanical assessment of an internal stability criterion. *Acta Geotechnica*, 8, 81-90.
- SIMMONS, C. J. L. A. 1849. Accident Returns: Extract for the Accident at Newark on 6th December 1849. Board of Trade.
- SIMON, A., CURINI, A., DARBY, S. E. & LANGENDOEN, E. J. 2000. Bank and near-bank processes in an incised channel. *Geomorphology*, 35, 193-217.
- SLANGEN, P. & FANNIN, R. J. 2017. The role of particle type on suffusion and suffosion. *Géotechnique Letters*, 7, 6-10.
- SMALE, K. 2019. *Flood repairs for West Highland railway line* [Online]. Available: <https://www.newcivilengineer.com/latest/flood-repairs-west-highland-railway-line-07-08-2019/> [Accessed].
- STIRLING, R. A., TOLL, D. G., GLENDINNING, S., HELM, P. R., YILDIZ, A., HUGHES, P. N. & ASQUITH, J. D. 2021. Weather-driven deterioration processes affecting the performance of embankment slopes. *Géotechnique*, 71, 957-969.
- SUWAL, L. P. & KUWANO, R. 2012. Poisson's ratio evaluation on silty and clayey sands on laboratory specimens by flat disk shaped piezo-ceramic transducer. *Bulletin of ERS*, 45, 141-158.
- TABARI, H. 2020. Climate change impact on flood and extreme precipitation increases with water availability. *Scientific Reports*, 10, 13768.

- TAKE, W. A. & BOLTON, M. D. 2004. Identification of seasonal slope behaviour mechanisms from centrifuge case studies. *Advances in geotechnical engineering: The Skempton conference*.
- THORNE, C. 1982. Processes and mechanisms of river bank erosion. In: R. D. HEY, J. C. B. C. R. T. (ed.) *Gravel-bed rivers*. Wiley.
- TRANSPORTATION RESEARCH BOARD, NATIONAL ACADEMIES OF SCIENCES, E. & MEDICINE 2016. *Minimizing Roadway Embankment Damage from Flooding*, Washington, DC, The National Academies Press.
- TRANSPORTATION SAFETY BOARD 1997. Interim railway safety recommendations concerning the identification and detection of railway roadbed instability. TSB Recommendation# 05/97. *Transportation Safety Board, Quebec, Canada*.
- TRUONG, Q. H., EOM, Y. H. & LEE, J. S. 2010. Stiffness characteristics of soluble mixtures. *Géotechnique*, 60, 293-297.
- TSUBAKI, R., BRICKER, J. D., ICHII, K. & KAWAHARA, Y. 2016. Development of fragility curves for railway embankment and ballast scour due to overtopping flood flow. *Natural Hazards and Earth Systems Sciences*, 16, 2455-2472.
- TSUBAKI, R., KAWAHARA, Y., SAYAMA, T. & FUJITA, I. 2012. Analysis of Hydraulic and Geomorphic Conditions Causing Railway Embankment Breach due to Inundation Flow. *Journal of hydroscience and hydraulic engineering*, 30, 87-99.
- TSUBAKI, R., KAWAHARA, Y. & UEDA, Y. 2017. Railway embankment failure due to ballast layer breach caused by inundation flows. *Natural Hazards*, 87, 717-738.
- UIC. 2018. *The definition of High Speed Rail* [Online]. Available: https://www.uic.org/com/uic-e-news/596-high-speed/article/the-definition-of-high-speed-rail?page=thickbox_enews [Accessed June 2018 2018].
- USACE 2000. Design and construction of levees. *Engineering and Design*. U.S. Army Corps of Engineers.
- USBR 2015. Best Practices in Dam And Levee Safety Risk Analysis. 4 ed.
- USGS. 2009. *Black Hills Area Floods - 2000 to 2009* [Online]. Available: <https://sd.water.usgs.gov/projects/FloodHistory/2001-2009/FH2001.html> [Accessed March 2018].
- UTLEY, B. C. & WYNN, T. M. 2008. Cohesive Soil Erosion: Theory and Practice. *World Environmental and Water Resources Congress 2008*.
- VAN ASCH, T. W. J., BUMA, J. & VAN BEEK, L. P. H. 1999. A view on some hydrological triggering systems in landslides. *Geomorphology*, 30, 25-32.
- VAN LEEUWEN, Z. & LAMB, R. 2014. Flood and scour related failure incidents at railway assets between 1846 and 2013. *Railway Safety & Standards Board*.
- VERMONT LOCAL ROADS. 2012. *Road Collapse- Maine 2008* [Online]. Available: <https://www.youtube.com/watch?v=NTbhyHNA1Vc> [Accessed].
- WAN, C. F. & FELL, R. 2008. Assessing the Potential of Internal Instability and Suffusion in Embankment Dams and Their Foundations. *Journal of Geotechnical and Geoenvironmental Engineering*, 134, 401-407.
- WATANABE, Y., LENOIR, N., OTANI, J. & NAKAI, T. 2012. Displacement in sand under triaxial compression by tracking soil particles on X-ray CT data. *Soils and Foundations*, 52, 312-320.
- WINTER, M., MACGREGOR, F. & SHACKMAN, L. 2005. *Scottish road network landslides study*.
- WINTER, M. G., SHEARER, B., PALMER, D., PEELING, D., HARMER, C. & SHARPE, J. 2016. The Economic Impact of Landslides and Floods on the Road Network. *Procedia Engineering*, 143, 1425-1434.
- WOLMAN, M. G. 1959. Factors influencing erosion of a cohesive river bank. *American Journal of Science*, 257, 204-216.

- XIAO, M. & SHWIYHAT, N. 2012. Experimental Investigation of the Effects of Suffusion on Physical and Geomechanic Characteristics of Sandy Soils. *Geotechnical Testing Journal*, 35, 890-900.
- YAMASHITA, S., FUJIWARA, T., KAWAGUCHI, T., MIKAMI, T., NAKATA, Y. & SHIBUYA, S. 2007. International parallel test on the measurement of Gmax using bender elements. *Organized by Technical Committee*, 29.
- YAMASHITA, S., KAWAGUCHI, T., NAKATA, Y., MIKAMI, T., FUJIWARA, T. & SHIBUYA, S. 2009. Interpretation of International Parallel Test on the Measurement of Gmax Using Bender Elements. *Soils and Foundations*, 49, 631-650.
- YANG, Y., CHEN, G., MENG, X., BIAN, S., CHONG, Y., SHI, W., JIANG, W., JIN, J., LI, C., MU, X. & YUE, D. 2022. Analysis of the microseismicity characteristics in landslide dam failure flume tests: implications for early warning and dynamics inversion. *Landslides*, 19, 789–808.
- YANG, Y., KUWANO, R. & XU, C. 2018. A preliminary study on the piping erosion of soils using glucose dissolution method. *Environmental Earth Sciences*, 77, 31.
- ZHANG, L. & CHEUK, J. 2014. Mechanical consequences of internal soil erosion AU - Chang, Dongsheng. *HKIE Transactions*, 21, 198-208.
- ZHANG, L. L., ZHANG, J., ZHANG, L. M. & TANG, W. H. 2011. Stability analysis of rainfall-induced slope failure: a review. *Proceedings of the Institution of Civil Engineers - Geotechnical Engineering*, 164, 299-316.
- ZHU, Y., VISSER, P. J., VRIJLING, J. K. & WANG, G. 2011. Experimental investigation on breaching of embankments. *Science China Technological Sciences*, 54, 148-155.

Appendix 1

Table of identified flood induced landslides.

Failure name	Failure country	Failure Date	Failure year	Reference
Julia Creek, Queensland	Australia	27-Dec	2015	(Australian Transport Safety Bureau, 2015)
Northern Territory	Australia	27-Dec	2011	(Josephs, 2011)
Bangladesh	Bangladesh	N/A	1998	(Ansary, 1998)
Stackpool	Canada	N/A	2011	(Railrodder, 2011)
RER B Paris	France	12-Jun	2018	(RATP, 2018)
Acquaviva	Italy	05-Oct	2005	(Polemio and Lollino, 2011)
Italy Road	Italy		2005	(Mossa, 2007)
Trnava – Kutý	Slovakia	30-Mar	2006	(RAIB, 2013b)
Loch Treig	United Kingdom	28-Jun	2012	(RAIB, 2013b)
Falls of cruchan	United Kingdom	18-Jul	2012	(RAIB, 2013b)
Rosyth	United Kingdom	18-Jul	2012	(RAIB, 2013b)
St Bees	United Kingdom	30-Aug	2012	(RAIB, 2013b)
Bargoed	United Kingdom	30-Jan	2013	(RAIB, 2013b)
Watford	United Kingdom	16-Sep	2016	(RAIB, 2017a)
Ousbeck North,	United Kingdom	04-Nov	2005	(RAIB, 2006a)
Moy	United Kingdom	26-Nov	2005	(RAIB, 2006b)
Farnley Haugh	United Kingdom	07-Jan	2016	(Petley, 2016, CML, 2016)
Gillingham tunnel	United Kingdom	28-Nov	2009	(RAIB, 2010)
Kemble	United Kingdom	15-Jan	2007	(RAIB, 2008)
Chorley Euxton	United Kingdom	19-Nov	1890	(Hutchinson, 1890)
Bessie Ghyll	United Kingdom	N/A	2000	(O'Kelly et al., 2008)
Conwy Valley	United Kingdom	Dec-15	2015	(Rail Engineer, 2016)
Nant Rhydycar, Wales	United Kingdom	Dec-79	1979	(RSSB, 2004)
Baildon	United Kingdom	07-Jun	2016	(RAIB, 2017b)
Knockmore, Northern Ireland	United Kingdom	28-Jun	2012	(RAIB, 2013c)
Newark	United Kingdom	05-Dec	1849	(Simmons, 1849)
Thorrington	United Kingdom	15-Mar	2018	(Duggan, 2018)
Highlands	United Kingdom	22-Jan	2018	(Drewett, 2018)
Oulton Broad	United Kingdom	N/A		(Network Rail, 2014)
Botley landslide	United Kingdom	N/A		(Network Rail, 2014)
Barrow Upon Soar	United Kingdom	27-Dec	2012	(RAIB, 2013a)
Conwy Valley	United Kingdom	N/A	1994	(Poole)
Corby	United Kingdom	13-Jun	2019	(BBC, 2020)
Oban	United Kingdom	N/A	2019	(Smale, 2019)
Churnet valley	United Kingdom	28-Oct	2019	(Holden, 2019)
Polmont	United Kingdom	N/A - Aug	2020	(Polmont, 2020)
Plymouth Road, Ann Arbor	USA	26-May	2011	(Heflin, 2011)
Black hills area, Hermosa, South Dakota	USA	17-Aug	2007	(USGS, 2009, National Weather Service, 2007)
Ideal Draw near Wilcox	USA	N/A	N/A	(Transportation Research Board et al., 2016)

Appendix 1

San Pedro on I-10 near Benson	USA	N/A	N/A	
Laguna wash on 163 near Kayenta	USA	N/A	N/A	
Middle Fork Snoqualmie River Road	USA	N/A	N/A	
IA 150 over Cedar River near Vinton	USA	N/A	N/A	
US 6 over Cedar River in Muscatine County	USA	N/A	N/A	
Route 103 over Mohawk River	USA	N/A	N/A	
1 Blaine Co SH 33 over creek 10.8 mi east of US 281 in Watonga	USA	N/A	N/A	
Alfalfa Co 17668-04 SH 8 from Major CL N 4.0 mi	USA	N/A	N/A	
Little South Fork Hunter Creek	USA	N/A	N/A	
Mt. Hood Highway, OR 35, Nov. 2006	USA	N/A	N/A	
Spruce Street Retaining Wall	USA	N/A	N/A	
FM 787 at Trinity River	USA	N/A	N/A	
US 79 at Tinity River Relief near Palestine Texas	USA	N/A	N/A	
Cannonville Bridge Embankment Failure ND 18 from Neche to Canadian border	USA	N/A	N/A	
Desert Road, , Freeport, Maine	USA	N/A	2008	(Vermont Local Roads, 2012)
Doon, Iowa	USA	23 - Jun	2018	(Independent, 2018)
Louisville, Nebraska	USA	N/A	2018	(Higgins, 2019)

References

- ANSARY, A. M. M. S. A. S. M. A. 1998. Damages to railway embankments during the 1998 flood in Bangladesh. *15th International Conference on Soil Mechanics and Foundation Engineering*. Istanbul.
- AUSTRALIAN TRANSPORT SAFERY BUREAU 2015. Derailment of freight train 9T92.
- BBC. 2020. *Corby train crash: 'Ineffective' flood system caused landslide* [Online]. Available: <https://www.bbc.co.uk/news/uk-england-northamptonshire-52807827> [Accessed].
- CML. 2016. *Farnley Haugh Landslide Repair* [Online]. Available: <https://www.cml.uk.com/case-studies/farnley-haugh-landslide/> [Accessed].

- DREWETT, Z. 2018. *Train pushed off the tracks by tonnes of mud in landslide* [Online]. Available: <http://metro.co.uk/2018/01/22/train-pushed-off-tracks-tonnes-mud-landslide-7250305/> [Accessed].
- DUGGAN, R. 2018. *Greater Anglia services will run tomorrow after engineers repair damage from landslide* [Online]. Essex Live. Available: <https://www.essexlive.news/news/greater-anglia-services-run-tomorrow-1355314> [Accessed March 2018 2018].
- HEFLIN, C. 2011. *Plymouth Road in Ann Arbor remains closed following embankment failure; midday reopening expected* [Online]. Available: <http://www.annarbor.com/news/plymouth-road-remains-closed-following-embankment-failure-midday-reopening-expected/> [Accessed].
- HIGGINS, J. 2019. *Midwest flooding washes out hundreds of miles of roads, rail lines* [Online]. Available: https://www.upi.com/Top_News/US/2019/04/04/Midwest-flooding-washes-out-hundreds-of-miles-of-roads-rail-lines/2351554328299/ [Accessed].
- HOLDEN, M. 2019. *Steam railway CLOSED after flood damage* [Online]. Available: <https://www.railadvent.co.uk/2019/10/steam-railway-closed-after-flood-damage.html> [Accessed].
- HUTCHINSON, C. S. 1890. *Lancashire and Yorkshire Railway*. Whitehall, London, S.W>,: Railway Department, Board of Trade.
- INDEPENDENT. 2018. *Crude oil pours into river after train derails in US* [Online]. Available: <https://www.independent.co.uk/news/world/americas/oil-spill-train-derailment-water-contamination-iowa-rock-river-doon-a8413626.html> [Accessed 2019].
- JOSEPHS, J. 2011. *Train derailed in Australia flood* [Online]. BBC. [Accessed].
- MOSSA, M. 2007. The floods in Bari: What history should have taught. *Journal of Hydraulic Research*, 45, 579-594.
- NATIONAL WEATHER SERVICE. 2007. *Hermosa, SD, Flash Flood of August 17, 2007* [Online]. Available: <https://www.weather.gov/unr/2007-08-17> [Accessed].
- NETWORK RAIL 2014. *Route Weather Resilience and Climate Change Adaptation Plans*, Anglia.
- O'KELLY, B. C., WARD, P. N. & RAYBOULD, M. J. 2008. Stabilisation of a progressive railway embankment slip. *Geomechanics and Geoengineering*, 3, 257-270.
- PETLEY, D. 2016. *The Farnley Haugh landslide in Northumberland, northern England* [Online]. Available: <https://blogs.agu.org/landslideblog/2016/01/09/farnley-haugh-landslide-1/> [Accessed].
- POLEMIO, M. & LOLLINO, P. 2011. Failure of infrastructure embankments induced by flooding and seepage: a neglected source of hazard. *Natural Hazards and Earth System Sciences*, 11, 3383.
- POLMONT, I. R. S. O. F. D. O. E. T. G. T. L. N. 2020. *Fiona Dobie* [Online]. Available: <https://www.falkirkherald.co.uk/news/transport/images-reveal-scale-flood-damage-edinburgh-glasgow-train-line-near-polmont-2946093> [Accessed].
- POOLE, G. *CONWY VALLEY RAILWAY FLOOD REPAIRS 1994*. [Online]. Available: <http://www.6gshed.co.uk/conwyvalleyrailwayfloodrepairs.html> [Accessed].
- RAIB 2006a. *Derailment at Oubeck North near Lancaster 4 November 2005*. Rail Accident Investigation Branch.
- RAIB 2006b. *Derailment near Moy, Inverness-shire on 26 November 2005*. Rail Accident Investigation Branch.
- RAIB 2008. *Derailment of a passenger train near Kemble, 15 January 2007*. Rail Accident Investigation Branch.
- RAIB 2010. *Derailment near Gillingham tunnel, Dorset, 28 November 2009*. Rail Accident Investigation Branch.

Appendix 1

- RAIB 2013a. Derailment of a freight train at Barrow upon Soar, Leicestershire. *Rail Accident Report*. Rail Accident Investigation Branch, Department for Transport.
- RAIB 2013b. RAIB Class investigation into landslips affecting Network Rail infrastructure between June 2012 and February 2013 April 2014. Rail Accident Investigation Branch.
- RAIB 2013c. Train ran onto a washed-out embankment near Knockmore, Northern Ireland 28 June 2012. Rail Accident Investigation Branch, Department for Transport.
- RAIB 2017a. Derailment due to a landslip, and subsequent collision, Watford 16 September 2016. Rail Accident Investigation Branch.
- RAIB 2017b. Report 03/2017: Trains passed over washed out track at Baildon.
- RAIL ENGINEER. 2016. *The Conwy Crisis* [Online]. Available: <https://www.railengineer.uk/2016/03/18/conwy-crisis/> [Accessed 2018].
- RAILRODDER. 2011. *CN Ruel Subdivision Roadbed Failure* [Online]. Available: <https://www.youtube.com/watch?v=Pb3pZIK6UFQ> [Accessed].
- RATP. 2018. *RER B accident - Update on work in progress and traffic forecasts* [Online]. Available: <https://www.ratp.fr/groupe-ratp/newsroom/rer/accident-du-rer-b-point-sur-les-travaux-en-cours-et-previsions-de-traffic> [Accessed 14/06/2018].
- RSSB 2004. Impact of scour and flood risk on railway structures (T112).
- SIMMONS, C. J. L. A. 1849. Accident Returns: Extract for the Accident at Newark on 6th December 1849. Board of Trade.
- SMALE, K. 2019. *Flood repairs for West Highland railway line* [Online]. Available: <https://www.newcivilengineer.com/latest/flood-repairs-west-highland-railway-line-07-08-2019/> [Accessed].
- TRANSPORTATION RESEARCH BOARD, NATIONAL ACADEMIES OF SCIENCES, E. & MEDICINE 2016. *Minimizing Roadway Embankment Damage from Flooding*, Washington, DC, The National Academies Press.
- USGS. 2009. *Black Hills Area Floods - 2000 to 2009* [Online]. Available: <https://sd.water.usgs.gov/projects/FloodHistory/2001-2009/FH2001.html> [Accessed March 2018].
- VERMONT LOCAL ROADS. 2012. *Road Collapse- Maine 2008* [Online]. Available: <https://www.youtube.com/watch?v=NTbhyHNA1Vc> [Accessed].